


INVESTIGATION OF THE THYROID PROTEOME AS A MOLECULAR ARCHIVE
OF THYROID DISEASE

by
Rosa Isela Gallagher
A Dissertation
Submitted to the
Graduate Faculty
of
George Mason University
in Partial Fulfillment of
The Requirements for the Degree
of
Doctor of Philosophy
Biosciences

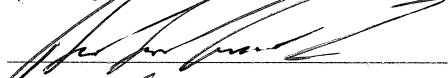
Committee:


Virginia Espina

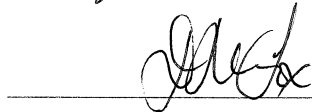
Dr. Lance Liotta, Dissertation Director




Dr. Virginia Espina, Committee Member


Waisman

Dr. Alessandra Luchini, Committee Member



Dr. Robin Couch, Committee Member


P. Agouris

Dr. Iosif Vaisman, Director, School of
Systems Biology

Dr. Donna M. Fox, Associate Dean, Office
of Student Affairs & Special Programs,
College of Science

Date: April 30, 2019

Dr. Peggy Agouris, Dean, College of
Science

Spring Semester 2019
George Mason University
Fairfax, VA

Investigation of the Thyroid Proteome as a Molecular Archive of Thyroid Disease

A Dissertation submitted in partial fulfillment of the requirements for the degree of
Doctor of Philosophy at George Mason University

by

Rosa Isela Gallagher
Master of Science
University of Texas-Pan American, 2006
Bachelor of Science
University of Texas-Pan American, 2000

Director: Virginia Espina, Research Assistant Professor
Center for Applied Proteomics and Molecular Medicine

Spring Semester 2019
George Mason University
Fairfax, VA

Copyright 2019 Rosa Isela Gallagher
All Rights Reserved

DEDICATION

To my husband Scott Gallagher for always believing in me and for being my faithful compass. To my son Joseph for inspiring me to pursue my dreams and motivating me to lead by example. To my grandmother for teaching me to work hard for the things that I aspire to achieve.

ACKNOWLEDGEMENTS

I would like to first thank Dr. Virginia Espina for her invaluable guidance throughout this process. Ginny's love for science and inquisitive mind lead to many discussions about possible research projects that sparked my interest into the area of thyroid cancer. Without her continuous thoughtful support and mentorship this project wouldn't have been possible. I would also like to thank Dr. Lance Liotta for his constant support and for being an inspiration to all at CAPMM. A special thanks to Dr. Alessandra Luchini and Dr. Robin Couch for their generous dedication and willingness to help graduate students reach their goals. All the members of CAPMM have my most sincere gratitude and appreciation for all of their help, especially Dr. Weidong Zhou, Dr. Paul Russo, Dr. Julia Wulfschlegel, and Dr. Emanuel Petricoin. Finally, I would like to thank my husband Scott for his unconditional support on everything I set my mind to do and to my son Joseph who inspires me to always do my best every day.

TABLE OF CONTENTS

	Page
List of Tables	vii
List of Figures	viii
List of Abbreviations	ix
Abstract	xii
Introduction	1
Thyroid Gland: Morphology and Physiology	2
Intrafollicular Colloid	8
Thyroid Disorders and Colloid Heterogeneity	10
Follicular Thyroid Adenomas	13
Papillary Thyroid Cancer	15
Signaling Pathways in Cancer	16
Autophagy Pathway	16
AMPK Pathway	18
Specific Aims and Project Overview	23
Project Overview	26
Materials and Methods	28
Preparation of frozen tissue sections	28
Laser capture microdissection	28
Protein extraction of microdissected material for downstream analysis	29
Sample preparation for mass spectrometry analysis	30
Sample incubation with nanoparticles	30
LC-MS/MS data analysis	32
Cell culture	33
Isolation of extracellular vesicles	34
Reverse phase protein microarrays	35

Statistical analysis	37
Aim of Study I	39
Investigation of the Proteomic Machinery in Thyroid Colloid by Mass Spectrometry....	40
Results	42
Protein profiling of colloid samples	42
Gene ontology analysis.....	44
The Kyoto encyclopedia of genes and genomes (KEEG) pathway analysis.....	46
RB221 nanoparticles effectively concentrate and harvest thyroid colloid proteins ..	48
Discussion	51
Aim of Study II.....	57
Protein Identification from Extracellular Vesicles Secreted by Thyroid Cells.....	58
Results	61
Extracellular vesicles are abundantly secreted by thyroid cell lines	61
Proteins involved in exosome biogenesis.....	61
Functional relevance of EVs-derived proteins	65
Protein cargo comparison of Nthy-ori3-1 and CRL-1803 EVs.....	66
RPPA characterization.....	70
Discussion	72
Aim of Study III.....	76
Phosphoproteomic Profile of Thyroid Colloid and Follicular Cells by RPPA.....	77
Results	79
RPPA reveals the presence of phosphoproteins in colloid.....	79
Autophagy pathway signaling is elevated in PTC follicular cells.....	82
DNA damage/repair response protein activation in colloid and epithelial cells	85
Discussion	88
Appendix 1	94
References.....	96

LIST OF TABLES

Table	Page
Table 1 List of proteins identified by MS in pilot study of thyroid colloid.....	24
Table 2 Colloid proteins common between non-carcinoma and PTC samples ranked according to their abundance ratio from averaged spectral hits	45
Table 3 Colloid proteins common between non-carcinoma and FTA samples ranked according to their abundance ratio from averaged spectral hits	46
Table 4 Proteins detected in Nthy-ori3-1 and CRL-1803 EVs previously identified in ExoCarta database.....	62
Table 5 Extracellular vesicles-derived proteins common between Nthy-ori3-1 and CRL- 1803 ranked according to their relative difference based on averaged spectral hits	69
Table 6 Characterization of Nthy-ori3-1 and CRL-1803 derived EVs via RPPA.....	71
Table 7 Specimen list and corresponding diagnosis analyzed by RPPA	79
Table 8 Endpoints with significant statistical differences in PTC and FTA colloid comparison.....	81

LIST OF FIGURES

Figure	Page
Figure 1 Thyroid morphology.....	2
Figure 2 Thyroid hormone synthesis	5
Figure 3 Iodothyronine deiodination pathways	7
Figure 4 Hematoxylin and eosinY stained thyroid tissue	12
Figure 5 Comparison of protein activation in significantly different signaling pathways in the colloid and epithelial cells through RPPA	14
Figure 6 Identified protein counts by LC-MS/MS analysis.....	43
Figure 7 Significantly enriched GO terms identified in the shared proteome of PTC, FTA, and non-carcinoma colloid samples.....	47
Figure 8 Identified protein counts by LC-MS/MS analysis after pre-processing colloid with RB221 nanoparticles.....	50
Figure 9 Exosomal proteins categorized by their biological function	66
Figure 10 CRL-1803 and Nthy-ori3-1 EVs comparison according to their biological function	67
Figure 11 Signal pathway mapping of thyroid colloid from PTC, FTA, and non-carcinoma samples.	80
Figure 12 Signal pathway mapping of follicular cells from PTC patients	83
Figure 13 Autophagy markers signaling activation by RPPA	84
Fig 14 DNA damage/repair protein activation in PTC epithelium.....	86
Fig 15 Subgroup of PTC samples revealed higher expression of proteins involved in DNA damage/repair pathway in both colloid and epithelium	88

LIST OF ABBREVIATIONS

Adenosine monophosphate	AMP
Adenosine monophosphate-activated protein kinase.....	AMPK
Adenosine triphosphate.....	ATP
Adenosine triphosphatase	ATPase
Anaplastic thyroid cancer	ATC
Autophagy Related Homolog 5	ATG5
Atypia of undetermined significance	AUS
Bovine serum albumin	BSA
Calcium	Ca ²⁺
Cryopreservation solution.....	OCT
Cytokeratin-10	CK10
Cytokeratin-19	CK19
Deoxyribonucleic acid	DNA
Diiodotyrosine.....	DIT
Differentiated thyroid cancer	DTC
Dithiothreitol.....	DTT
Epithelial mesenchymal transition.....	EMT
Extracellular vesicle.....	EV
Extracellular signal related kinase	ERK
Fetal bovine serum.....	FBS
Fibronectin 1	FN1
Fine needle aspiration	FNA
Follicular lesion of undetermined significance.....	FLUS
Follicular thyroid adenoma	FTA
Follicular thyroid cancer	FTC
Formalin fixed paraffin embedded.....	FFPE
Glutathione peroxidase 3	GPx3
Growth regulating estrogen receptor binding 1	GREB-1
Hector Battifora Mesothelial-1	HBME-1
Hematoxylin and Eosin.....	H&E
Hydrogen Peroxide	H ₂ O ₂
Immunohistochemistry	IHC
Interleukin	IL
Interleukin 11 receptor alpha	IL11R α
Iodide	I ⁻
Iodothyronine deiodinase type 3	DIO3

Kilodalton	kDa
Kirsten renin-angiotensin system.....	KRAS
Light chain	LC
Liquid chromatography-coupled tandem mass spectrometry	LC-MS/MS
Liver hepatocellular cells	HepG2
Mass spectrometry	MS
Medullary thyroid cancer	MTC
Methanol	MeOH
Microtubule-associated protein-1 Light Chain 3 Beta.....	LC3B
Mitogen activated protein kinase	MAPK
Monoiodotyrosine	MIT
Mammalian target of rapamycin	mTOR
Papillary thyroid cancer	PTC
Paired box gene-8	PAX8
Phosphate buffered saline	PBS
Phosphatidylinositol 3-kinase	PI3K
Plasma Membrane Calcium ATPase isoform2	PMCA2
Post-translational modification	PTM
Potassium	K
Protein kinase B	AKT
Reactive blue 221	RB221
Reactive oxidative species	ROS
Receptor tyrosine kinases	RTK
Renin-angiotensin system	RAS
Reverse phase protein microarray	RPPA
Ribosomal protein S6 kinase	p70S6K
Selenocystein insertion binding protein 2	SECISBP2
Serine	Ser
Sodium	Na
Sodium dodecyl sulfate	SDS
Sodium-iodide symporter.....	NIS
Tissue culture	TC
Threonine	Thr
Thyroglobulin	Tg
Thyroid hormone receptor	TR
Thyroid hormone receptor alpha.....	TR α
Thyroid hormone receptor beta.....	TR β
Thyroid stimulating hormone	TSH
Thyroid transcription factor	TTF
Thyroperoxidase	TPO
Thyrotropin releasing hormone.....	TRH
Thyroxine.....	T ₄
Thyroxine binding globulin	TBG
Tissue protein extraction reagent	T-PER

Transthyretin	TTR
Trifluoroacetic acid	TFA
Triiodothyronine	T ₃
Tyrosine	Tyr

ABSTRACT

INVESTIGATION OF THE THYROID PROTEOME AS A MOLECULAR ARCHIVE OF THYROID DISEASE

Rosa Isela Gallagher, Ph.D.

George Mason University, 2019

Dissertation Director: Dr. Virginia Espina

Very little is known about the molecular composition and function of thyroid colloid beyond its role as a thyroglobulin, iodine, and thyroid hormone storage depot. Colloid morphologic heterogeneity is observed in all major thyroid disorders with reduced colloid volume being a hallmark of thyroid cancer. Elucidating colloid protein content and its interactions with epithelial cells in thyroid follicles may provide new insights into tumor progression along with potentially actionable information on new therapeutic modalities to test in thyroid cancer patients. Multiplatform proteomic analyses of laser capture microdissected (LCM) follicular cells and colloid indicate that intracellular colloid is a heterogeneous proteinaceous fluid with the potential of regulating more than thyroid hormone synthesis. Presence of extracellular vesicles and protein expression of autophagy markers in tumor-associated thyroid cells suggests that cellular components are being degraded/recycled for energy while depleting essential proteins from the

colloid, thus creating constant cell stress contributing to tumor proliferation. Establishing signatures of post-translational modifications within the colloid and epithelial cells could potentially be useful in effectively categorizing patients for prognostic and therapeutic purposes. Furthermore, the colloid characteristics may aid in early identification of patients showing key modifications indicative of tumor progression.

INTRODUCTION

According to the most recent statistics given by the American Cancer Society, the incidence of thyroid cancer has tripled over the last three decades, approximating 60,000 new cases in the United States alone in 2017¹. Thyroid gland carcinoma is a very prevalent neoplasia and its incidence is about three times higher among females than males worldwide. It is currently the fastest-increasing cancer in the United States and has become the fifth most common type of cancer in women. More than 95% of thyroid tumors arise from thyroid follicular cells, most often as differentiated thyroid cancers (DTCs), including papillary thyroid cancer (PTC), and follicular thyroid cancer (FTC). By retaining the differentiated features of normal thyrocytes, including the ability to concentrate iodine, these tumors are in most cases surgically removed followed by radioactive iodine treatment². At the opposite pole, both medullary thyroid cancer (MTC) and anaplastic thyroid carcinoma (ATC) are poorly differentiated with the latter considered the most aggressive and invasive^{3,1,4}.

Diagnosis of thyroid neoplasms is primarily based on cytological criteria using biopsies obtained by fine needle aspiration (FNA). While this is the most important diagnostic test in the initial evaluation of a patient with a thyroid nodule, more often than not patients displaying either indeterminate or suspicious results undergo a diagnostic surgical procedure (thyroid lobectomy or total thyroidectomy) to exclude malignancy.

Despite the benefits of fine needle aspiration cytology for diagnosis of thyroid cancers, FNAs are not necessarily useful at distinguishing malignant and benign thyroid adenoma lesions⁵⁻⁸.

Improving diagnostic accuracy is therefore of crucial clinical importance and molecular biomarkers are desperately needed to provide a definitive diagnosis and help expedite patient treatment based on their individual molecular profile.

The following introduction presents morphologic and molecular features of non-diseased and diseased thyroid gland to highlight the under-appreciated of colloid molecular heterogeneity in thyroid follicles, which is the underlying basis of this research project.

Thyroid Gland: Morphology and Physiology

The thyroid gland is a butterfly-shaped bilobed organ anchored to the trachea by lateral suspensory ligaments (Fig. 1). The follicle is the functional unit of the thyroid gland and has a distinctive spherical structure⁴. On average, normal thyroid glands contain between 500,000 and 1.5 million follicles.⁹ Each follicle is comprised of a single layer of follicular cells actively shielding the colloid material at its center. Follicular cells vary in size and shape from cuboidal to columnar

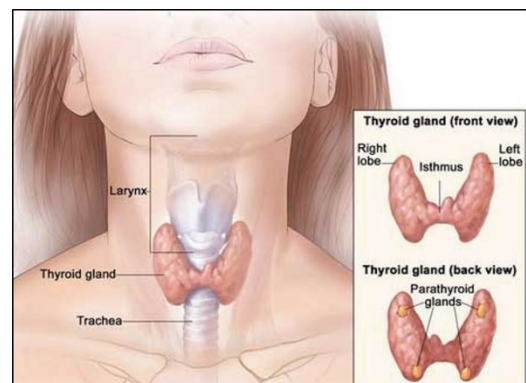


Fig. 1. Thyroid gland morphology. Thyroid gland is a butterfly-shaped organ, located below the larynx and anchored to the trachea. The thyroid gland secretes hormones to regulate heart rate, blood pressure, temperature, and metabolism. Illustration for the National Cancer Institute ©(2012) Terese Winslow LLC, U.S. Govt. has certain rights.

appearance which directly correlates with their level of thyroid hormone synthesis. The most abundant component in colloid is thyroglobulin, an iodinated glycoprotein that is the precursor of triiodothyronine (T₃) and thyroxine (T₄). Interestingly, small vacuoles and larger oval clear spaces are frequently detected within the colloid as well as particulate-like clumps that have no clear purpose. Thyroid hormones are produced from follicular cells through iodination of tyrosine and are released to the circulation in their biologically active forms (T₃ and T₄). C cells, or parafollicular cells, are another component of the thyroid follicle. These cells produce calcitonin, a hormone involved in calcium and phosphate homeostasis as well as bone growth, located between or adjacent to the follicular cells. Calcitonin is of clinical importance since its measurement serves as a sensitive and specific tumor marker for patients with MTC^{4,10-12}.

Thyroid hormone synthesis involves several biochemical steps that take place within the follicular cells (Fig. 2)¹³. First, thyroid iodide (I⁻), the negatively charged form of the iodine atom, accumulation is stimulated by the thyroid stimulating hormone (TSH) produced by the pituitary gland. TSH secretion and production is in turn regulated by the thyrotropin-releasing hormone (TRH) produced by the hypothalamus. Accumulated iodide is then actively transported into follicular cells by the sodium-iodide symporter (NIS)^{14,15}. NIS, a transmembrane glycoprotein, mediates iodide uptake by follicular thyroid cells and is also a thyrocyte differentiation marker that is lost in the course of thyroid carcinogenesis¹⁶⁻¹⁸.

Na⁺/I⁻ symporter transports two sodium ions and one iodide ion into the cell requiring an electrochemical gradient, which is generated by the Na, K-ATPase system.

Iodide then reaches the apical membrane and is released into the follicular lumen (filled with colloid). Pendrin, a chloride/iodide anion transporter expressed on the apical membrane has been shown to assist in iodide transport¹⁷.

The function of NIS is closely regulated by post-translational glycosylation. This protein carries three N-linked glycosylations, resulting in a mature protein that migrates at a molecular weight of 80–90 kDa. In addition, a partially glycosylated form can also be seen migrating at a molecular weight of 60 kDa on SDS-PAGE. As shown by Levy et al., NIS glycosylation is not required for the correct targeting of the protein to the plasma membrane, nonetheless it plays a role in protein stabilization and folding^{16,19}. The cytoplasmic carboxyl-terminal domain of NIS contains a PDZ target motif and a dileucine motif tail that are important for protein-protein interactions. A recent study reported that the deletion of these motifs prevented the transport and insertion of NIS protein into the plasma membrane, hence these motifs are likely to be involved in the post-translational regulation of NIS by TSH^{15,20}.

Pendrin is capable of regulating I^- efflux at the apical membrane in several heterologous expression systems, including *Xenopus oocytes* and particularly in mammalian cell systems^{14,16,21,17}. Normally, about 120 micrograms of iodide are taken up by the thyroid gland for the synthesis of thyroid hormones. Iodide transport into cells is inhibited when colloidal iodine levels become elevated. Excess iodine results in expression inhibition of both NIS and pendrin, thus reducing the number of both transporters available to import iodide and export iodine^{17,22}. This entire process allows

the thyroid cell to regulate the amount of iodide entering the follicular cell and lumen in order to maintain appropriate levels for colloid production²².

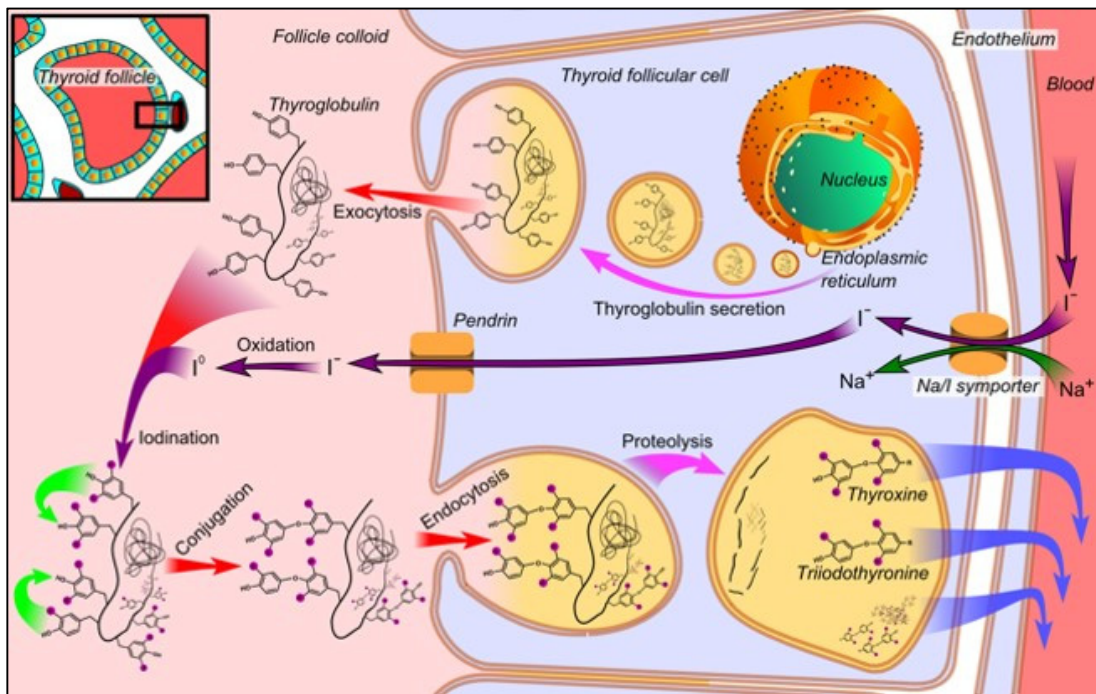


Fig. 2. Thyroid hormone synthesis. The thyroid gland is responsible for the synthesis, storage, and secretion of thyroxine (T_4), and triiodothyronine (T_3) and for the peripheral control metabolism of T_3 and T_4 ¹⁶. Illustration by Mikael Häggström, used with permission.

Once in the colloid, iodide is oxidized by thyroperoxidase (TPO) in the presence of hydrogen peroxide (H_2O_2)^{23,24}. TPO is a membrane-bound glycoprotein that catalyzes both the organification and the coupling reactions of iodotyrosines. Some of the more common causes of defective thyroid hormone synthesis are due to TPO defects ²⁵. Iodide excess has been demonstrated to be toxic to the thyroid gland and consequently may lead

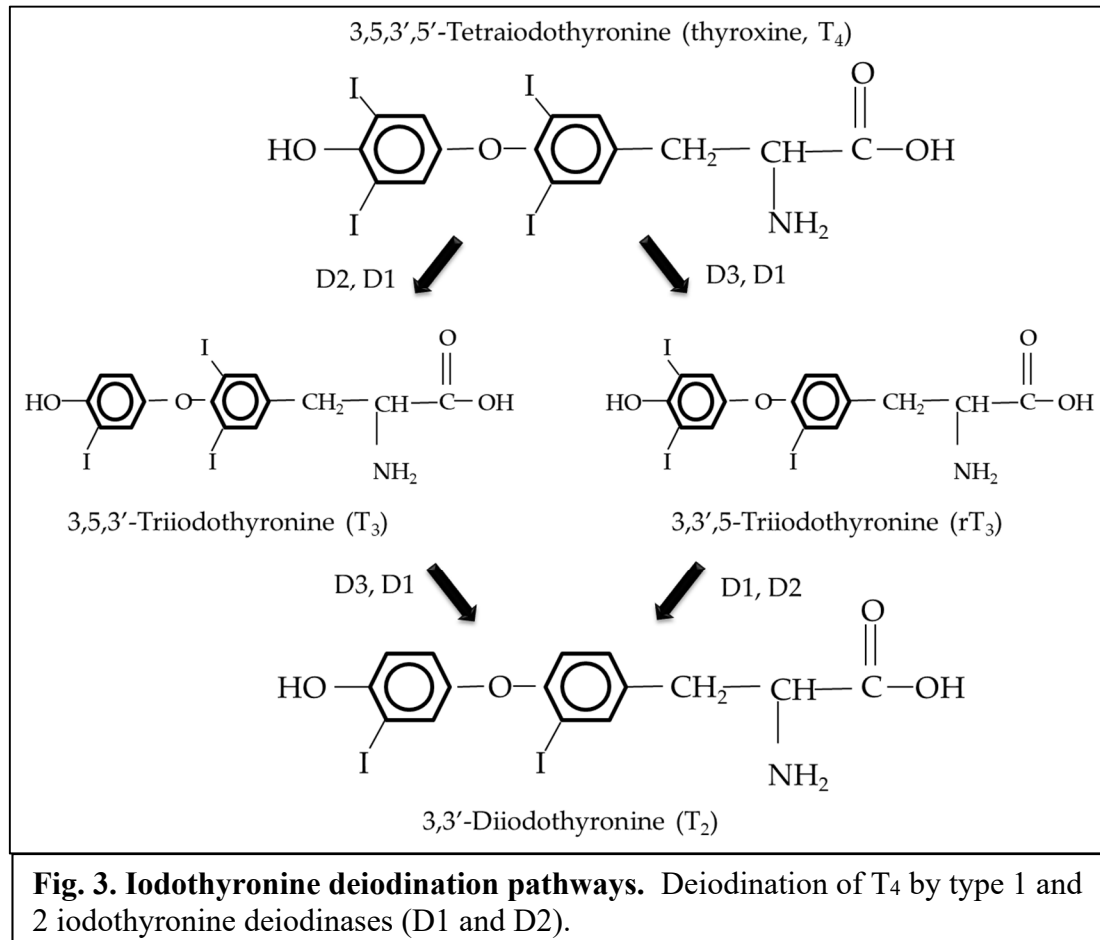
to hypothyroidism, hyperthyroidism, euthyroid goiter, or thyroid autoimmunity, with oxidative stress being one of the primary mechanisms^{26,27}.

The presence of H₂O₂ is critical for the oxidation of iodide, as well as its organification and coupling reactions. However, it is not entirely clear whether H₂O₂ is formed directly or through a process that includes the formation of O₂⁻ as an intermediate step in a dual oxidase system. H₂O₂ generation is considered a limiting step in thyroid hormone biosynthesis, and biochemical studies are now suggesting that H₂O₂ may be generated by a thyroid NADPH oxidase.^{24,28,4}

Thyroglobulin (Tg), a large glycoprotein found in the colloid, functions as a matrix for the synthesis and storage of T₄ and T₃. TPO iodinates certain tyrosyl residues on Tg, this organification reaction generates monoiodotyrosine (MIT) and diiodotyrosine (DIT). Both iodotyrosines are released in very small amounts into the circulation, therefore, they are significantly more abundant in the Tg molecule than in the T₄ and T₃. Iodotyrosines are then fused in the coupling reaction by TPO to form T₄ and T₃. In order to release thyroid hormones, Tg is internalized into the follicular cell through micropinocytosis and accordingly digested in lysosomes. Thyroid hormones, T₄ and T₃ are subsequently released into the blood stream while MIT and DIT are predominantly deiodinated by a thyroidal dehalogenase, prompting the recycling of iodide back into the follicular lumen and reused for hormone synthesis (Fig. 3)^{13,29-31,4,32,23}.

Mutations in the Tg gene can lead to goiter and in some cases to hypothyroidism. Clinically, the measurement of Tg in serum is used in the follow up of patients with well-differentiated thyroid cancer and serves as specific and sensitive tumor marker^{33,34}.

Although Tg is localized in the colloid, it can be reabsorbed in to the peripheral circulation, allowing it to be readily detected in the patient's serum⁶.



Thyroid hormones circulate in the blood stream bound to three major plasma proteins, thyroxine binding globulin (TBG), transthyretin (TTR), and albumin (or apolipoprotein B100). T₄ is predominantly secreted by the thyroid gland, however, T₃ is the more active of the two and it has a higher affinity to the nuclear thyroid hormone receptors (TRs). Thyroid hormone receptor alpha (TR α) and thyroid hormone receptor

beta (TR β), two main nuclear transcription factors, mediate most actions of thyroid hormones, which alter the expression of numerous genes throughout organism^{35,36}. Evidence from human, animal, and in vitro studies show that both TRs play a dual role, since they are key components for growth and proliferation of different cell types and organs, while at the same time are able to act as inhibitors of cell proliferation and inducing differentiation in other types of cells. T₄ and T₃ are essential hormones necessary for normal growth and development, primarily of the central nervous system, and they both play a key role in regulating metabolism^{35,37}. Undeniably, the site of hormone production is also of vital metabolic interest but surprisingly little is known about follicular colloid beyond its role as a Tg, I⁻, and thyroid hormone storage depot^{10,38}.

Intrafollicular Colloid

Thyroid colloid was first recognized in 1892 as a secretion product of the thyroid epithelium and described as a proteinaceous fluid inside thyroid follicles³⁹. Since then very few attempts have been made to describe the nature of colloid most likely due to technical complications in obtaining pure colloid material and/or lack of sensitive methodology. Some attempts were made to measure total protein content using single rat thyroid follicles. This was performed by means of micropuncture technique of the colloid in which thyroglobulin was found to be the predominant protein fraction via polyacrylamide microgel electrophoresis. Despite contamination issues of the colloid

specimen and the inability to identify specific proteins at the time, significant amounts of more slowly and faster migrating proteins were observed⁴⁰⁻⁴². Protein composition reported in rat colloid samples clearly varied between the follicles in the same gland and it was proposed early on that alterations of the colloid composition and the concentrations of its proteins could probably reflect functional changes in the follicle^{42,43}. Analytical ion microscopy techniques have also revealed surprisingly uneven distributions of iodine and possibly Tg within and between individual follicles in rats^{44,45}. Furthermore, colloidal Tg from bovine thyroid glands has been isolated in at least two reported forms of aggregation, primarily soluble and insoluble Tg⁴⁶. The existence of different colloidal aggregates with possibly multiple iodine compartments is without a doubt deserving of further attention in relation to thyroid function.

In a more recent study, glutathione peroxidase 3 (GPx3), a selenoprotein, was extracted from globular Tg colloid obtained from post mortem thyroid glands incubated in 0.5% sodium dodecyl sulfate (SDS). This finding suggested GPx3 is secreted into the follicular lumen and loosely attached to the colloidal thyroglobulin with the purpose of protecting the thyroid gland from possible damage by H₂O₂⁴⁷. Much is left to learn about the molecular composition and function of colloid beyond its role in producing thyroid hormones.

Thyroid colloid and the surrounding epithelial cells exist in harmonious molecular equilibrium to maintain normal thyroid function. Therefore, the presence or absence of proteins and biomolecules within the colloid and/or thyrocytes likely modulate DNA transcription and protein translation resulting in changes in DNA transcription/translation

cell signaling pathways, and thyroid gland phenotype^{48,49}. It has been suggested that in addition to TSH, even slight alterations of Tg secondary or tertiary structures (and possibly other proteins) may be involved in dramatically changing iodination kinetics by altering its diffusion velocity^{50,51}. We propose that the follicular colloid composition may include signature molecules, exosomes, autophagosome, and lysosomes involved in thyroid disease/carcinogenesis.

Thyroid disorders and colloid heterogeneity

All major thyroid conditions exhibit colloid heterogeneity throughout the gland. Thyroid cancer generally exhibits a reduction in the colloid volume, as seen by smaller colloid diameters on histological sections (Fig. 4). In contrast, abundant colloid is a pathological occurrence of goiter resulting from overproduction of colloid or damaged transportation in thyroid cells²².

Interestingly, the size of a thyroid follicle has been shown to depend on the size and number of follicular cells surrounding the colloid⁴. In rats, under physiological conditions, an increase in the colloid volume has been associated with a higher number of follicles with a constant size distribution instead of a larger volume of each follicle⁵². In some cases when the thyroid gland is inactive, the follicles often appear large in size, the lining cells are flat, and the colloid is abundant. On the other hand, if the gland is over-active, the follicles tend to be smaller, the lining cells change to a cuboidal or columnar shape, and the colloid appears scanty^{52,53}.

Graves' disease, also known as hyperthyroidism, is an autoimmune disorder that occurs due to highly unregulated synthesis and secretion of thyroid hormone^{54,55}.

Autoantibodies to thyroid stimulating hormone receptor (TSHR) stimulate thyroid hormone synthesis and diffuse proliferation of the follicular cells. The amount of colloid can vary in different areas of the gland depending on the degree of epithelial hyperplasia present and the colloid has a lighter appearance compared to normal follicles⁴. In contrast, the most common cause of hypothyroidism is chronic thyroiditis, an autoimmune disorder notorious for exhibiting varying degrees of lymphocytic infiltration, destroying follicular cells with elevated thyroid antibody concentrations resulting in an underactive thyroid gland⁵⁶. Another common cause of hypothyroidism is thyroid resection surgery. Removal of the entire thyroid gland (thyroidectomy) causes hypothyroidism in 30 to 50% of patients in which half of the thyroid gland is removed (lobectomy)⁴. A recent *in vitro* study by Xu et al. showed decreases in autophagy-related protein LC3B, indicative of autophagy suppression, due to excess iodine resulting in activation of the AKT/mTOR signaling pathway⁵⁶.

Ageing also induces morphological and functional changes in the thyroid leading to a gradual loss in its ability to maintain homeostasis. Increases in both gland size and number of follicles have been reported in aged male albino rats, however the thyroid of a human over the age of 60 undergoes progressive fibrosis and atrophy, leading to a reduction in thyroid volume⁵⁷⁻⁵⁹.

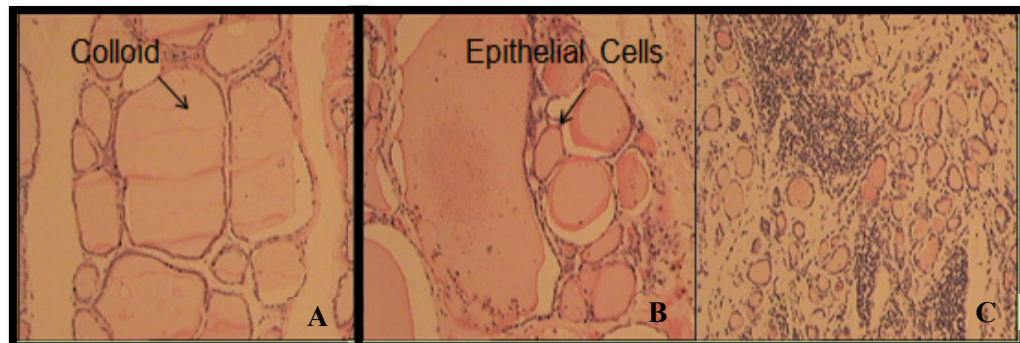


Fig. 4. Hematoxylin and Eosin Y Stained Thyroid Tissue 40x. Fixed frozen sections of thyroid tissue exhibiting colloid size variability found in (A) Normal, (B) Goiter, and (C) Tumor tissue.

The thyroid gland tissue architecture is like a fort – epithelial cells surrounding a core of colloid. Very little is known about colloid-composition and function beyond its role as a Tg, I^- , and thyroid hormone storage depot³⁸. We propose that the colloid is much more than a simple repository. Preliminary histological observations of protein expression from selected thyroid epithelium and colloid collected via laser capture microdissection revealed individual protein profiles with evident differences in Cu-Zn Superoxide Dismutase, Prolactin, PMCA2 and STAT3 Ser727 both between patient specimens and between the epithelial cells and colloid samples (Fig. 5). We hypothesize that colloid is an ongoing “chemical factory” and serves as a molecular information archive of thyroid metabolic activity. Thus, it is the intent of this study to generate the first detailed molecular portrait of thyroid colloid heightening follicular adenomas and papillary carcinomas of the thyroid.

Follicular Thyroid Adenomas

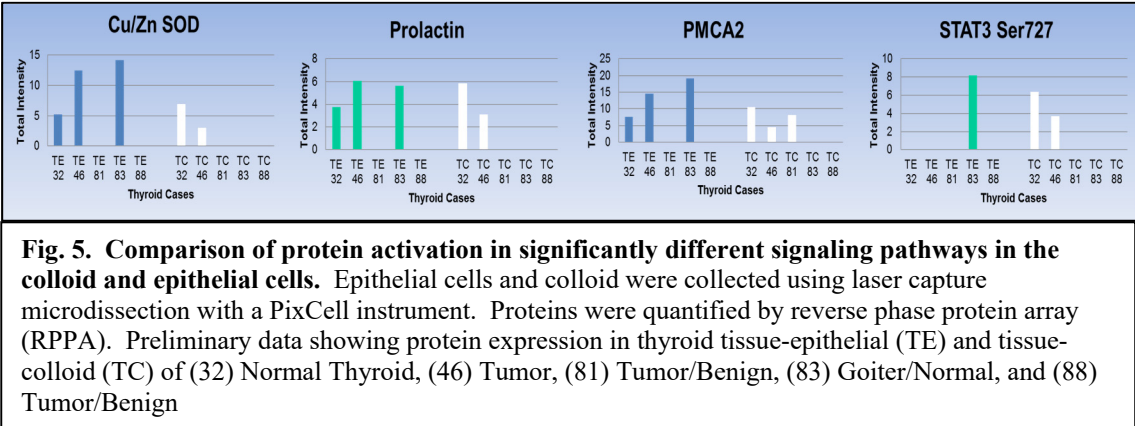
Follicular thyroid adenomas (FTA) are benign, encapsulated, noninvasive tumors originating from thyroid follicular cells. FTA incidence is difficult to assess since these tumors cannot be reliably discriminated from other variants, including solitary hyperplastic nodules. Radiation exposure and iodine deficiency are some of the main risk factors of FTA⁶⁰. The exact mechanism of how iodine deficiency promotes adenoma formation is not clear, but it likely involves an increase in TSH levels that stimulate proliferation of thyroid cells. Preexisting solitary thyroid adenomas increase the carcinoma risk by approximately 30-fold and multiple hyperplastic nodules (multinodular goiter) by close to 10-fold⁴. Approximately 20% of nonfunctioning follicular adenomas possess oncogene mutations that may predispose them to progression to follicular thyroid carcinoma⁶¹.

Mutations in Renin-angiotensin system (RAS) genes are also commonly detected in FTA and may be precursors of malignant transformation⁶². RAS mutation is responsible for chronic stimulation of various down-stream signaling pathways, including the Mitogen-Activated Protein kinase (MAPK) pathway and Phosphatidylinositol 3-kinase (PI3K)/Protein Kinase B (AKT) pathway, by the mutant RAS protein⁶³. This mutation is more than likely an initiating event in the development of FTAs.

FTAs display a variety of follicle sizes, some of which are very cellular and almost depleted of colloid and yet others are classified as microfollicular with very round follicles and small amounts of colloid^{4,64}. Furthermore, normofollicular adenomas include follicles comparable in size to normal thyroid follicles and macrofollicular

adenomas have large follicles filled with colloid. Despite of this evident diversity in colloid volume within FTAs, these observations do not bare any diagnostic significance and are seldom mentioned in the diagnostic line of a pathology report^{4,53,61,65}.

Follicular thyroid carcinoma (FTC) and benign FTA have very similar histological features and in most cases are indistinguishable by preoperative diagnosis⁶². Diagnosis of thyroid adenomas is primarily based on microscopic evaluations and some cases do benefit from additional immunohistochemical (IHC) examination. FTA cells stain positively for Tg, TTF1, Paired box gene-8 (PAX8) and low to intermediate molecular weight cytokeratins⁴. Some authors have reported the diagnostic usefulness of Cytokeratin-19 (CK19) reactivity in thyroid carcinomas to differentiate carcinomas from follicular adenomas⁶⁶. Additionally, immunoreactivity of Galectin-3 and Hector Battifora Mesothelial-1 (HBME-1) is rarely observed in FTAs and both are being considered to aid in the differential diagnosis of FTA and FTC⁶⁷. Although promising, none of these immunohistochemical markers seem to be specific for malignancy, and may only help in diagnosis when used in combination.



Papillary thyroid carcinoma

Papillary thyroid carcinoma (PTC) is the most common type of thyroid cancer. Its incidence in women has more than tripled over the past several decades in United States^{68,69}. Multiple factors are responsible for this increase, including the use of ultrasonography, which aids in detection. Ultrasonography is able to detect very small thyroid nodules and guide FNA procedures to successfully retrieve aspirates from affected areas⁴. Updated histopathologic criteria have also provided better tools to recognize and correctly diagnose follicular variants of papillary carcinomas. Unfortunately, a history of benign thyroid disease is a well-known risk factor for PTC⁷⁰. PTC has a papillary growth pattern, represented by finger-like projections typically covered by a single layer of epithelial cells surrounded by loose myxoid stroma⁴. Intrafollicular colloid is scant but varies in volume and some PTC cases may even exhibit calcified colloid material.

Galectin-3 has been shown to promote K-RAS signaling to RAF and PI3K which affects apoptosis and has been utilized to increase diagnostic specificity of differentiated cancer types^{71,72}. Interestingly, PTC reveals abnormal mitogenic signaling to the nucleus via the RET/RAS/BRAF-MAPK pathway and promotes irregular methylation of tumor suppressor TSHR gene⁷¹. This pathway has also been investigated to understand the relationship between PTC and oncogenic changes seen in Hashimoto's thyroiditis (chronic thyroiditis).

One of the most studied molecular mutations that has been most studied in PTC is BRAF, in particular the V600E point mutation. A BRAF V600E mutation in PTC tumors

usually indicates aggressive tumors and association with a greater risk of metastasis^{70,73}. Furthermore, this point mutation has been recently associated with an increase in autophagy. Kim et al. observed higher expression levels of autophagy-related proteins in PTCs with BRAF V600E mutation compared to those without it⁷⁰. The limitation of this study was assessment of autophagy only by immunohistochemistry on FFPE (formalin fixed paraffin embedded) tissue sections. The authors suggested a more functional approach is needed to confirm these results. To address concerns regarding quantifying autophagy related markers in thyroid cells and colloid, I used laser capture microdissection (LCM) of frozen thyroid tissue sections to procure enriched thyroid epithelial cells and colloid, with minimal contamination between the cellular and colloid specimens. Reverse phase protein arrays (RPPA) were used to quantify proteins and their post-translationally modified forms to compare activation states of autophagy-related proteins. Moreover, the ability to quantify numerous proteins by RPPA within the colloid from PTC follicles may yield information to explain the paucity of colloid observed in this type of thyroid cancer.

Signaling Pathways in Cancer

Autophagy Pathway

In the 1950-1980 era, autophagy was generally studied through the use of biochemical methods and electron microscopy. Yeast genetics was introduced to this field and autophagy-based research has exploded in the past decade, particularly in the area of tumorigenesis⁷⁴⁻⁷⁷. Autophagy is a cyclical cellular pathway that can be

catabolic, producing ATP in times of cellular stress, or it can be apoptotic, resulting in cell death^{78,79}. Autophagy regulates cell homeostasis through either cell survival or cell death, via an alternative mechanism to apoptosis. In addition, autophagy appears to operate in a variety of cell types as an essential process for maintaining ATP levels and free amino acid availability, breaking down protein aggregates and for controlling cell death^{80,81}. Given its role in homeostasis, autophagy acts as a double-edge sword in many cancers⁷⁹.

Beclin-1 and microtubule-associated protein light chain 3 (LC3) genes play an important role in mammalian autophagy. Beclin-1 is an autophagy-specific protein that regulates autophagosome formation and may also act as a tumor suppressor⁷⁶. When heterozygous disruption occurs in mice, a decrease in autophagy expression is observed along with an increase in cellular proliferation and spontaneous tumor development⁸². LC3, a mammalian homolog of yeast Atg8, was the first mammalian protein identified that specifically associates with autophagosome membranes and therefore, serves as a widely used marker for autophagosomes⁸³.

Extremely aggressive tumors have high metabolic demands that cannot be satisfied by angiogenesis and/or glycolysis alone, resulting in activation of autophagy as an alternate metabolic pathway to recycle cytoplasmic components as a source of cellular energy^{84,85}. However, unrestrained autophagy has also been shown to eventually lead to cell death following the progressive consumption of cellular components⁸⁶. Furthermore, it has been proposed that autophagy is required to guard against oxidative damage to the genome by clearance of dysfunctional mitochondria; however, once tumorigenic

mutations have been established, autophagy provides a survival advantage to the tumor cells in nutrient deprived conditions and supports chemoresistance in tumor cells^{75,87}.

Thus, autophagy inhibitors, such as chloroquine and chloroquine derivatives, have been evaluated as cancer therapy⁸⁷.

In thyroid tissue, autophagy activation may vary according to the thyroid disorder or tumor subtype. For example, LC3A and LC3B, lipidated forms of LC3, have been reported to exhibit higher levels of expression in medullary cancer (MC) via IHC analysis⁸⁵. In contrast, LC3B displayed a decrease in activation in a study of patients diagnosed with thyroiditis⁵⁶. As follicle size decreases in most thyroid cancers, consequently so does colloid volume. We propose that depletion of essential proteins/biomolecules in the colloid and follicle reduction is due to upregulation of autophagy creating constant cell stress which contributes to tumor proliferation.

AMPK Pathway

Another pathway that has been associated with thyroid cancer and recently, with autophagy is AMPK. Activation of AMPK is a direct effect of energy depletion in the cell primarily caused by stress. AMPK is a metabolic stress-sensing cytosolic enzyme whose expression has recently been reported as highly activated in PTC⁸⁸⁻⁹⁰. Loss of energy triggers an increase in the intracellular AMP-to-ATP ratio promoting conformational changes of AMPK making it a substrate for upstream phosphorylation by kinases, thus resulting in its activation. In its activated state, AMPK is able to inhibit

processes that consume energy and upregulates energy-producing pathways in an attempt to replenish intracellular ATP⁸⁹. The mTOR/p70S6K pathway (involved in cell proliferation and metabolism) is one of the main downstream targets strategically inhibited by AMPK in an attempt to restore ATP levels by blocking proliferation in thyroid cancer cells¹⁸.

TSH has been shown to inhibit AMPK phosphorylation and activation, thus directly influencing iodide regulation and glucose uptake in thyroid cells leading to a higher cell proliferative rate⁹¹. Interestingly, PTC seems to also express high levels of mTOR and together with high expression of AMPK over-activation of these signaling pathways may be associated with tumor cell survival under stressful conditions and/or are even essential for tumor growth and invasion^{18,92,93}. Activation of mTOR is shown to suppress cell autophagy through directly inhibiting Ulk1, which is the upstream kinase generally initiating cell autophagy⁹⁴. However, it has been reported that mTOR blockade can also induce feedback autophagy activation, which might serve as a pro-survival factor to inhibit cancer cell death⁹⁵.

Different cancer studies have demonstrated that AMPK activation mediated by the reduction of the ATP/AMP ratio promotes cellular survival under stressful metabolic conditions that are characteristic of the tumor microenvironment^{18,88}. Cytokines can also generate an inflammatory microenvironment that may result in reactive oxidative stress, which in turn may stimulate MAPK pathway and increase thyroid tumorigenesis⁹⁶. Additionally, the MAPK and PI3K-AKT pathways are known to be involved in PTC and FTC, respectively, and recently it has been suggested that simultaneous activation of

these two pathways may become more frequent as the grade of thyroid tumors increase⁹⁷.

Establishing characteristic signatures of post-translational modifications within the colloid and epithelial cells of follicular adenomas and papillary carcinomas could potentially be useful in effectively classifying patients according to their molecular profile and aid in the early prognostic identification of patients likely to develop tumor progression. In this study, I microdissected follicular cells and intrafollicular colloid from thyroid tissue for proteomic profiling with the intent of identifying the colloid composition and its protein interactions with neighboring epithelial cells. The rationale for this approach is strongly supported by previous proteomic characterization of vitreous humor in patients with age related macular degeneration, which revealed vitreous fluid to be a repository of post-translationally modified proteins derived from the retinal pigment epithelium⁹⁸. Proteomic profiling of individual patients' colloid and follicular cells could generate signatures that may discriminate between thyroid neoplasms and significantly improve diagnosis of particularly challenging cases. This study is the first to examine both thyroid colloid content and epithelial cell proteome utilizing LCM, mass spectrometry, and RPPA for a comprehensive proteomic analysis.

The aim of this research study was to elucidate the colloid proteome and signal transduction pathways of thyroid epithelium. The results revealed the first detailed colloid proteome analysis and autophagy pathway interactions in individual thyroid tissues.

Hypothesis: The paucity of colloid in thyroid cancer is due to upregulation of autophagy in surrounding epithelial cells

Autophagy is a cellular catabolic process by which damaged or long-lived cellular proteins and organelles are degraded or recycled for energy (ATP)⁹⁹. Autophagy may act as a tumor suppressor mechanism during the initial steps of tumorigenesis; conversely, autophagic activation can also function as a protective mechanism promoting tumor survival thereby creating constant cell stress which contributes to tumor proliferation^{100–102}. We propose that the proteome of the human colloid contains soluble proteins, protein fragments and extracellular vesicles (EVs). These soluble proteins, along with EVs may provide cargo for sequestration within autophagosomes of thyroid epithelium. We hypothesize that the paucity of colloid in thyroid cancer is due to upregulation of autophagy, which depletes essential proteins from the colloid, thereby creating a constant state of epithelial cell stress. Conversely, abundant colloid in thyroiditis-like disorders may reflect autophagy inhibition.

Although PTC is considered the most common and treatable of all thyroid cancers, a subset of PTC patients are refractory to surgery and radioactive iodine treatment¹⁰³. Advanced PTC is in most cases highly resistant to external beam radiation and to doxorubicin treatment, thus novel therapies are indeed needed for patients

suffering with this advanced type of cancer^{103,104}. Several studies have reported autophagy induction by both external radiation and chemotherapy agents in cancer cells *in vitro*. In some cancer cells, autophagy has been observed to play a protective role under stressful conditions, however, prolonged autophagy leads to a shortage of the apoptosis machinery resulting in a non-apoptotic programmed cell death^{87,103,105,106}. Thus, autophagy expression activity has been established and linked to the tumor subtype in various types of cancer⁷⁸. Profiling of PTC and FTA thyroid components could generate signatures that may discriminate between thyroid neoplasms and significantly improve diagnosis of challenging undifferentiated cases. A long term goal emanating from this current study is the ability to potentially identify PTC patients who could benefit from autophagy inhibition therapy.

An under-studied and under-appreciated area in cancer research is the contribution of exosome cargo to cell signaling, both locally at the tissue microenvironment level and globally at the organism level. We propose that secreted EVs may contribute to autophagy induction of thyroid cancer. Exosomes convey intercellular communications via transport of proteins, lipids, and nucleic acids. Initiating and/or maintaining autophagic flux through exosome cargo via the Na/I symporter and pendrin may be possible especially during metabolic stress. These modes of EV transport may also facilitate iodinated molecules import/export for autophagy induction in thyroid cancer. Up-regulation of autophagy may deplete essential proteins from the colloid, thereby creating a constant state of epithelial cell stress, thus contributing to tumor cell proliferation.

SPECIFIC AIMS AND PROJECT OVERVIEW

Analyzing the thyroid colloid proteome may potentially contribute to the discovery of new protein and metabolic targets for the identification, treatment, and possibly prevention of thyroid disease. Our results show the wealth of previously unknown protein information contained within the thyroid colloid, which may provide a better understanding of thyroid function and colloid composition (Table 1).

The term proteomics describes the global analysis of the proteome, which is composed of the total collection of all proteins expressed at a given time point and physiological state in a specific biological entity. Many cellular processes are regulated post-transcriptionally and genomic studies are incapable of determining protein post-translational modifications such as phosphorylation and cleavage that affect tumor biology. Consequently, proteomics is an essential tool to enhance our understanding of thyroid disease process.

Specific Aims

We have demonstrated that thyroid colloid can be successfully isolated from follicles using an automated laser capture microdissection (LCM) system. A detailed molecular portrait of thyroid colloid is thus attainable using a proteomic approach integrating both mass spectrometry (MS) and reverse phase protein arrays (RPPA). We identified molecular differences in protein expression within 20 frozen thyroid tissue

biopsies from different thyroid disorders. By incorporating harvesting nanoparticle technology to concentrate low abundance proteins in the colloid lysate, we expanded the breadth of detectable colloid proteins via liquid chromatography tandem mass spectrometry (LC-MS/MS). In addition, we investigated protein characterization of secreted thyroid exosomes and their role in cell signaling communication in thyroid cell lines. The aim of this study was to establish the first detailed molecular portrait of human thyroid colloid and provide assessment of extracellular vesicles activity in thyroid cells, which could provide additional therapeutic & diagnostic targets for thyroid cancer patients.

Table 1. List of proteins identified by MS in pilot study of thyroid colloid

Protein	MW	Accession	Case 32: Adjacent Normal	Case 46: Tumor	Case 81: Tumor/Benign	Case 83: Goiter and Normal	Case 88: Tumor and Benign
thyroglobulin [Homo sapiens]	304592.4	55770862	x	x	x	x	x
keratin 1 [Homo sapiens]	65998.9	119395750	x	x	x	x	x
albumin preproprotein [Homo sapiens]	69321.6	4502027	x	x	x	x	x
keratin 10 [Homo sapiens]	58765.5	195972866	x	x	x	x	
beta globin [Homo sapiens]	15988.3	4504349	x	x	x	x	
keratin 9 [Homo sapiens]	62026.7	55956899	x	x	x	x	
histone cluster 1, H2b1 [Homo sapiens]	13897.6	4504271		x	x	x	
keratin 6B [Homo sapiens]	60030.3	119703753	x	x			x
keratin 2 [Homo sapiens]	65393.2	47132620	x	x			x
prostatic binding protein [Homo sapiens]	21043.7	4505621		x			x
histone cluster 1, H4a [Homo sapiens]	11360.4	4504301		x	x		
galectin 3 binding protein [Homo sapiens]	65289.4	5031863			x	x	
peripherin [Homo sapiens]	53618.5	21264345			x	x	
heat shock 90kDa protein 1, beta [Homo sapiens]	83212.2	20149594			x	x	
vimentin [Homo sapiens]	53619.2	62414289		x			
actin, gamma 1 propeptide [Homo sapiens]	41765.8	4501887		x			
actin, gamma 2 propeptide [Homo sapiens]	41849.8	4501889		x			
glutathione peroxidase 3 precursor [Homo sapiens]	35386.0	6006001		x			
fibrillin 1 precursor [Homo sapiens]	312022.0	24430141		x			
fructose-bisphosphate aldolase A [Homo sapiens]	39395.3	193794814		x			
calcitonin-related polypeptide, beta [Homo sapiens]	13697.1	9945304		x			
keratin 27 [Homo sapiens]	49791.6	153945736	x				
serum amyloid P component precursor [Homo sapiens]	25371.1	4502133			x		
cystatin C precursor [Homo sapiens]	15789.1	4503107			x		
heterogeneous nuclear ribonucleoprotein D isoform d [Homo sapiens]	30653.1	51477708			x		
profilin 1 [Homo sapiens]	15044.6	4826898				x	
peroxiredoxin 1 [Homo sapiens]	22096.3	4505591				x	
keratin 16 [Homo sapiens]	51236.3	24430192				x	
calmodulin 1 [Homo sapiens]	16826.8	5901912				x	
PREDICTED: similar to C4A protein isoform 1 [Homo sapiens]	192753.6	239740684					x
serine proteinase inhibitor, clade A, member 1 [Homo sapiens]	46707.1	50363217					x
transferrin [Homo sapiens]	76999.7	4557871					x
clusterin isoform 1 [Homo sapiens]	57795.7	42716297					x
keratin 2 [Homo sapiens]	65393.2	47132620					x
Total Hits			9	18	14	14	11

Specific Aim 1. Investigate the proteomic machinery of thyroid colloid by Mass Spectrometry. Analyze and identify proteins present in microdissected material of pure thyroid colloid via mass spectrometry. Develop methodologies and demonstrate the utility of hydrogel nanoparticle technology for harvesting, concentrating, and identifying low abundance biomolecules that might be present in thyroid colloid. Evaluate protein harvesting affinity of RB221 (reactive blue 221) nanoparticles via LC-MS/MS.

Specific Aim 2. Identify extracellular vesicles-related proteins secreted by thyroid cells. Harvest extracellular vesicles secreted from normal and tumorigenic thyroid cultured cell lines. Isolate and purify EVs via ultracentrifugation and ExoQuick-TC kit. Identify EVs cargo via LC-MS/MS and quantify cargo protein by RPPA to elucidate potential intercellular communication that could drive thyroid cancer progression.

Specific Aim 3. Characterize the phosphoproteomic profile of thyroid colloid and follicular cells by RPPA. RPPA is a highly sensitive protein array technology for multiplex mapping of tissue and cellular phosphoprotein signal pathways. By probing printed arrays with validated antibodies both colloid and follicular cells can be evaluated under identical experimental conditions. 52 previously validated antibodies to proteins involved in thyroid hormone synthesis, cytokine signaling, transcription, glucose/energy metabolism, cell migration, angiogenesis, and autophagy were used to quantify the state of protein signaling interactions. RPPA technology has the required sensitivity and

precision for small numbers of cells and provides a means of quantifying protein post-translational modifications indicative of activated signal pathways^{107–109}.

Specific Aim 3a. Explore possible DNA lesions found in thyroid colloid and epithelial cells. Detect potential DNA damage via RPPA through expression of phosphorylated DNA-dependent protein kinases and other related proteins that are active and become phosphorylated in response to DNA double strand breaks and/or involved in DNA damage response and maintenance of genomic stability.

Project Overview

Isolation of pure colloid material was performed by LCM and analyzed by MS for molecular profiling. Hydrogel RB221 nanoparticles were tested on microdissected intrafollicular colloid for the harvesting, concentration, and identification of additional biomolecules via LC-MS/MS (*Specific Aim 1*). Normal and tumorigenic human thyroid cell lines were cultured and secreted EVs were harvested, isolated and purified. Ultracentrifugation methods were first attempted resulting in inconclusive results in two different occasions. Isolation and purification of harvested EVs was successfully achieved by using ExoQuick-TC kit. Exosome markers and EVs cargo were characterized via LC-MS/MS and RPPA (*Specific Aim 2*). Characterization of the phosphoproteomic profile of both follicular cells and colloid material was conducted via RPPA. Tissue material was lysed, printed on microarrays, probed with selected antibodies, and the spot intensities were compared to quantify the state of protein post-translational modifications, particularly in relation to the autophagy signaling pathway,

taking place within the thyroid follicle for a comparative analysis of PTC, FTA, and non-carcinoma samples (*Specific Aim 3*). DNA lesions/breaks were also investigated in microdissected material of both colloid and follicular cells via RPPA through the expression of DNA damage response protein markers (*Specific Aim 3a*).

MATERIALS AND METHODS

Preparation of Frozen Tissue Sections

Frozen tissue samples were collected under a previously funded, IRB approved project, with patient consent, to procure thyroid tissue (NCI IMAT 1R33CA157403-01) with Inova Health System in Northern VA. Frozen thyroid biopsies (n=20) were embedded in cryopreservation solution (OCT) (Sakura Finetek Corp.) over dry ice and stored at -80 °C until ready to be sectioned. Frozen sections, 8µm thick, were obtained using a cryostat at -20°C or colder. Sections were placed on labeled, uncharged, pre-cleaned glass microscope slides (Fisher), positioning the tissue section near the center of the slide, avoiding the top and bottom thirds of the slide. Glass slides holding frozen sections were stored at -80 °C until ready for further processing.

Laser Capture Microdissection (LCM)

A total of 20 frozen thyroid samples were collected under a previously funded, IRB approved project (NCI IMAT 1R33CA157403-01) with Inova Health System. In order to preserve protein phosphorylation during LCM, tissue sections were first fixed in 70% ethanol (Sigma-Aldrich), then stained with Mayer's hematoxylin solution (Sigma-Aldrich) and Scott's tap water (Fisher Scientific) containing complete protease inhibitors tablets (Roche), followed by an ethanol gradient and xylene (Sigma-Aldrich) dehydration step. LCM was performed to procure colloid material from 8µm thick frozen sections of thyroid tissue. Initially, a PixCell II instrument (Arcturus) was used for microdissection.

However, this instrument relies on manual user control of a joystick to move and guide the stage/microdissection. The variability in microdissection and subsequent inadvertent capture of epithelial cells with the colloid necessitated using an automated LCM instrument with a graphical user interface. Subsequently, an Arcturus^{XT}™ LCM system (ThermoFisher) equipped with both, an IR laser and UV cutting capabilities, was used to microdissect intrafollicular colloid and follicular cells as per manufacturer's recommendations and previously published protocol¹¹⁰. The Arcturus^{XT}™ features imaging software for creating stitched images of the tissue, allowing the user to identify differences in cellular morphology during cell selection more accurately. The Graphical User Interface permits the control of all operations in the system, including stage translation, slide selection, focus and light intensity, laser parameters, objective selection, cap transfers, and camera settings.

Protein Extraction of Microdissected Material for Downstream Analysis

Extraction of proteins from tissue cells procured by LCM must be performed just before the chosen downstream analysis. Protein extraction buffer consisted of 500µl tissue protein extraction reagent (T-PER, Pierce), 475µl Tris-glycine 2x SDS loading buffer (Invitrogen), and 25µl 2-mercaptoethanol (BME, Sigma-Aldrich). LCM caps (Agilent) were thawed at room temperature on a flat-clean surface with film side up. A specific amount (dependent on the number of captured cells/shots) of extraction buffer was directly pipetted on the cap film and incubated for 1 min. The maximum volume of extraction buffer that can be used to cover the surface of an LCM cap is 15 µl, however, a

maximum of 10µl was preferred. Gentle pipetting (up and down motion) of delivered extraction buffer was performed several times, using a circular motion, and being careful not to scrape the polymer on the cap. Extraction buffer containing solubilized cells was collected in a 0.5mL Safe-Lock Eppendorf tube. If more than one LCM cap was used to microdissect the cells of interest, solubilized cells from these caps were pooled into the same eppendorf tube. Lysates were incubated on a heat plate at 100°C for 6 minutes and later stored at -20 °C until ready downstream analysis.

Sample Preparation for Mass Spectrometry Analysis

Microdissected material was lysed with 8M urea (Sigma-Aldrich) (volume depending on the number of cells/shots isolated per sample). Lysates were spun at 16,000 x g for 5 minutes and supernatant (small molecule solution) was then dried in SpeedVac. Dried supernatant was reconstituted in 10µl of MeOH (Sigma-Aldrich) and stored at -20°C until analyzed with MS. Pellet was re-solubilized with 10ul of 8M urea, reduced with 10mM DTT, alkylated with 50mM iodoacetamide, and lastly digested with trypsin (Promega) overnight at 37°C. Digest was stopped with the addition of 1µl TFA. Digest was desalted with Zip-Tip (Millipore), dried in SpeedVac and reconstituted with 10µl of 0.1% formic acid.

Sample Incubation with Nanoparticles

High-affinity dye RB221 (Organic Dyes and Pigments) was covalently bound to hydrogel nanoparticle cages as reported by Tamburro et al.¹¹¹. RB221 nanoparticles were

prepared by Michael Harpole following a standard operating procedure. Briefly, RB221 dye (100mg) was dissolved in 50ml water with 200mg sodium carbonate and shaken on a rotator for 30min. The dye was filtered with a 0.22um membrane and added to 50ml of 10% allylamine (AA) nanoparticles. Excess dye was washed off the nanoparticles by repeatedly washing the particles and spinning the nanoparticle solution in a centrifuge, and discarding the supernatant after each wash until the supernatant was clear. The RB221-AA nanoparticles were verified to bind glycoproteins by performing a western blot with erythrocytes and an antibody to glycosylated hemoglobin. I microdissected additional colloid material and lysed it with 8M urea (volume depending on the number of cells/shots isolated per sample) and diluted 1:10 in PBS. 200µl of RB221 nanoparticles was added to the lysate, incubated at room temperature for 30 minutes under rotation, and centrifuged for 20 minutes at 16.1 x rcf. Supernatant was discarded and pellet was resuspended in 1mL of water. Samples were incubated at room temperature for 5 minutes under rotation and then centrifuged for 20 minutes at 16.1 x rcf. After removing water wash, nanoparticle-pellet was re-suspended in 300µl of elution buffer and incubated for 30 minutes under rotation. Sample was centrifuged for 20 minutes at 16.1 x rcf, elution was recovered and transferred into a new tube. Nanoparticle elution was dried with Nitrogen, followed by the addition of 10uL of 8M urea and then reduced with 10mM DTT, alkylated with 50mM iodoacetamide, and finally digested with trypsin overnight at 37°C. Digestion was stopped with the addition of 1uL TFA and samples were desalted with ZipTip, dried in SpeedVac then reconstituted with 10µl of 0.1% formic acid.

Liquid Chromatography Tandem Mass Spectrometry (LC-MS/MS)

LC-MS/MS experiments were performed on an Orbitrap Fusion (Thermo Fisher Scientific) equipped with a nanospray EASY-nLC 1200 HPLC system (Thermo Fisher Scientific) with the assistance of Dr. Weidong Zhou. Peptides were separated using a reversed-phase PepMap RSLC 75 μm i.d. \times 15 cm long with 2 μm , C18 resin LC column (Thermo Fisher Scientific). The mobile phase consisted of 0.1 % aqueous formic acid (mobile phase A) and 0.1 % formic acid in 80% acetonitrile (mobile phase B). After sample injection, the peptides were eluted by using a linear gradient from 5% to 50 % B over 30 min and ramping to 100 % B for an additional 2 min. The flow rate was set at 300 nL/min as per Dr. Zhou's suggested protocol. The Orbitrap Fusion was operated in a data-dependent mode in which one full MS scan (60,000 resolving power) from 300 Da to 1500 Da using quadrupole isolation, was followed by MS/MS scans in which the most abundant molecular ions were dynamically selected by Top Speed, and fragmented by collision-induced dissociation (CID) using a normalized collision energy of 35%. "Peptide Monoisotopic Precursor Selection" and "Dynamic Exclusion" (8 sec duration), were enabled, as was the charge state dependency so that only peptide precursors with charge states from +2 to +4 were selected and fragmented by CID. Tandem mass spectra were searched against the National Center for Biotechnology Information (NCBI) human database using Proteome Discoverer v 2.1 with SEQUEST using tryptic cleavage constraints. Mass tolerance for precursor ions was 5 ppm, and mass tolerance for

fragment ions was 0.5 Da. Data were analyzed with oxidation (+15.9949 Da) on methionine, iodination (+125.8966) and di-iodination (+251.7932) on tyrosine and histidine as a variable post translation modifications, and carbamidomethyl cysteine (+57.0215) as a fixed modification. A 1 % false discovery rate (FDR) was used as a cut-off value for reporting peptide spectrum matches (PSM) from the database.

Cell Culture

Human thyroid follicular epithelial cell line Nthy-ori3-1 (Sigma-Aldrich) and human thyroid carcinoma CRL-1803 (ATCC) were stored in liquid nitrogen at a temperature of approximately -196°C. For thawing, vials of frozen cells were placed in a warm (37 °C) water bath for 5 minutes and then suspended in 10mL of the appropriate nutrient medium. Cells were centrifuged at 125 x g for 5 minutes and pellets were re-suspended in 2mL of nutrient medium and added to a pre-equilibrated 75 cm² flask (Corning) containing 8mL of nutrient medium.

Nthy-ori3-1 was cultivated in RPMI-1640 (ATCC) medium supplemented with 10% fetal bovine serum (ATCC) and 2mM L-glutamine (Sigma-Aldrich) as per manufacturer's instructions. CRL-1803 was cultivated in F-12K medium (Kaighn's modification of Ham's F-12) with L-Glutamine (ATCC) as per manufacturer's instructions. Nthy-ori3-1 cells were passaged by 1:4 split every 4 days. CRL-1803 were slow growing and were therefore transferred to 25 cm² flasks instead and only passaged once by 1:2 split. For each passage, media was removed from flask, cells rinsed using 2mL of PBS, and trypsinized by adding 3mL of 0.25% w/v of Trypsin (ATCC) and

incubated for 6 minutes at 37°C and 5% CO₂. Upon detachment, cells were washed with their nutrient medium, transferred into a centrifuge tube and pelleted at 125 x g for 5 minutes. Pellet was then re-suspended in a 2mL of appropriate nutrient medium and finally transferred to a flask containing 8mL of pre-equilibrated nutrient medium.

Isolation of extracellular vesicles

In my first attempt to isolate EVs, I followed Dr. Ramin Hakami's protocol used in his laboratory to isolate exosomes from bacterial cell cultures. Briefly, exosome free nutrient medium was supplemented as above except FBS was ultra-centrifuged at $100,000 \times g$ for 70 min to remove bovine exosomes. Collected supernatants were centrifuged at 2,000 rpm for 10 min at 4°C to eliminate dead cells. Supernatants were then filtered through 0.22 µm filters to remove most apoptotic bodies, but allow exosomes to pass through the filter. The filtrate was then processed through a series of ultracentrifugation steps. In the first step, filtrate was ultracentrifuged at $10,000 \times g$ for 30 min at 4°C. Supernatants were transferred to clean ultracentrifuge tubes and ultracentrifuged again at $100,000 \times g$ for 70 min at 4°C. Supernatants were removed and EVs pellets were resuspended in PBS without calcium and magnesium and ultracentrifuged again at $100,000 \times g$ for 70 min at 4°C. Pellets were resuspended in 50–100 µl of sterile PBS without calcium and magnesium. These semi-purified EVs were stored at 4°C until ready for downstream analysis. The protein concentrations of EVs preparations were determined by running Bradford assay on EVs lysates. Unfortunately, after three attempts at isolating exosomes from both thyroid cell lines following the

above protocol, the protein concentrations of “crude” EVs was too low to read by Bradford assay. Therefore, I decided to take a different approach for the isolation of thyroid EVs.

ExoQuick-TC® ULTRA EV (System Biosciences) isolation kit for tissue culture media was used according to manufacturer’s instructions. Briefly, exosome free nutrient medium was supplemented as above except we used Exo-FBS™ exosome-depleted FBS (System Biosciences). Collected supernatants were centrifuged at 1500 x g for 10 minutes to pellet dead cells and cell debris. Supernatant was transferred to a new collection tube and 2mL of ExoQuick-TC per 10mL of supernatant was added and mixed well by inverting the tube 5 times. ExoQuick-TC mixture was incubated on ice overnight at 4°C and then centrifuged at 3000 x g for 10 minutes at room temperature. Extracellular vesicles (EVs) appeared as a small beige pellet at the bottom of the tube. The supernatant was removed and the tube was pin down one more time to remove any residual solution. EVs pellet was resuspended in 100µl of buffer B and protein concentration measured by Bradford assay. For purification of isolated EVs, we added 200µl of buffer A to each sample and added to a preconditioned purification column loaded with 100µl of buffer B. Column was incubated at room temperature on a rotating shaker for 10 minutes. Sample was eluted and immediately transferred to a 2mL tube for centrifugation at 1000 x g for 30 seconds to obtain purified EVs.

Reverse Phase Protein Arrays (RPPA)

The microdissected material was lysed with a SDS-TPER-BME extraction buffer, lysates were incubated on a heat plate at 100°C for 6 minutes and stored at -20°C until ready to print on arrays. RPPAs were printed, stained, and analyzed as previously published protocol¹¹². Briefly, thyroid samples were printed in triplicate spots on nitrocellulose-coated glass slides (Oncyte Avid, GRACE Bio-Labs) using an Aushon 2470 arrayer (Aushon Biosystems) equipped with 185 µm pins as per manufacturer's instructions. Reference standards were printed in 10-point dilution curves as procedural calibrators and as positive controls for antibody staining. Each reference standard curve was printed in triplicate at concentrations of 0.125 µg/µl total protein. For estimation of total protein amounts, selected arrays were stained with Sypro Ruby Protein Blot Stain (Invitrogen) according to the manufacturer's instructions and imaged on a Power-scanner fluorescent scanner (Tecan US, Inc.). In preparation for antibody staining, printed arrays were treated with 1× ReBlot Mild Solution (Chemicon) for 15 minutes followed by two 5 minutes PBS (Invitrogen) washes with constant rocking. Arrays were the incubated in blocking solution (1g I-block (Applied Biosystems), 0.5% Tween-20 in 500 mL of PBS for at least 1 hour with constant rocking. Immunostaining was performed on an automated slide stainer (DakoCytomation) using the Catalyzed Signal Amplification System kit according to the manufacturer's recommendation (CSA; Dako). The arrays were probed with 52 antibodies (one antibody per array) against total or phosphoprotein endpoints (Table3). Primary antibody binding was detected using a biotinylated goat anti-rabbit immunoglobulin G (IgG) H+L (1:7500; Vector Laboratories) or rabbit anti-

mouse IgG (1:10; DAKO) followed by streptavidin-conjugated IRDye680 fluorophore (LI-COR Biosciences). All antibodies used were subjected to extensive specificity validation by western blot for a single band at the appropriate molecular weight as well as phosphorylation specificity through the use of cell lysate controls. For normalization of RPPA arrays, the staining of selected arrays with SyproRuby blot stain for total protein and a negative control slide (incubated only with a secondary antibody) was used in each run to account for background noise are required.

RPPA spot intensity was analyzed with MicroVigene v4.0 (VigeneTech), in which spots were detected, local background was subtracted, negative control was subtracted, replicates were averaged, and each spot was normalized to total protein, producing a single value for each sample.

Statistical Analysis

Statistical analyses were performed using the data analysis software system R v3.5.1. To compare findings between groups parametric and non-parametric univariate tests were used (Student's t-test, Wilcoxon rank-sum test). The two-sample t-test was used to compare the means of two independent populations while assuming that the two populations are normally distributed and have the same variance. The Wilcoxon test, on the other hand, is the non-parametric analog of the two-sample t-test used to compare the means between two independent populations without the assumption of normally distributed data. Cluster mapping of thyroid data was conducted using the Ward method

for 2-way unsupervised hierarchical clustering using JMP v14 (SAS Institute). GraphPad Prism v7.05 (GraphPad Software) was used to generate graphs.

AIM OF STUDY I

**Investigation of the Proteomic Machinery of Thyroid Colloid by Mass
Spectrometry**

Specific Aim 1. Investigate the proteomic machinery of thyroid colloid by mass spectrometry.

Advances in proteomic analysis are now able to provide a comprehensive picture of changes taking place in both, protein expression and post-translational modifications (PTMs) in cells^{113,114}. Liquid chromatography-coupled tandem mass spectrometry (LC-MS/MS) is routinely used for large-scale protein identification and global profiling of PTMs in complex biological mixtures. Therefore, several attempts have been made to identify diagnostic markers for thyroid lesions by using biochemical, immunohistochemical or genetic markers^{115,116}. Proteomic techniques are increasingly used in the search for diagnostic and prognostic markers in cancer with the purpose of distinguishing benign and malignant thyroid tumors. These techniques can similarly be applied for the identification and characterization of colloid proteinaceous components.

Thyroid colloid has been characterized mainly by the presence of thyroglobulin, a high abundance protein produced by the follicular cells that functions as a matrix for the synthesis and storage of T₄ and T₃. We propose that the colloid fluid space is much more than a simple repository of thyroid hormones and may likely contain several undiscovered small protein molecules and protein fragments generated within the thyroid follicle that could play a key role in tumor survival and even metastasis.

In order to investigate the proteomic composition of colloid, laser capture microdissection was used to procure pure intrafollicular colloid from frozen thyroid

biopsies. A LC-MS/MS-based approach was used to perform an initial global proteomic analysis of PTC, FTA, and non-carcinoma samples. Early thyroid studies were primarily based on analysis of the entire tissue biopsy. LCM provides the unique ability in this study to procure individual cell populations within the context of the microenvironment that may reveal distinctive information useful in the identification and classification of thyroid disease.

Furthermore, LC-MS/MS analysis was coupled with a core-shell nanoparticle capture technique in order to identify additional low-weight and low-abundant proteins, not previously described in thyroid colloid. MS-based proteomic technologies generally have a limited range of detection and may not be as sensitive at avoid abundant proteins potentially masking detection of low abundant and scarcer proteins/peptides¹¹¹. Thus, depletion of high abundant proteins is often necessary before analysis. A new class of chemical affinity bait, a copper complex reactive dye, Reactive Blue 221 {RB221; cuprate(4-),[2-[[[3-[[4-chloro-6-[ethyl[4-[[2-(sulfooxy)ethyl]sulfonyl]phenyl]amino]-1,3,5-triazin-2-yl]amino]-2-hydroxy-5-sulfophenyl]azo]phenylmethyl]azo]-4-sulfobenzoato(6-)]-, tetrahydrogen} has been previously utilized to harvest low abundance glycolipids with high efficiency while simultaneously dissociating interfering substances in solution that mask their presence¹¹⁷. RB221 dye was selected because copper moieties are known to preferentially interact with glycans. In this study, RB221 core-shell nanoparticles, were tested on microdissected colloid for the harvesting, concentrating, and identifying additional low abundance biomolecules.

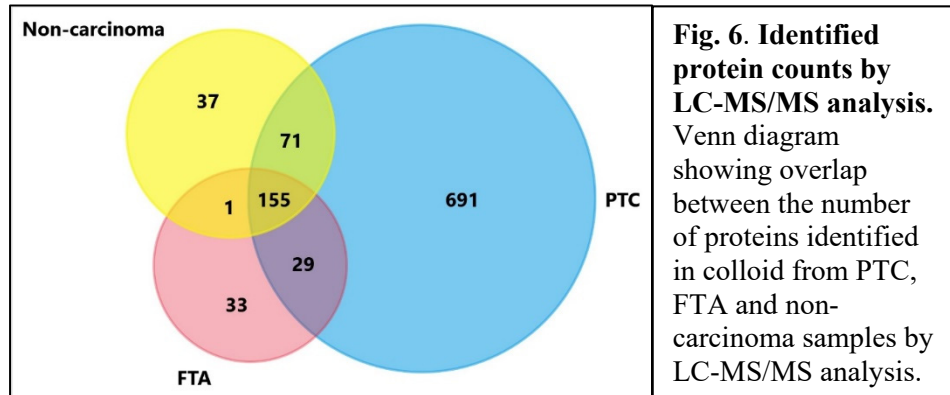
RESULTS

Protein profiling of colloid samples

Colloid microdissected from thyroid samples were analyzed by LC-MS/MS for protein identification and spectral counting to determine qualitative protein differential abundances between thyroid disorders. LC-MS/MS results using eight independent samples from PTC (n=3), FTA (n=3), and non-carcinoma (n=2) samples detected peptides from a total of 1,017 NCBI annotated proteins collectively. PTC group produced the largest amount of identifiable proteins and out of 1,017 proteins 155 shared proteins were found present at least twice in their respective group with spectral count of at least 1 unique peptide (Fig. 6). Non-carcinoma and PTC groups had 71 unique proteins in common, while non-carcinoma and FTA only had 1 unique protein in common. Additionally, 29 unique proteins were shared by both PTC and FTA groups. As expected in thyroid colloid, the most abundant protein across all samples was the large glycoprotein thyroglobulin, followed by albumin.

Relative differences were calculated as $[(\text{number of PTC or FTA spectra} - \text{number of non-carcinoma spectra}) / (\text{average number of spectra for PTC or FTA and non-carcinoma}) \times 100]^{118}$. Spectral count comparisons from non-carcinoma and PTC revealed 18 proteins with at least 120% relative difference (Table 2). Proteins related to processing and transport of secreted proteins into the extracellular space showed higher abundance in PTC samples when compared to non-carcinoma samples. Whereas proteins involved in cell motility activity were found in lower abundance in PTC samples. Interestingly, cytokeratin-19 (CK 19) was detected in all PTC samples and showed higher

abundance in comparison to non-carcinoma samples. CK 19 has recently being considered as a possible biomarker to differentiate between benign and malignant thyroid lesions along with galectin-3 and Hector Battifora Mesothelial-1 (HBME-1)^{66,67}. Galectin-3 was also identified in PTC samples but showed little difference when compared to non-carcinoma samples. Several cytokeratins have been suggested to have a role in cell biology beyond that of structural cytoskeletal proteins¹¹⁹. Elevated CK 8 protein expression, for instance, is an established diagnostic cancer biomarker in several epithelial cancers, including anaplastic thyroid carcinoma (ATC). It has also been shown to bind to annexin A2, a protein known to mediate apoptosis as well as the redox pathway¹¹⁹. On the other hand, trefoil factor 3 (TFF3) was only detected in non-carcinoma samples. TFF3 expression levels have been reported to decrease in FTC and PTC tumors with high risk of invasion or metastasis^{120,121}.



While comparing non-carcinoma and FTA groups, we observed 10 proteins with at least 120% relative difference (Table 3). Top differential proteins belonged to the cytokeratin family, which are able to form highly dynamic intermediate filament

structures that get reorganized during apoptosis. This reorganization can be mediated by post-translational modifications or interaction with proteins such as 14-3-3.

Cytokeratins in FTA samples displayed a higher relative abundance when compared to non-carcinoma samples. On the other hand, proteins involved in positive regulation of apoptotic cell removal and cell motility showed a decrease in abundance.

Gene ontology analysis

A global gene ontology (GO) analyses was performed to obtain a general overview of functional classes within the identified proteins that overlapped all three groups using the Database for Annotation, Visualization and Integrated Discovery (DAVID v6.8). Figure 7 shows representative categories of the most significantly enriched GO terms; within the molecular function (GO: MF) category, the top terms were related to chromatin-related maintenance, nucleosome activity and cytoskeletal organization. In the cellular component (GO: CC) category, the top terms were linked to extracellular exosome, nucleus, cytoplasm, and extracellular space; inferring the involvement of exosomes in colloid. The biological process (GO:BP) category highlighted protein heterodimerization activity, DNA binding, and structural integrity processes. Overall similar results were obtained while considering GO analysis for each thyroid group individually. However, an interesting observation designated “negative regulation of apoptotic process” as one of the selective significant terms found in the biological process (GO: BP) category in PTC samples, which may suggest a connection to lysosome formation and autophagy as an alternative to apoptosis activity.

Table 2. Colloid proteins common between non-carcinoma and PTC samples ranked according to their relative difference based on averaged spectral hits.

Accession	Protein	Non-carcinoma	PTC	Relative Difference	Status
27436946	lamin isoform A	1	13	171%	↑
383792150	lamin isoform D	1	9	160%	↑
4507677	endoplasmin precursor	2	14	150%	↑
41582239	immunoglobulin superfamily containing leucine-rich repeat protein precursor	1	6	143%	↑
372466572	keratin, type II cytoskeletal 8 isoform 1	1	6	143%	↑
16507237	78 kDa glucose-regulated protein precursor	2	10	133%	↑
118582275	extracellular superoxide dismutase [Cu-Zn] precursor	1	5	133%	↑
4557888	keratin, type I cytoskeletal 18	1	5	133%	↑
10863927	peptidyl-prolyl cis-trans isomerase A isoform	1	5	133%	↑
5174735	tubulin beta-4B chain	1	5	133%	↑
4502107	annexin A5	1	5	133%	↑
67782365	keratin, type II cytoskeletal 7	1	5	133%	↑
629266065	basement membrane-specific heparan sulfate proteoglycan core protein isoform a precursor	1	4	120%	↑
126012571	basement membrane-specific heparan sulfate proteoglycan core protein isoform b precursor	1	4	120%	↑
24234699	keratin, type I cytoskeletal 19	1	4	120%	↑
574584803	tubulin beta-4A chain isoform 1	1	4	120%	↑
4501881	actin, alpha skeletal muscle	4	1	-120%	↓
4501889	actin, gamma-enteric smooth muscle isoform 1 precursor	4	1	-120%	↓

Table 3. Colloid proteins common between non-carcinoma and FTA samples ranked according to their relative difference based on averaged spectral hits.

Accession	Protein	Non-carcinoma	FTA	Relative Difference	Status
5031839	keratin, type II cytoskeletal 6A	1	12	166.7%	↑
24430192	keratin, type I cytoskeletal 16	1	8	163.6%	↑
195972866	keratin, type I cytoskeletal 10	2	9	127%	↑
55956899	keratin, type I cytoskeletal 9	3	13	120%	↑
4501881	actin, alpha skeletal muscle	4	1	-120%	↓
4501889	actin, gamma-enteric smooth muscle isoform 1 precursor	4	1	-125%	↓
578818565	PREDICTED: vimentin isoform X1	9	2	-127%	↓
67190748	complement C4-A isoform 1 preproprotein	10	1	-155.6%	↓
356582273	complement C4-A isoform 2 preproprotein	10	1	-169%	↓
178557739	complement C4-B preproprotein	11	1	-164%	↓

The Kyoto encyclopedia of genes and genomes (KEGG) pathway analysis

KEGG pathway analysis was performed on the identified colloid proteins to evaluate which pathways were significantly represented in PTC, FTA, and non-carcinoma samples respectively. These results showed that PTC proteins were involved in processes such as phagosome (19 proteins), PI3K-Akt signaling pathway (19 proteins), viral carcinogenesis (24 proteins), gap junction (16 proteins), pathogenic *Escherichia coli* infection (20 proteins), glycolysis / gluconeogenesis (9 proteins), protein digestion and absorption (8 proteins), thyroid hormone synthesis (7 proteins), and estrogen signaling pathway (7 proteins) among others. PTC samples exhibited the most protein-pathway diversity along with a larger number of proteins.

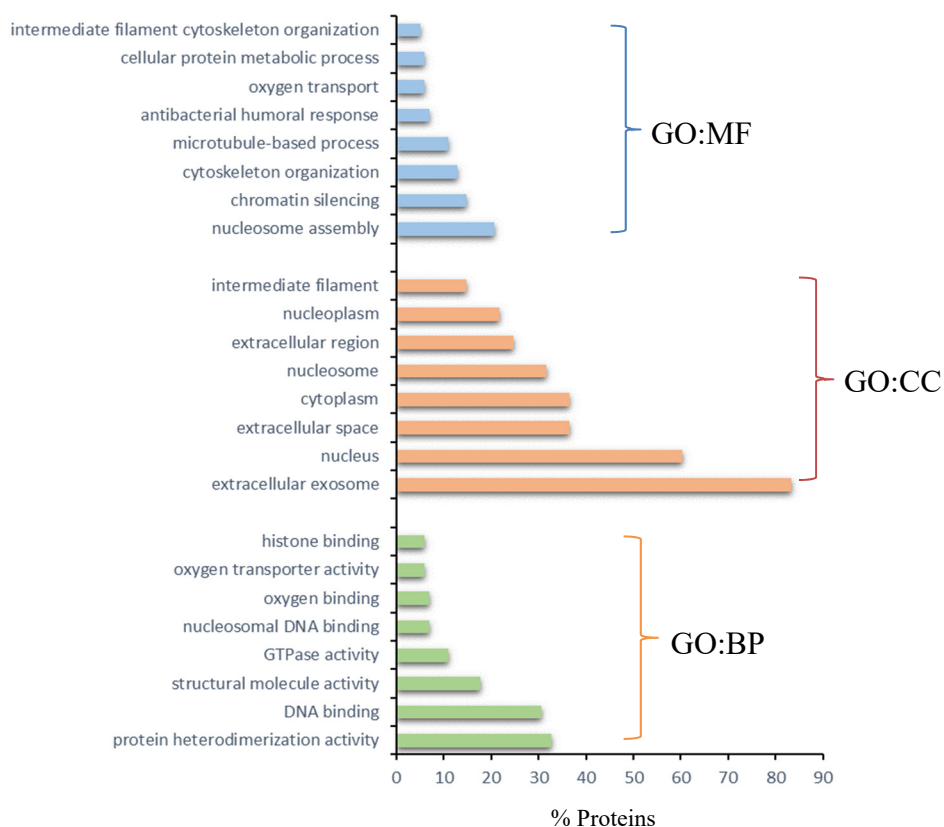


Fig.7. Significantly enriched GO terms identified in the shared proteome of PTC, FTA, and non-carcinoma colloid samples. Gene ontology (GO) search within the molecular function (MF) chromatin-related maintenance including nucleosome activity. Extracellular exosome was identified as the top cellular component (CC.) Protein heterodimerization activity and DNA binding were recognized as the primary drivers of biological processes (BP).

FTA proteins revealed processes involving phagosome (14 proteins), viral carcinogenesis (15 proteins), pathogenic *Escherichia coli* infection (14 proteins), gap junction (12 proteins), focal adhesion (7 proteins), ECM-receptor interaction (6 proteins), and thyroid hormone synthesis (4 proteins). Non-carcinoma proteins showed similar pathway involvement with PTC samples including phagosome (13 proteins), PI3K-Akt signaling pathways (10 proteins), viral carcinogenesis (21 proteins), gap junction (11 proteins), pathogenic *Escherichia coli* infection (14 proteins), and thyroid hormone

synthesis (5 proteins); additionally, Hippo signaling pathway (8 proteins), cell cycle (7 proteins), protein processing in endoplasmic reticulum (7 proteins) were identified as part of the active pathways in non-carcinoma samples.

This analysis implicates colloid proteins in the regulation of numerous diverse biological functions not just exclusively to thyroid hormone synthesis as previously speculated. It is interesting to note that some of the proteins found in all thyroid samples are also associated with pathways of viral origin and transmission of pathogens. Although literature searches could biologically justify our findings, functional studies are required to better understand the specific role of the identified proteins and to offer new insights on thyroid cancer pathogenesis.

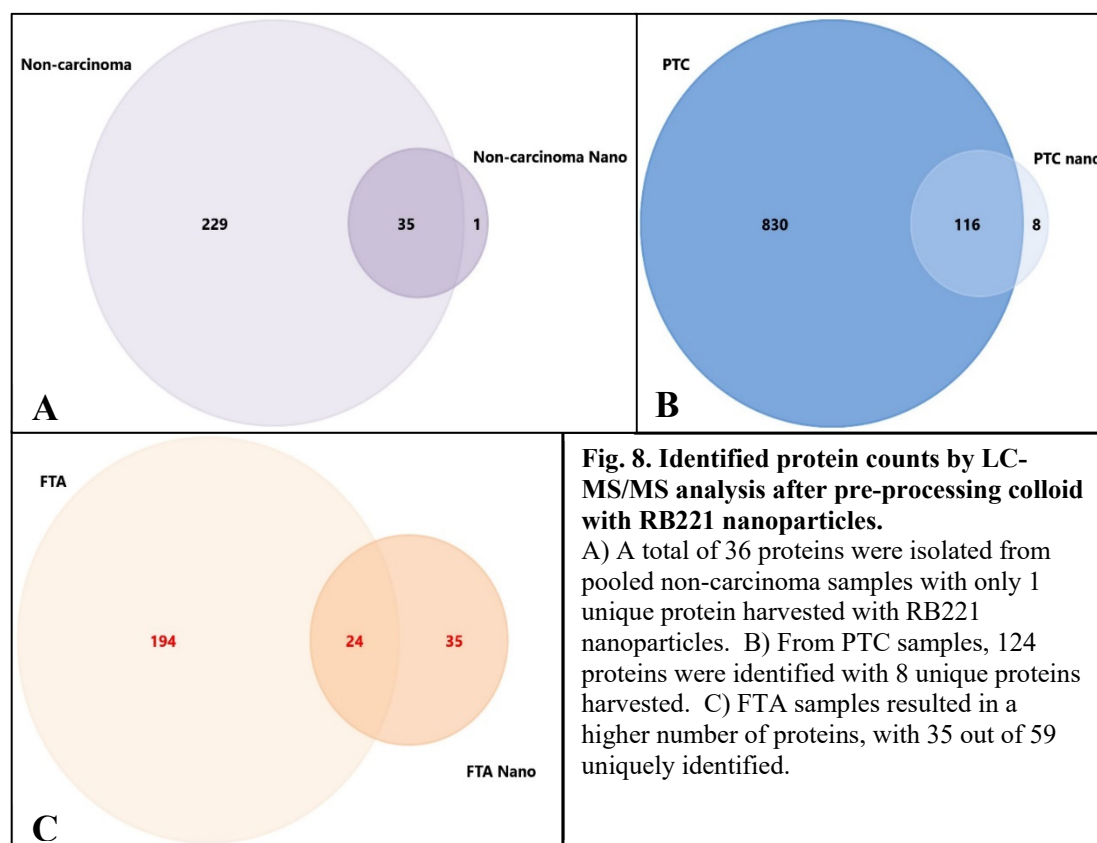
RB221 nanoparticles effectively concentrate and harvest thyroid colloid proteins

The potential of RB221 nanoparticles as a method of colloid pre-processing for harvesting low molecular and low abundance proteins was developed and evaluated. Additional thyroid colloid was microdissected from the same set of eight frozen biopsies used for the previous LC-MS/MS analysis. Colloid samples were processed according to the protocols described in the Materials and Methods section for incubation with nanoparticles and identification of proteins via LC-MS/MS. Peptides for a total of 219 NCBI annotated proteins were detected in non-carcinoma, FTA, and PTC samples collectively. Pooled non-carcinoma samples resulted in a total of 36 proteins; 35 of these proteins were commonly identified in the first study with only 1 unique protein harvested when compared with the initial results (Fig. 8). A total of 124 proteins were identified

from PTC samples, 116 of these proteins had been previously detected but only 8 exclusive proteins were captured by RB221 nanoparticles mainly from the cytokeratin family origin CK 13, CK 24, and CK 28. Surprisingly, FTA samples had the largest number of unique proteins identified with 35 distinctive proteins out of a total of 59 captured by the nanoparticles including interleukin 11 receptor alpha (IL11R α), zinc finger protein 846, protein S100A9, growth regulator estrogen receptor binding 1 (GREB-1), selenocysteine insertion sequence-binding protein 2 (SECISBP2), hepatic and glial cell adhesion molecule (HepaCAM) family member 2, and CK 4, 13, 15, 24, 25, 26, 27, 28. Expression of IL11 and its co-receptor IL11R α , which is required for signal transduction, have been correlated with invasion and proliferation in breast, gastric, and colorectal cancers, suggesting that IL11 and IL11R α are important factors in cancer progression¹²². Cytokeratins, on the other hand, are cytoskeletal intermediate filaments often used as important markers of tissue differentiation via immunohistochemistry for cancer classification^{123,124}. Abnormal expression of CK 4 and CK 13 specifically has been reported to indicate dysregulation of epithelial differentiation in oral squamous cell carcinoma and associated up-regulation of other cytokeratins may be one of the contributing factors for morphological alterations in affected epithelium¹²⁵. RB221 nanoparticles appear to have a high affinity for capturing low abundant cytokeratin proteins present in FTA colloid, which grants further research into their role in thyroid carcinogenesis beyond that of structural cytoskeletal proteins.

Interestingly, S100A9 a member of the S100 calcium-binding protein family was also captured by RB221 nanoparticles in FTA colloid. S100A8/A9 protein complex has been shown to be released from activated phagocytes increasing Beclin-1 expression and interaction with Bcl2 in MCF7 cells, thus resulting in autophagy and lysosomal activation

126.



Even though nanoparticles are used to improve sensitivity of LC-MS/MS analysis, finding the optimal dye with a high protein-binding affinity is essential for the successful isolation and identification of low abundance proteins in a given sample. In

this study, additional low molecular weight glycoproteins were targeted with RB221 nanoparticles. Screening samples with nanoparticles of different organic chemistries to recognize bait selectivity for specific proteins or classes of proteins prior to this colloid study would have been pursued if adequate quantities of thyroid tissue had been available.

DISCUSSION

The thyroid colloid was investigated in this study and as hypothesized, in addition to thyroglobulin, several other small protein molecules were identified by LC-MS/MS in PTC, FTA, and non-carcinoma samples. This first broad, LCM-based proteomics analysis of colloid from PTC, FTA, and non-carcinoma samples provides an original proteome characterization of this physiologically unique thyroid follicle component. Thyroid colloid is generally recognized by the site for thyroid hormone synthesis, however, this study portrays colloid as a fluid space of much greater diversity and a rich source of proteins.

PTC samples exhibited the most protein-pathway diversity, analysis of these samples revealed proteins involved in processing and transport of secreted proteins into the extracellular space and phagosome formation, suggesting the occurrence of extracellular vesicles and/or exosomes. Normally, iodinated thyroglobulin is stored as colloid in the follicular lumen upon thyroid hormone demand. It is then processed by lysosome peptidases to release iodide that can be recycled for the following round of

thyroid hormone synthesis. Furthermore, the lower molecular weight proteome identified in this study may also encompass many clinically important markers released in the colloid resulting in signaling communication between neoplastic cells and tumor microenvironment mediated by microvesicles or exosomes that could also reflect early-stage pathophysiological changes in thyroid tissue. These proteins will need to be investigated further and validated in a larger cohort.

β -tubulins belong to the core protein families that heterodimerize to form α/β -tubulin dimers, which assemble into microtubules, one of the essential cytoskeletal structures¹²⁷. β 4-tubulin protein levels were found higher in PTC samples when compared to non-carcinoma; β -tubulin expression has previously been reported in the cytoplasm of thyroglobulin producing thyrocytes but not in thyroid colloid¹²⁸. Fluctuations in the levels of this protein certainly alters microtubule properties necessary for adequate thyroid development and function. Normal thyroid cell proliferation and thyroid migration are essential to thyroid gland development, therefore thyroid hormone secretion requires β -tubulins incorporation into the microtubules, suggesting a specific function of β -tubulins isotypes in intracellular transport of vesicles¹²⁸.

Additionally, several type I and type II cytokeratins were also identified in the PTC, FTA, and non-carcinoma groups. Cytokeratins are epithelial cytoskeletal proteins whose expression pattern differs between epithelial tissues and their developmental stages but is maintained when a malignant transformation occurs making them useful in tumor differentiation¹²⁹. Both CK 8 and CK 18 showed upregulated differential spectral counts in PTC samples. These cytokeratins are intermediate filament phospho-

glycoproteins of simple-type epithelia that have been reported to protect hepatocytes from apoptosis and their mutations predispose to liver disease¹³⁰. Elevated CK 8 protein expression is an established diagnostic cancer biomarker in several epithelial cancers, including anaplastic thyroid carcinoma. On the other hand, CK 18 glycosylation appears to serve as a cytoprotective and anti-apoptosis buffer during cellular stress and links glycosylation of the keratin cytoskeleton to activation of cell survival kinases¹³⁰. In lung cancer, for example, profiles of CK 5/6, CK 7, CK 10/13, CK 14, CK 17, and CK 18 enable discrimination between squamous cell carcinoma and adenocarcinoma of the lung¹²³. Furthermore, cytokeratins can provide prognostic information and even enable therapy monitoring. Upon release from proliferating or apoptotic cells, cytokeratins provide useful markers for epithelial malignancies, distinctly reflecting ongoing cell activity. In this study, CK 19 protein was found upregulated in PTC samples, supporting its consideration as a possible biomarker to differentiate between benign and malignant thyroid lesions. The combination of CK 19 and CK 8 high expression levels may postulate a role for cytokeratins in predicting high degree of malignancy in thyroid lesions. Several cytokeratins have been suggested to have a role in cell biology beyond that of structural cytoskeletal proteins¹¹⁹. Overall, cytokeratins serve several diverse functions that include cytoprotection from cell stress and apoptosis, regulation of epithelial polarity and protein targeting to subcellular compartments and regulation of translation^{130,131}.

Hydrogel nanoparticles, harvest and trap low molecular weight proteins, and protein fragments from biological fluids. The proteins captured are protected from

degradation and stabilized inside the particles. Colloid preprocessing with hydrogel nanoparticles permitted the identification of low abundance proteins in FTA samples, never identified by LC-MS/MS before and/or never measured in colloid. These promising results suggest that multifunctional hydrogel nanoparticles can be further investigated for the discovery of novel biomarkers of disease in thyroid colloid. In this study, we applied RB221 nanoparticles to analyze a small cohort of PTC, FTA, and non-carcinoma colloid samples. Unique protein profiles were observed for each analyzed sample, which included low abundance proteins such as cytokeratins, IL 11R α growth factors, receptors, enzymes, and both structural and nuclear proteins.

Interleukins and cytokines play an important role in the pathogenesis of several cancers. IL 11 belongs to the IL 6 cytokine family and mediates its function via the IL11R α . On ligand binding to IL11R α , the glycoprotein 130 subunit, critical for signal transduction of IL11, is recruited to form an IL11/IL11R α /GP130 complex activating signal transduction pathways to modulate target gene expression¹²². Expression of IL11 and its co-receptor IL11R α are correlated with invasion and proliferation in breast, gastric, and colorectal cancers, suggesting that IL11 and IL11R α are important factors in thyroid cancer progression. Recent studies have shown that IL11/IL11R α binding and downstream signaling via STAT3 activation may be a leading molecular pathway in metastasis¹³². This global-LC-MS/MS analysis revealed weak/low abundance for only a few CKs, indicating that CK levels are low among the total protein colloid content. Validation and further investigation to understand the biological

meaning and clinical value of the identified proteins is needed with careful consideration of potentially contaminating structural and stratified epithelial CKs.

Of special interest is the detection of S100A9, a member of the S100 calcium-binding protein family, sequestered by the nanoparticles in FTA colloid. S100 proteins are small (10–12 kDa) acidic proteins with high-affinity for Ca^{2+} ¹³³. Alterations of the expression levels of S100 proteins have been reported to be associated with tumors and their malignancy. S100A4 was found to be associated with poor survival rates in breast cancer and expressed in PTC and ATC, including colorectal, esophagus and gall bladder cancer¹³³. The S100A8/A9 heterodimers are the best characterized S100 family members with respect to extracellular functions. Moreover, S100A8/A9 protein complex has been associated with autophagy and lysosomal activation¹²⁶.

External signals are constantly taken in by the follicular cells through specific receptors and translated in modification of intracellular pathways, including autophagy, growth and differentiation, transcription, and cytoskeletal organization, that determine the activation of the required cellular function in the thyroid gland. Therefore, it is only reasonable to assess colloid, a major component of thyroid follicles, as an active participant and contributor of cancer survival and proliferation. In this initial global proteomic analysis, we have detected and identified several proteins in the colloid of PTC, FTA, and non-carcinoma samples that, to our knowledge, either had not yet been associated with thyroid tissue nor previously identified in colloid. One of the main limitations of our study lies in the small sample number, though this was unavoidable due to the relatively low prevalence of thyroid surgeries performed at INOVA hospital during

the allowed collection period, the wealth of information provided by the analyzed samples provides a solid foundation to validate our findings in a larger study set. Further investigation is also needed to understand the biological meaning and clinical value of the newly identified proteins in the thyroid colloid.

In conclusion, we have demonstrated that the proteomic composition of colloid comprises several proteins involved in the regulation of numerous diverse biological functions not just exclusively to thyroid hormone synthesis as previously speculated. This is the first study to identify and quantify exosomes and/or microvesicle-related proteins in the thyroid colloid. Bi-directional exocytosis of exosomes and microvesicles into the blood and colloid is a novel concept with implications for signal transduction in thyroid disease. EVs cargo consisting of total and phospho-proteins were identified in the thyroid colloid. In addition, the preprocessing of colloid with RB221 nanoparticles revealed the presence of unique proteins in FTA samples that were not initially detected in the LC-MS/MS analysis, which can be further explored as a method for early detection of prognostic biomarkers of disease progression. Our results supported our hypothesis that the colloid fluid space is much more than a simple repository of thyroid hormones and it does indeed contain several undiscovered low abundance proteins generated within the thyroid follicle that are currently known to be involved in tumor survival and metastasis.

AIM OF STUDY II

**Protein Identification from Extracellular Vesicles Secreted
by Thyroid cells**

Specific Aim 2. Identify extracellular vesicles-related proteins secreted by thyroid cells.

Exosomes are part of an alternative mechanism for protein export and intercellular communication via transport and release of proteins, lipids, and nucleic acids¹³⁴. These nano-molecules (30–100 nm) are secreted from most cell types and its production has been observed in a variety of cell types *in vitro*. In relation to cancer, there is evidence that exosomes play a role in carcinogenesis by influencing several processes including angiogenesis, metastasis, anchorage-independent growth, immune system evasion and proliferation^{135,136}. Thus, EVs/exosomes in thyroid colloid could potentially serve as rich reservoirs of tumor-specific proteins capable of acting as functional biomarkers for disease detection and progression.

The protein composition of *in vitro* produced exosomes has been studied using a variety of techniques, including western blotting, flow cytometry of exosomes-coated beads, and mass spectrometry¹³⁷. These techniques have helped demonstrate that exosomes from different cellular origins share common groups of proteins^{136–141}. These groups are proteins actively participating in antigen binding and presentation (heat-shock proteins), proteins involved in intracellular membrane fusion and transport (annexins and rab proteins), proteins involved in targeting and cell adhesion (tetraspanins and integrin proteins), cytoskeletal proteins (actin and tubulin) and metabolic enzymes^{136–141}. These previous studies suggest that exosomes express a limited set of proteins and can be used as antigen sources in cancer treatments.

We have learned that thyroid colloid is indeed comprised of several proteins, peptides and likely EVs involved in anabolic and catabolic activities regulated by the thyroid epithelium. We hypothesize that EVs transport of iodinated molecules may contribute to autophagy induction during thyroid carcinogenesis. Levels of iodine intake are highly correlated with thyroid diseases, such as goiter and nodularity, hyperthyroidism, hypothyroidism, and thyroid cancer. Autophagy activation/deactivation within the thyroid epithelium may influence the composition of the colloid. The paucity of colloid in thyroid cancer may be due to up-regulation of autophagy, which depletes essential proteins from the colloid, thereby creating a constant state of epithelial cell stress, thus contributing to tumor cell proliferation. In order to investigate the differences between tumor-derived EVs and normal-cell EVs, researchers often characterize the proteome of tumor exosomes. Exosomes are representative of the cell from which they were derived, therefore, it is reasonable to assume that proteome signatures would exhibit unique qualities dependent on the cellular origin.

Microvesicles have been isolated and characterized from distinct cells under normal and stressed conditions. At present, the most commonly used methods for EV isolation include ultracentrifugation combined with a sucrose gradient for purification. This methodology was initially adapted earlier in this study to isolate and purify secreted EVs from normal and cancer thyroid cell lines prior to MS analysis. MS proteomic analysis revealed the presence of 16 distinctive proteins including histones and proteins involved in cell adhesion, protein transport, cell structure, and signal transduction (Table 2). Presence of EVs was confirmed only by RPPA positive staining (not MS) of CD9 in

lysates made from cell culture medium of normal thyroid cells. Information provided in this pilot study, demonstrated that a detailed molecular portrait of thyroid colloid is achievable with the use of mass spectrometry. Moreover, molecular differences are identifiable by RPPA within follicular cells of different thyroid disorders and proteome characterization of secreted thyroid EVs can be analyzed by LC-MS/MS and further validated by RPPA. As part of our continuing investigation, we repeated this study with a different methodology and larger number of thyroid cells to increase the yield of isolated EVs for LC-MS/MS analysis and confirmation of related protein markers by RPPA to enhance specificity and allow for a more complete proteomic analysis of diseased thyroid tissue. Therefore, the objective of this study was to determine if EVs are secreted by normal and tumorigenic human thyroid cell lines and to analyze their protein composition.

RESULTS

Extracellular vesicles are abundantly secreted by thyroid cell lines

Nthy-ori3-1 (normal) and CRL-1803 (carcinoma) human thyroid cell lines were cultured in triplicates and secreted EVs were harvested, isolated, and purified using ExoQuick-TC® ULTRA EV (System Biosciences) isolation kit for tissue culture media as per manufacturer's instructions. In recent years, the use of ExoQuick kit for the successful isolation of exosomes has increased, especially in the infectious disease area^{142–144}. Exosome markers and exosome cargo were characterized via LC-MS/MS (see Materials and Methods section). Mass spectrometry analysis of cell culture conditioned media from Nthy-ori3-1 and CRL-1803 detected peptides from a total of 1,537 NCBI categorized proteins collectively. Of the 1,537 total proteins found, 1,312 proteins were present at least twice in their respective cell line with spectral count of at least 1 unique peptide. The majority of currently accepted exosome markers were also found in common among all analyzed proteomics data and included membrane surface markers of the tetraspanin family (CD9, CD81), annexin-2 (ANXA2) and heat shock proteins (Hsp70 and Hsp90)^{145–147}. This evidence suggests that proteins found in thyroid EVs preparations are relatively abundant.

Proteins involved in exosome biogenesis

Several additional proteins were identified when compared to the most abundant EVs cargo proteins listed in ExoCarta, an exosome database (<http://exocarta.org/>),

developed to identify exosomal contents. (Table 4). Nthy-ori3-1 cells yielded a larger number of identifiable exosomes in ExoCarta compared to CRL-1803 cells. These results categorized beta actin (ACTB), gamma actin 1 (ACTG1), alpha actinin 4 (ACTN4), albumin (ALB), fructose-bisphosphate A aldolase (ALDOA), CD9, eukaryotic translation elongation factor 1 alpha 1 (EEF1A1), glyceraldehyde-3-phosphate dehydrogenase (GAPDH), RAP1B, member of RAS oncogene family (RAP1B), tubulin alpha 1a (TUBA1A), tubulin alpha 1b (TUBA1B), tubulin alpha 1c (TUBA1C), and tyrosine 3-monooxygenase/tryptophan 5-monooxygenase activation protein zeta (YWHAZ) as present in both normal and carcinoma exosomes with no significant relative differences when compared to each other.

Table 4. Proteins detected in Nthy-ori3-1 and CRL-1803 exosomes previously identified in ExoCarta database.

ACCESSION	Previously detected in exosomes (ExoCarta)	Present in both	Nthy-ori3-1	CRL-1803
4501885	actin beta(ACTB)	X		
316659409	actin gamma 1(ACTG1)	X		
12025678	actinin alpha 4(ACTN4)	X		
9951915	adenosylhomocysteinase(AHCY)		X	
4502201	ADP ribosylation factor 1(ARF1)		X	
4502027	albumin(ALB)	X		
4557305	aldolase, fructose-bisphosphate A(ALDOA)	X		
578822814	alpha-2-macroglobulin(A2M)			X
4502101	annexin A1(ANXA1)		X	
50845388	annexin A2(ANXA2)		X	
530412286	ATP citrate lyase(ACLY)		X	
4757944	CD81 molecule(CD81)		X	
4502693	CD9 molecule(CD9)	X		

89903012	cell division cycle 42(CDC42)		X	
311771535	chaperonin containing TCP1 subunit 2(CCT2)		X	
63162572	chaperonin containing TCP1 subunit 3(CCT3)		X	
567757609	chloride intracellular channel 1(CLIC1)		X	
530411491	clathrin heavy chain(CLTC)		X	
578798587	enolase 1(ENO1)		X	
767942082	eukaryotic translation elongation factor 1 alpha 1(EEF1A1)	X		
4503483	eukaryotic translation elongation factor 2(EEF2)		X	
767943537	e_zrin(EZR)			X
41872631	fatty acid synthase(FASN)		X	
160420317	filamin A(FLNA)		X	
5031863	galectin 3 binding protein(LGALS3BP)			X
7669492	glyceraldehyde-3-phosphate dehydrogenase(GAPDH)	X		
767980445	heat shock protein 90 alpha family class A member 1(HSP90AA1)		X	
767970091	heat shock protein family A (Hsp70) member 8(HSPA8)		X	
4504323	histone cluster 2 H4 family member a(HIST2H4A)		X	
4505257	moesin(MSN)			X
768024950	myosin heavy chain 9(MYH9)		X	
10863927	peptidylprolyl isomerase A(PPIA)		X	
32455266	peroxiredoxin 1(PRDX1)		X	
32189392	peroxiredoxin 2(PRDX2)		X	
4505763	phosphoglycerate kinase 1(PGK1)		X	
767984412	pyruvate kinase, muscle(PKM)		X	
5453555	RAN, member RAS oncogene family(RAN)		X	
7661678	RAP1B, member of RAS oncogene family(RAP1B)	X		
10835049	ras homolog family member A(RHOA)		X	
9845509	ras-related C3 botulinum toxin substrate 1 (rho family, small GTP binding protein Rac1)(RAC1)		X	
61744477	solute carrier family 3 member 2(SLC3A2)			X
57863259	t-complex 1(TCP1)		X	
767985152	thrombospondin 1(THBS1)			X
393715095	tubulin alpha 1a(TUBA1A)	X		
57013276	tubulin alpha 1b(TUBA1B)	X		
14389309	tubulin alpha 1c(TUBA1C)	X		
4507951	tyrosine 3-monooxygenase/tryptophan 5-monooxygenase activation protein eta(YWHAH)		X	

5803227	tyrosine 3-monooxygenase/tryptophan 5-monooxygenase activation protein theta(YWHAQ)		X	
21735625	tyrosine 3-monooxygenase/tryptophan 5-monooxygenase activation protein zeta(YWHAZ)	X		
768033354	ubiquitin like modifier activating enzyme 1(UBA1)		X	
6005942	valosin containing protein(VCP)		X	

Galectin 3 binding protein (LGALS3B) is a known tumor-associated antigen suppressing immune surveillance and promoting proliferation/survival of tumor cells and has been previously associated with shorter cancer survival and drug resistance¹⁴⁸. LGALS3B is usually not expressed in normal cells but displays pathological expression in many tumors including those affecting the pancreas, liver, colonic mucosa, breast, lung, prostate, head and neck, nervous system and the thyroid gland¹⁴⁹. The up-regulation of galectins and significant hyper N-glycosylation of LGALS3BP in tumor tissue may imply an increased cell–cell interaction to facilitate tumor cell aggregation and metastatic diffusion¹⁵⁰. Of note, ezrin (EZR) and moesin (MSN) were identified in CRL-1803-derived EVs and their activation has been linked to the regulation of invasion and migration of PTC cells along with podoplanin and metalloproteins¹⁵¹. Additionally, thrombospondin 1 (THBS1), also identified in CRL-1803 EVs, has been reported as a potential regulator of angiogenesis and tumor progression in differentiated thyroid carcinomas¹⁵².

Tumor-specific EVs are distinct from EVs secreted by normal thyroid cells and thus, may provide more information of tumor-related pathways. Interestingly, low spectral counts of annexin 2 were identified only in the Nthy-ori3-1 EVs and not in EVs derived from CRL-1803 cells. annexin 2 has been reported as highly expressed in EVs

from malignant and pre-metastatic breast cancer cells promoting angiogenesis and facilitating the formation of favorable microenvironment for metastasis, therefore, it was unexpected to find this protein expressed in EVs from Nthy-ori3-1 cells¹⁵³. The use of LC-MS/MS for the characterization of exosome-derived proteins in our study may offer a possible explanation for the detection of annexin 2 in the normal thyroid cell line. However, it doesn't explain why it is not identified in CRL-1803 cells unless it is only specific to certain tumors.

Functional relevance of EVs-derived proteins

Analysis of these results using Database for Annotation, Visualization and Integrated Discovery (DAVID v6.8) and Functional Enrichment Analysis tool (FunRich v3.1.3) determined the percentage of proteins attributable to the resulting top biological functions from harvested EVs (Fig. 9).

Secreted EVs from Nthy-ori3-1 cells exhibited high protein percentages involved in the following biological functions: cell growth and/or maintenance (21.4%), protein metabolism (20.3%), and regulation of nucleobase, nucleoside, nucleotide and nucleic acid metabolism (17%). On the other hand, CRL-1803 EVs-derived proteins were primarily involved in cellular growth and/or maintenance (46.1%), transport (11.2%), and protein metabolism (10.5%). Cancer cells generally promote cellular growth, angiogenesis, and overall metastasis in order to survive, divide, and form tumors in thyroid tissue, therefore, it is not surprising to find CRL-1803 EV-cargo predominantly involved in cellular growth and/or maintenance (Fig.10).

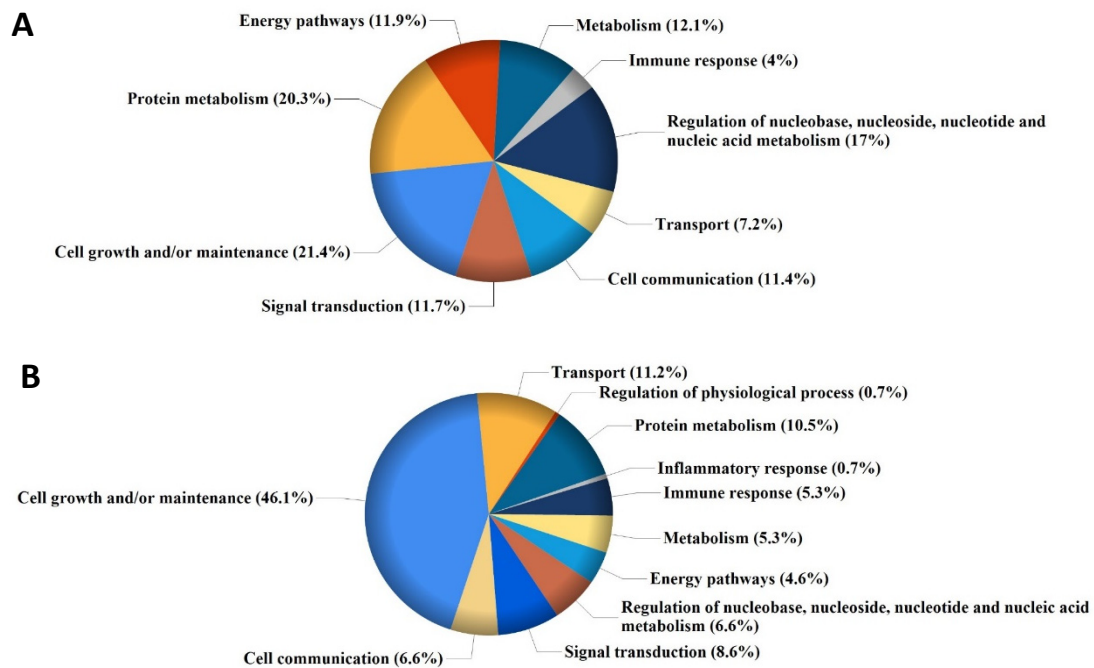
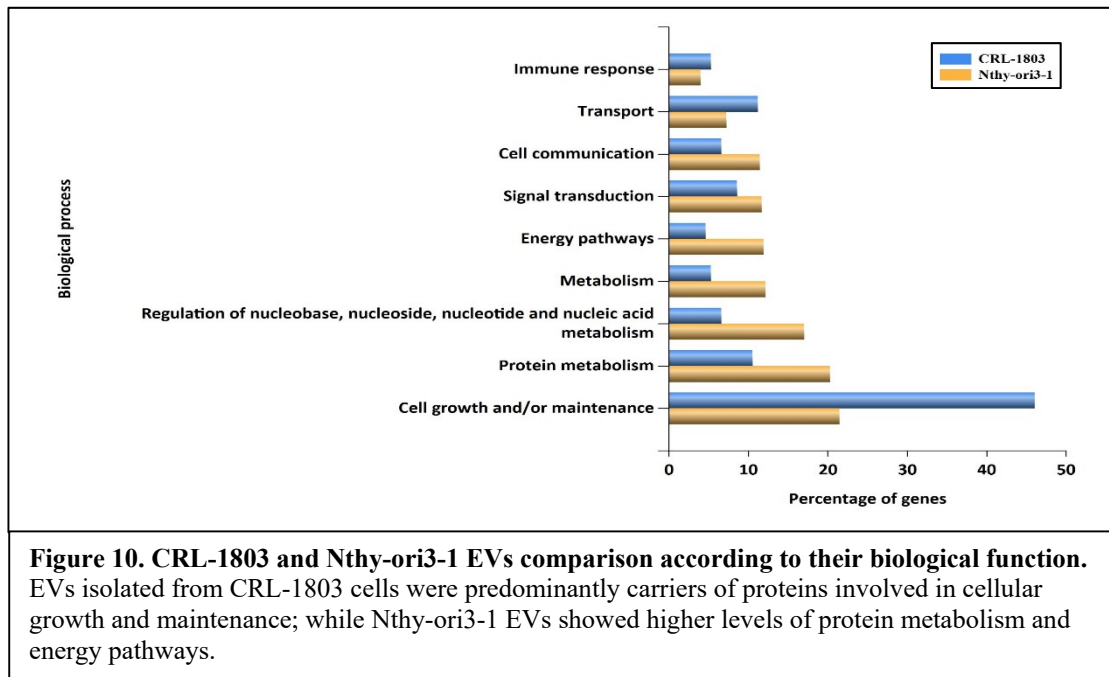


Figure 9. Extracellular vesicles-derived proteins categorized by their biological function. (A) Secreted EVs proteins isolated from Nthy-ori3-1 thyroid cells. (B) EVs-derived proteins isolated from CRL-1803 thyroid carcinoma cells.

Protein cargo comparison of Nthy-ori3-1 and CRL-1803 EVs

Spectral count comparisons from Nthy-ori3-1 and CRL-1803 EVs produced 19 EV-derived proteins with at least 120% relative difference (Table 3). Relative differences were calculated as $[(\text{number of CRL-1803 spectra} - \text{number of Nthy-ori3-1 spectra}) / (\text{average number of spectra for CRL-1803 and Nthy-ori3-1}) \times 100]$. The identified proteins were considered to be up or down regulated based on the relative difference percentage obtained.



The majority of the identified shared cell-derived EVs were downregulated in CRL-1803 when compared to Nthy-ori3-1 EVs, with the exception of cytokeratin 10 (CK 10) (Table 5). Expression of this particular high molecular weight cytokeratin seems to be a characteristic of aggressive thyroid tumors since it has been previously reported in anaplastic carcinomas¹⁵⁴. Complement C4-B-like preprotein and fibronectin isoform 1 preprotein were among the top downregulated proteins found in CRL-1803 EVs compared to Nthy-ori3-1. Complement C4-B is a member of the complement pathway and its activation has generally been considered part of the body's immune-surveillance against cancer. Evidence for the classical pathway of complement activation has been reported earlier via IHC in patients with papillary thyroid carcinoma¹⁵⁵. Inhibitory mechanisms of complement activation allow cancer cells to escape from complement-

regulated elimination and interfere with cancer immunotherapies¹⁵⁶. Thus, it can only be implied that upregulation of the complement C4-B results in recognition signals being secreted by thyroid normal cells via exosomes for the identification and tagging of malignant cancer cells. Fibronectin 1(FN1) encodes fibronectin, which is present in the plasma, at the cell surface, and in the extracellular matrix¹⁵⁷. As an epithelial–mesenchymal transition (EMT) marker (an essential step in cancer progression) fibronectin is involved in cell adhesion and migration, including embryogenesis, wound healing and metastasis¹⁵⁷. Several reports have described overexpression of FN1 in thyroid cancer based on analysis of tumor tissue specimens or fine needle aspiration biopsies^{158,159}. FN1 expression has also been proposed as a molecular marker for identifying malignant lesions with indeterminate diagnosis and there is even some IHC evidence that increased FN1 expression is localized mainly in the invasive front of thyroid cancers¹⁶⁰. These studies indicate that FN1, similarly to other EMT-related proteins, is a negative prognostic marker in patients with PTC^{160–162}. Additional studies have revealed that surface bound fibronectin mediates exosome-cell interactions^{163,164}. It has been demonstrated that other extracellular matrix component, (i.e. heparan sulphate proteoglycans), influences the production of extracellular vesicles by triggering intracellular signaling¹⁶⁵. Syndecan heparan sulfate proteoglycans and their cytoplasmic adaptor syntenin have been shown to interact with fibronectin 1, thus controlling the formation of exosomes¹⁶³. Elevated heparanase expression in tumor cells correlates with increased tumor angiogenesis, tumor invasiveness and metastasis, thus, overexpression of heparanase promotes exosome secretion^{166,167}.

Table 5. EVs-derived proteins common between Nthy-ori3-1 and CRL-1803 ranked according to their relative difference based on averaged spectral hits.

Accession	Protein	Nthy-ori3-1	CRL-1803	Relative Difference	Status
338858017	complement C4-B-like preproprotein	21	1	-181.8%	↓
47132557	fibronectin isoform 1 preproprotein	92	5	-179.4%	↓
126012562	prolow-density lipoprotein receptor-related protein 1 precursor	15	1	-175%	↓
7669492	glyceraldehyde-3-phosphate dehydrogenase isoform 1	13	1	-171.4%	↓
67190748	complement C4-A isoform 1 preproprotein	20	2	-163.6%	↓
767981764	PREDICTED: alpha-actinin-1 isoform X2	10	1	-163.6%	↓
223029410	talin-1	10	1	-163.6%	↓
5031863	galectin-3-binding protein precursor	19	2	-161.9%	↓
767985152	PREDICTED: thrombospondin-1 isoform X2	26	4	-146.7%	↓
316659409	actin, cytoplasmic 2	12	2	-142.9%	↓
119964726	cation-independent mannose-6-phosphate receptor precursor	6	1	-142.9%	↓
4503635	prothrombin preproprotein	6	1	-142.9%	↓
40317626	thrombospondin-1 precursor	22	5	-125.9%	↓
115298678	complement C3 precursor	16	4	-120%	↓
24638446	histone H2A type 2-C	4	1	-120%	↓
4557888	keratin, type I cytoskeletal 18	4	1	-120%	↓
13562114	tubulin beta-1 chain	4	1	-120%	↓
195972866	keratin, type I cytoskeletal 10	1	4	120%	↑

RPPA characterization

Extracellular vesicles secreted by Nthy-ori3-1 and CRL-1803 thyroid cell lines were further characterized via RPPA analysis primarily to confirm exosome protein markers CD63 and CD9 expression. A total of 52 endpoints (total and phospho-proteins) were used to expand our investigation of protein content in EVs shed by thyroid cell lines. RPPA data was normalized to CD63 expression values prior to protein level comparison between exosomes from each cell line. Activation of CD63 and CD9 was observed in both cell lines, confirming exosomal origin, with no significant differences in protein expression values between cell lines.

An interesting aspect of these results was the detection of protein expression in their phosphorylated state; phosphorylation indicates the activation state of signaling pathways, consequently, phosphoprotein content may be a key component in defining the role of EVs in intercellular signaling. Compared to normal thyroid cell line, the levels of AMPK β 1 S108, IRS S612, and mTOR S2448 proteins were significantly altered in EVs shed by the CRL-1803 cell line (Table 6). These phosphorylated members are involved in pathways regulating cell growth, apoptosis, protein synthesis, and cell metabolism. Fibronectin expression was significantly higher ($p=0.0002$) in Nthy-ori3-1 derived EVs, confirming earlier obtained MS results. Additionally, autophagy marker LC3B and thyroid hormone metabolic enzyme type 3 iodothyronine deiodinase (DIO3) expression were significantly higher in Nthy-ori3-1-derived EVs compared to CRL-1803 exosomes. On the other hand, calcium pump-plasma membrane calcium ATPase2 (PMCA2) was significantly elevated in CRL-1803-derived EVs. Calcium (Ca^{2+}) signaling has been

linked either directly or indirectly to the main processes altered in carcinogenesis such as regulation of proliferation, cell survival, migration and/or invasion through the remodeling of cellular calcium homeostasis^{168,169}. The expression of several Ca^{2+} channels show distinctive changes during these processes, resulting in altered Ca^{2+} signal patterns, thus affecting downstream signaling pathways. PMCA2 is a major regulator of Ca^{2+} signaling and it plays an essential role in the regulation of processes closely related to tumorigenesis^{168,169}.

Table 6. Characterization of Nthy-ori3-1 and CRL-1803 derived EVs via RPPA. Listed endpoints show significantly different protein expression of EVs content between cell lines, p-values (≤ 0.05).

Endpoint	<i>p</i> -value	Nthy-ori3-1	CRL-1803
Fibronectin	0.0002	↑	↓
LC3B	0.01	↑	↓
AMPK β 1 S108	0.04	↑	↓
DIO3	0.05	↑	↓
IRS1 S612	0.05	↓	↑
PMCA2	0.05	↓	↑
mTOR S2448	0.05	↑	↓

A number of alternative ways are exploited by cancer cells to promote proliferative signaling, including auto-stimulation of growth factor ligands production themselves. Cancer cells may also send signals to stimulate normal cells within the surrounding tumor-associated microenvironment, which in turn supplies the cancer cells with needed growth factors¹⁷⁰. It is thus likely that exosomes are active contributors

having an effect in intercellular signaling within the tumor microenvironment aiding in the survival and proliferation of cancer cells.

DISCUSSION

Exosomes are effective communication vehicles that transfer bioactive proteins and genetic material between cells¹⁷¹. Recently, studies have indicated that, based on the property of proteins, either as a tumor promoter or suppressor, the export of proteins by exosomes impacts the tumor environment¹⁷². Additionally, exosomes from malignant cells have shown the potential to induce normal cell transformation. For instance, prostate cancer cell-derived exosomes could induce neoplastic transformation of adipose-derived stem cells, which has been associated with trafficking of oncogenic proteins (Ras superfamily of GTPases), mRNA (K-ras and H-ras), as well as miRNAs (miR-125b, miR-130b, and miR-155) by exosomes^{173,174}. Because exosomes carry genomic and proteomic materials known to mediate these hallmarks of cancer, it is hypothesized that exosomes secreted by tumor cells have a role in the growth and propagation of tumor cells¹⁷⁵.

In this study, EVs secreted by Nthy-ori3-1 and CRL-1803 thyroid cell lines were isolated and their protein composition analyzed via LC-MS/MS and quantitatively evaluated by RPPA. MS results generated previously identified exosome markers including tetraspanins (CD9, CD81), annexin-2 (ANXA2) and heat shock proteins

(Hsp70 and Hsp90) confirming successful sequestration of exosome-derived proteins from thyroid cell lines^{145–147}. Galectin 3 binding protein, ezrin, moesin, and thrombospondin 1 were specific proteins identified uniquely in CRL-1803 tumor thyroid cell line. Collectively, this group of proteins have been found to promote proliferation/survival of tumor cells, angiogenesis, and regulation of invasion and migration of PTC cells^{148,151,152}. Cancer cells communicate with the surrounding and distant cells via exosomes, which constitutes a bi-directional interaction network promoting cancer development, progression, metastasis, and drug resistance. However, the exact mechanisms mediating the complex roles of exosomes in cancer have not yet been fully elucidated¹⁷⁶. Contrary to the current literature, annexin 2 was identified only in normal-derived thyroid exosomes and not in CRL-1803-derived exosomes. Annexin 2 has been reported overexpressed in exosomes from several malignant cancer cells resulting in stimulation of angiogenesis and metastasis^{153,177}. Although not found in the cancer thyroid cell line in this study, annexin 2 is still localized on the cell surface of endothelial cells and is essential for lipid raft formation and signal transduction through its interaction with CD44 and mediates interferon gamma-induced inflammation via calcium-dependent regulation of protein tyrosine kinase 2¹⁷⁸.

Analyses of the data using DAVID functional annotation revealed cellular growth/maintenance and transport as the main biological functions exhibited by CRL-1803-derived exosome proteins. Spectral count comparisons from Nthy-ori3-1 and CRL-1803 exosomes produced several proteins with relative differences. With the exception of CK10, most of the shared cell-derived exosomes exhibited lower spectral counts in

CRL-1803 compared to Nthy-ori3-1 exosomes. There continues to be increasing evidence associating exosomes with initiation, growth, progression, and drug-resistance of tumors involving interactions with the microenvironment by the transferring of oncogenic proteins and nucleic acids to receiving cells¹⁷⁹. Thus, microvesicles represent heterogeneous populations of membrane vesicles, budding directly from the plasma membrane and carrying a number of nuclear, cytosolic, and endoplasmic reticulum-derived proteins. Furthermore, exosomes released under hypoxic conditions are able to stimulate angiogenesis through interactions with endothelial cells¹⁸⁰. Altogether, these findings indicate that exosome may contribute to tumor development and progression by acting as a mediator in the transformation of normal cells to malignant cells¹⁷⁶.

RPPA analysis demonstrated that exosome cargo harvested from human thyroid cell lines contained not only total proteins but also proteins in their phosphorylated state. In addition to exosome markers CD9 and CD63, protein expression of phosphorylated AMPK β 1 S108, IRS1 S612, and mTOR S2448 were found to be significantly different while comparing Nthy-ori3-1 and CRL-1803 exosome-derived proteins. Activation of several other phospho-proteins was also observed, including NFkBp65 S536, STAT3 S727 and ATF2 T71, though no significant differences ($p=0.067$) between both cell lines was found. These phosphorylated transcription factors may play important roles in thyroid cell signaling, during cell cycle regulation, proliferation, cytokine production, growth factor receptors, and cell death. On an interesting note, HSP90 α T5/7 expression was elevated in CRL-1803 exosome-derived cargo. This protein is required for activation of DNA-PK, γ -H2AX formation, DNA fragmentation, and apoptotic body

formation, suggesting the involvement of DNA damage/repair pathway¹⁸¹. Moreover, LC3B expression was significantly elevated in Nthy-ori3-1 exosomes, indicating activation of the autophagy pathway. The remaining molecules, such as cytoskeletal proteins, could contribute to a protective shell stabilizing vesicular structure, and may carry targeting information.

In conclusion, I was able to develop a simple protocol for exosome harvesting using ExoQuick-TC kit on human thyroid cell lines. Nthy-ori3-1 and CRL-1803 secreted exosomes that were successfully harvested and further characterized via LC-MS/MS. This supports the hypothesis that exosomes may contribute to cellular signaling processes within the colloid. Mass spectrometry results generated previously identified exosome markers including tetraspanins (CD9 and CD81), annexin-2, and heat shock proteins (Hsp70 and Hsp90) confirming isolation of exosome-derived proteins from thyroid cell lines. Galectin-3, ezrin, moesin, and thrombospondin-1 were unique proteins identified in thyroid tumor-cell line derived exosomes. Collectively, these proteins have been reported to promote proliferation of tumor cells, angiogenesis, and regulation of migration of papillary thyroid carcinoma cells. In addition, a variety of signaling proteins (total and phosphorylated) can be quantified via RPPA and statistically differences identified between both thyroid cell lines. Future studies are needed to characterize exosomes in more detail, including electron microscopy characterization, and clarify the biological significance of these exosomes in thyroid disease.

AIM OF STUDY III

**Phosphoproteomic Profile of Thyroid Colloid and Follicular
Cells by RPPA**

Specific Aim 3. Characterize the phosphoproteomic profile of thyroid colloid and follicular cells by RPPA.

Post-translational modifications of protein networks can be profiled employing protein microarrays by comparing the proportion of total protein to the phosphorylated protein. In general, this reflects the state of information flow through a protein network. Monitoring the total and phosphorylated proteins over time between disease and non-diseased states may allow us to infer the activity levels of the proteins in a particular pathway in real-time^{182–184}. The utility of protein microarrays lies in their ability to quantify signaling kinases, which allows pathway maps to be constructed for specific samples and/or proteins. Identification of critical interactions within the network is a potential starting point for drug development and individualized therapies^{182,183}.

Quantifying a large number of protein signal pathway endpoints and post-translational modifications by conventional western blotting with limited amount of thyroid material would be extremely labor intensive and costly. Consequently we used RPPA analysis of 52 cell signaling kinase endpoints, representing autophagy, adhesion, invasion, and pro-survival pathways (Index 1). RPPA technology has the required sensitivity and precision for small numbers of cells and provides a means of quantifying protein post-translational modifications indicative of activated signal pathways^{107–109}. We applied the reverse phase protein microarray phosphoprotein pathway mapping to evaluate the hypothesis that the paucity of colloid in thyroid cancer is due to upregulation of autophagy in surrounding epithelial cells.

Laser capture microdissection can be used to procure enriched colloid material and surrounding epithelial cells without contamination from the surrounding cells/colloid. Earlier thyroid studies were mostly based on analysis of the entire tissue biopsy, LCM plays a unique role as it allows for the isolation of individual cell populations that may reveal accurate distinctive information useful in the identification and classification of thyroid disease. The state of protein signal transduction pathways within epithelial cells surrounding colloid material may be identified for comparative analysis of thyroid disorders.

Characterization of the phosphoproteomic profile of both follicular cells and colloid material was conducted via RPPA. Tissue material was microdissected, lysed, printed on microarrays, stained by selected antibodies, and analyzed to quantify the state of protein post-translational modifications, particularly in relation to the autophagy signaling pathway, taking place within the thyroid follicle for a comparative analysis of non-carcinoma, FTA, and PTC samples.

Thyroid biopsies were obtained from 20 patients with PTC (n=13), FTA (n=5), and non-carcinoma (n=2) diagnosis after thyroidectomy or lobectomy (Table 7). Thyroid tissues were processed according to LCM, protein extraction, and RPPA protocols listed under the Methods and Materials section of this study. Enrichment of epithelial cells by LCM was done before analysis to ensure that the cells being analyzed were only taken from within the follicular cell population of the thyroid follicle.

Table 7. Specimen list and corresponding diagnosis analyzed by RPPA

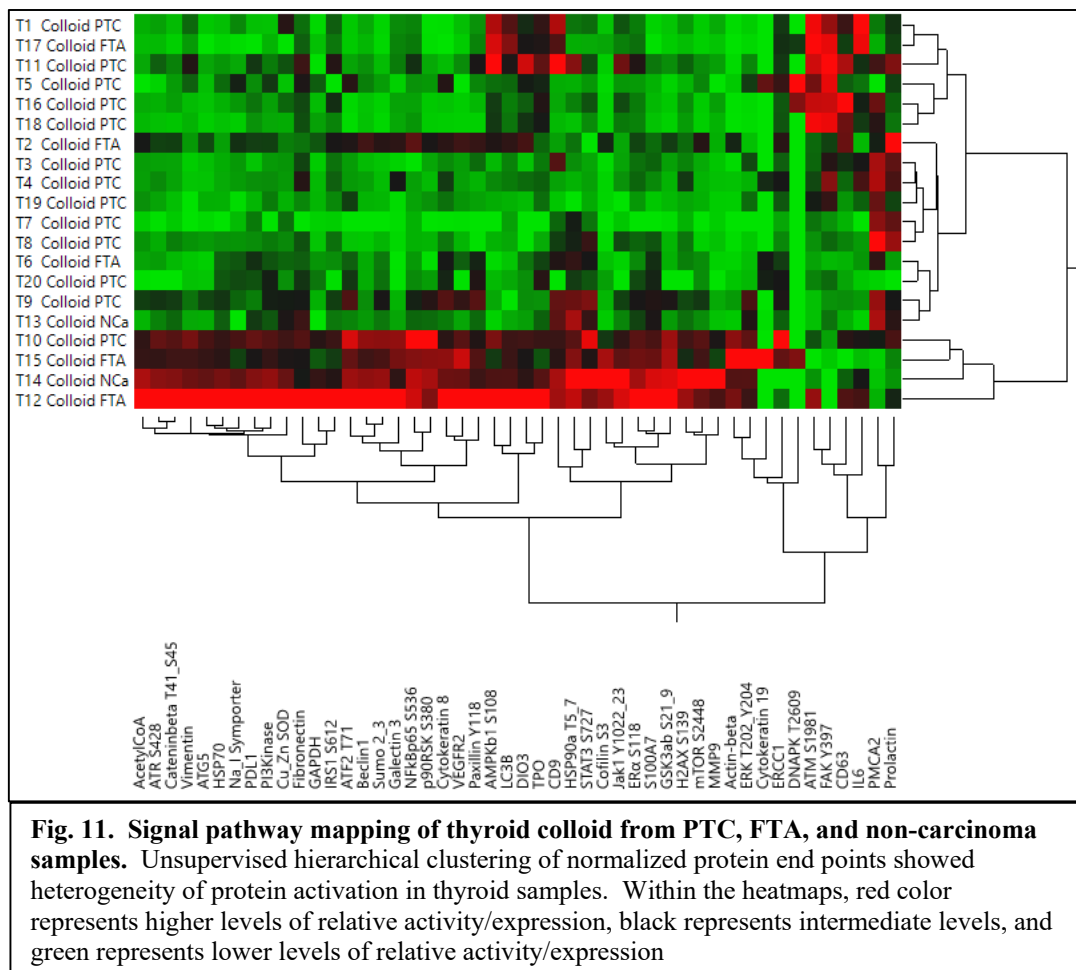
Patient ID	Diagnosis
T1	Papillary Thyroid Carcinoma
T2	Follicular Thyroid Adenoma
T3	Papillary Thyroid Carcinoma
T4	Papillary Thyroid Carcinoma
T5	Papillary Thyroid Carcinoma
T6	Follicular Thyroid Adenoma-Thyroiditis
T7	Papillary Thyroid Carcinoma
T8	Papillary Thyroid Carcinoma
T9	Papillary Thyroid Carcinoma
T10	Papillary Thyroid Carcinoma
T11	Papillary Thyroid Carcinoma
T12	Follicular Thyroid Adenoma
T13	Non-Carcinoma
T14	Non-Carcinoma-Hyperthyroidism
T15	Follicular Thyroid Adenoma
T16	Papillary Thyroid Carcinoma
T17	Follicular Thyroid Adenoma
T18	Papillary Thyroid Carcinoma
T19	Papillary Thyroid Carcinoma
T20	Papillary Thyroid Carcinoma

RESULTS

RPPA reveals the presence of phospho-proteins in Colloid

Unsupervised hierarchical clustering of RPPA data reveals that both PTC (n=13) and FTA (n=5) patients possess heterogeneous signaling pathway activation but few significant changes that do not necessarily distinguish these pathologies as a whole from each other (Fig. 11). Despite the known heterogeneity of thyroid disease, common

groupings are apparent based on commonly shared phosphorylation-driven signaling networks. In order to explore the potential for such functional groupings, we generated a broad-scale signaling activation map to determine which signaling pathways are activated across a variety of colloid specimens, and if pathway-based clustering was apparent. As shown in Figure 11, while patient specific signaling is certainly apparent, there appears to be clustering of patients into subgroups broadly based on FAK Y397, autophagy and DNA damage/repair activation markers.



Statistical analysis demonstrated that expression of individual endpoints including calcium pump-plasma membrane calcium ATPase2 (PMCA2) and focal adhesion kinase-tyr397 (FAK Y397) were significantly elevated in the colloid of PTC vs. FTA samples, while Cytokeratin 8, mTOR S2448, and NFkBp65 S536 were significantly downregulated in PTCs (Table 8). Interestingly, PMCA2 was also found to be significantly elevated in CRL-1803-derived exosomes in our earlier study. Calcium signaling has been linked to carcinogenesis via the regulation of proliferation, cell survival, migration and/or invasion through the remodeling of cellular calcium homeostasis^{168,169}. PMCA2 is a major regulator of Ca²⁺ signaling and it plays an essential role in the regulation of processes closely related to tumorigenesis^{168,169}. FAK is expressed in all cells at a low basal level, however it is significantly overexpressed in solid tumors, including papillary carcinomas, with even more elevated levels of expression in metastatic tumors¹⁸⁵. Activation of FAK by integrin clustering leads to auto-phosphorylation at Tyr397, which is a binding site for the Src family kinases PI3K and PLC γ . Phosphorylated FAK results in increased cell survival, motility, and proliferation, leading to angiogenesis, metastasis, and invasion of tumors¹⁸⁵.

Table 8. Endpoints with significant statistical differences in PTC and FTA colloid comparison.

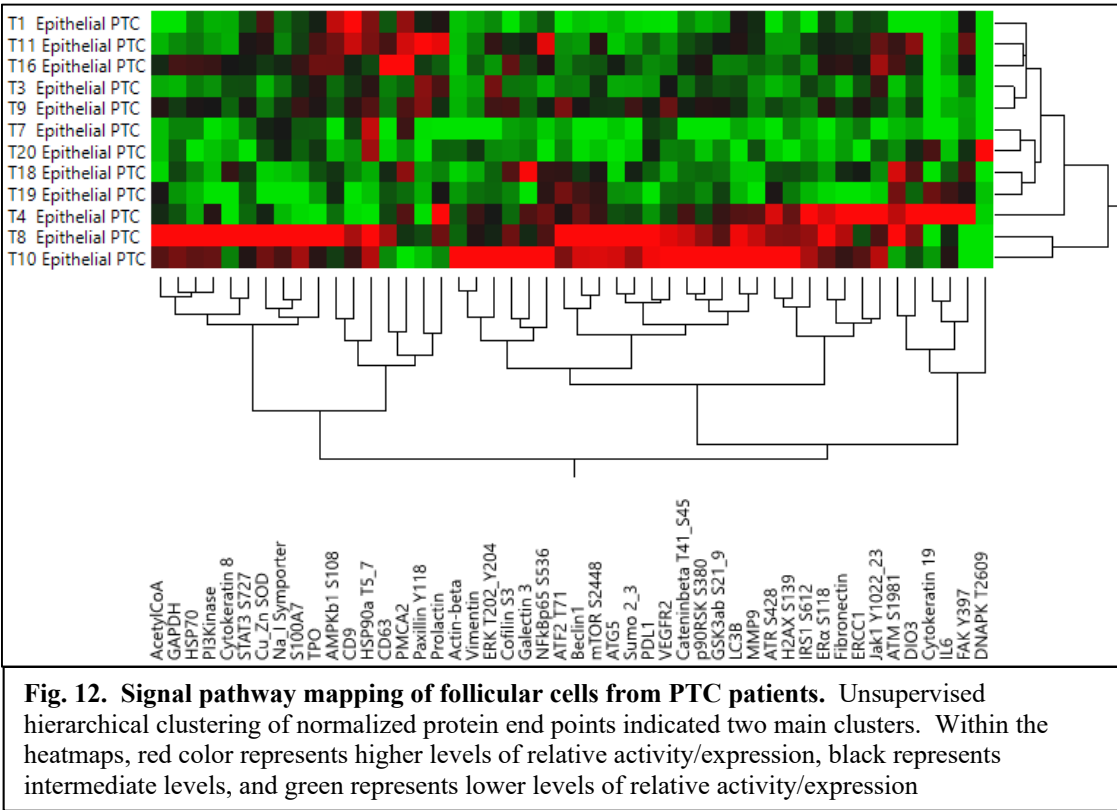
	<i>p</i> -value	Colloid PTC	Colloid FTA
PMCA2	0.004	↑	↓
FAK Y397	0.005	↑	↓
Cytokeratin 8	0.010	↓	↑
Actin-beta	0.015	↓	↑
mTOR S2448	0.023	↓	↑
NFkBp65 S536	0.045	↓	↑

Autophagy pathway signaling is elevated in PTC follicular cells

We first sought to investigate the activation state of 52 proteins that constituted a broad survey of several signaling pathways, in particular autophagy, in microdissected thyroid follicular cells by RPPA. Unsupervised hierarchical clustering analysis of the 52 specific end points revealed high activation of autophagy markers (Beclin-1 and LC3B) in epithelial cells from a subset of PTC patients (Fig. 12). Comparatively elevated AMPK and PMCA2 activation/phosphorylation was also displayed on a separate PTC-epithelial subgroup. Mean comparisons of protein signaling intensity values of microdissected epithelial cell populations confirmed higher (but not statistically significant) expression in autophagy markers LC3B and Beclin-1 in PTC samples when compared to both FTA and non-carcinoma epithelial cells (Fig. 13). Furthermore, it appears that some samples have tumors with predominant signaling activation across a number of pathways, while the rest of the samples' signaling portraits seem associated with specific pathway activation groupings. These results suggest that phosphorylation and cell signaling profiles may be useful for the classification of thyroid cancer into functional direct groupings. The number of samples used in this study is too small to statistically postulate if these groupings would hold across larger sample sets. Therefore, broader and deeper analysis of larger thyroid cancer study sets are needed in order to generate a functional map of signaling activities in thyroid cancer.

Autophagy (a Greek word that means "self-eating") is a catabolic process that delivers cytoplasmic components and organelles to lysosomes for digestion which can be advantageously recycled by tumor cells for energy, thus in some cases supporting

survival and proliferation^{80,78,74,87}. Autophagy activation in response to stress and starvation is also seen in normal cells, a low level of basal autophagy promotes homeostasis through housekeeping functions⁷⁸.



Upregulation of autophagy has been reported in cancer cells during several major events leading towards metastasis, including hypoxia and metabolic stress¹⁸⁶. By promoting survival during cellular stress, autophagy lessens tumor cell necrosis and associated macrophage infiltration of the primary tumor^{74,186}.

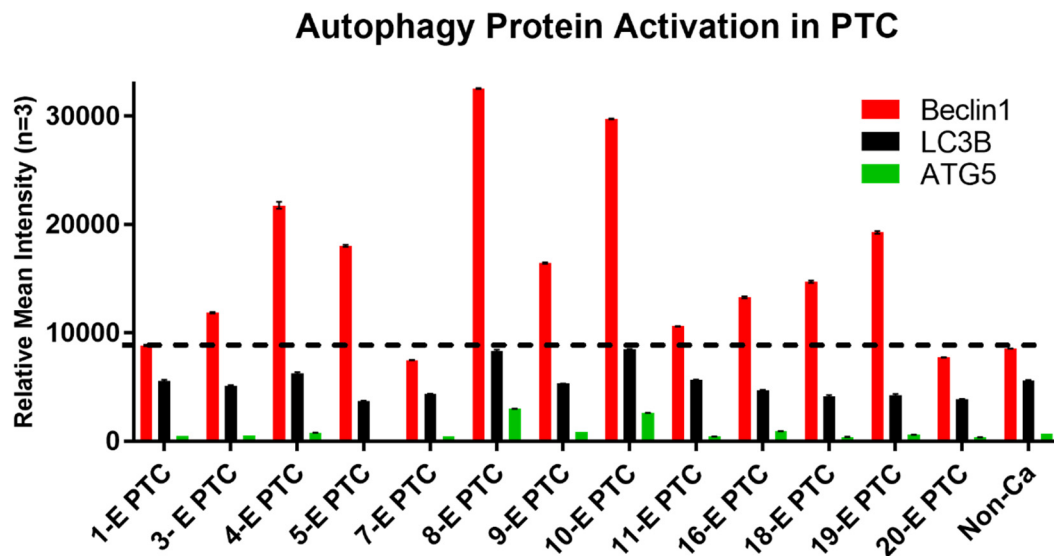


Fig 13. Autophagy protein quantification by RPPA. Follicular cells from papillary thyroid carcinoma patients show elevated Beclin-1 expression (relative mean intensity \pm SEM (N=3). “Non-ca” is a non-cancer, normal thyroid specimen used to establish the threshold level of Beclin-1 protein expression (black dotted line).

Several proteins are known to regulate the autophagy process, including AMP-activated protein kinase (AMPK). AMPK is activated by an elevated AMP/ATP ratio due to cellular and environmental stress, such as heat shock, hypoxia, and ischemia¹⁸⁷. This protein activates catabolic pathway for energy homeostasis. Reports have shown that lysosomal-dependent catabolic program, autophagy, plays important roles in macromolecular nutrient degradation, such as glycogen and lipid droplets. Autophagy-dependent glycogen degradation is reported as an important glucose-supplying alternative like gluconeogenesis^{18,187}. Protein expression of AMPK β 1 S108 showed no significant

differences in PTC follicular cells when compared to FTA and non-carcinoma, suggesting this protein is not responsible for autophagy pathway activation. It is important to emphasize that tumor cells are subjected to metabolically stressful conditions and a shift toward glucose metabolism, known as the 'Warburg Effect' occurs. Therefore, it is tempting to speculate whether AMPK activation could be implicated in this phenomenon⁸⁸. However, it is possible that any other of the AMPK- kinases, not included in this study, do contribute to the activation of autophagy markers. Interestingly, RPPA colloid results indicated higher expression of AMPK β 1 S108 in PTC samples compared to FTA and non-carcinoma colloid.

DNA damage/repair response protein activation in colloid and epithelial cells

DNA lesions/breaks were investigated in microdissected material of both colloid and follicular cells via RPPA through the expression of phosphorylated DNA-dependent protein kinases (DNA-PKcs T2609, ATM S1982, ATR S428, ERCC1, and H2AX S139). These protein kinase complexes play an important role in the DNA damage response and maintenance of genomic stability. DNA damage is linked to hormonal dysregulation, therefore, prevalence of hormone-linked nucleotides in DNA may have an effect in hormone regulation during tumorigenesis. Electrophilic metabolites that enter the nucleus of thyroid cells may covalently bond with the nucleobases, forming DNA-adducts and if not repaired, these adducts can create points of mutagenesis^{28,188}.

Neither PTC epithelial nor colloid samples showed significant difference in DNA damage/repair signaling pathway activation when compared to FTA or non-carcinoma samples. However, while looking at the PTC samples by themselves, a specific subgroup consistently showed higher protein expression of ATM S1981, ATR S428, ERCC1, and H2AX S139 (Fig 14).

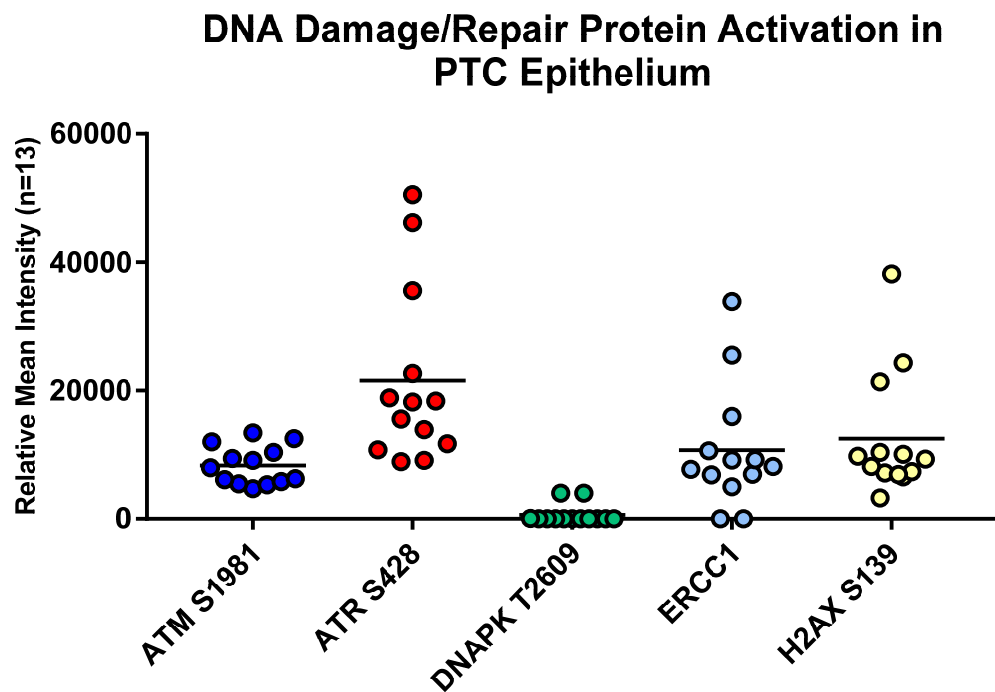
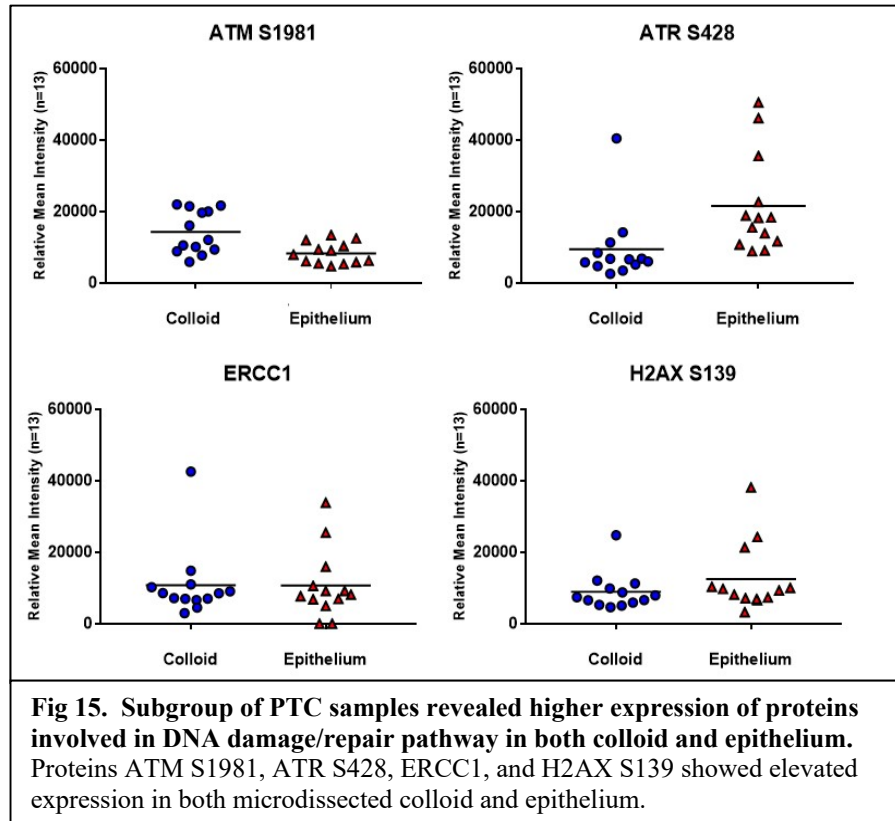


Fig 14. DNA damage/repair protein activation in PTC epithelium. DNA damage/repair protein markers revealed a subgroup of PTC samples that showed consistent elevated expression of ATR S428, ERCC1, and H2AX S139.

Furthermore, while reviewing the colloid results from PTC samples, the same subgroup exhibited similarly higher expression of proteins involved in the DNA damage/repair pathway. The thyroid follicular cell is known to be at a higher risk of

oxidative stress resulting in oxidative DNA damage produced by reactive oxidative species (ROS)¹⁸⁹. In particular, a disproportion between pro- and antioxidative factors has been suggested as a key mechanism in thyroid tumorigenesis. In thyroid epithelial cells, H₂O₂ is generated by thyroid oxidases in response to thyrotropin and acts as an essential cofactor for thyroid peroxidase during thyroid hormone synthesis^{190,191}. Excess of H₂O₂ is generally eliminated by superoxide dismutase, glutathione peroxidases and peroxiredoxins as part of the antioxidant system¹⁸⁹. A recently published study by Zhang et al. showed that metallothionein-I/II deficiency showed enhanced mitochondrial superoxide production with elevated expression level of peroxiredoxin 3 when challenged with excess iodide¹⁹². Increased respiration leads to production of mitochondrial reactive oxygen species, which in turn causes oxidative stress and DNA double-strand breaks and triggers a DNA damage response that ultimately leads to premature senescence of susceptible cells^{191,193}. In this case, autophagy might be cytoprotective during the response to DNA damage suggesting that activation of oxidative stress is involved in the cell's decision to undergo autophagy^{106,194}. Our results can shed some light onto the mechanisms by which thyroid hormonal regulation affects DNA damage and activation of the autophagy pathway.



DISCUSSION

RPPA is a novel technology that has been widely used in cancer research for its ability to study complex cellular signaling networks through quantitative analysis of protein levels within normal and diseased tissue¹⁹⁵. Coupled with LCM, RPPA has the required sensitivity and precision for small numbers of cells and provides a means of quantifying protein post-translational modifications indicative of activated signal pathways^{107–109}. In order to measure phosphorylation states and total protein levels, we probed thyroid colloid and epithelial cells printed on arrays with antibodies that covered

multiple functional processes, including thyroid hormone synthesis, cytokine signaling, transcription, glucose/energy metabolism, cell migration, angiogenesis, autophagy and DNA damage/repair response. Protein profiles did not vary significantly with tumor histotype and strongly suggested that pathway activation profiles in thyroid tumors may be rather patient-specific.

Since phosphorylation reflects activation of signaling pathways and the colloid in thyroid follicles has no cellular characteristics our results support our previous hypothesis that phospho-proteins found in colloid are likely exosome cargo secreted by the thyroid follicular cells. This illustrates the importance of proteomic technology coupled to signal pathway profiling in providing new and unexpected insights into cellular processes. PCMA2 and FAK Y397 were found to be significantly upregulated in PTC colloid. Additionally, PMCA2 was significantly elevated in CRL-1803-derived exosomes in our earlier study. Calcium signaling has been associated with several biological processes that induce carcinogenesis, including proliferation, survival, migration and/or invasion through the remodeling of cellular calcium homeostasis^{168,169}. FAK is expressed in all cells at a low basal level, but significantly overexpressed in papillary carcinomas¹⁸⁵. FAK activation by integrins leads to auto-phosphorylation at Tyr397 increasing cell survival, motility, and proliferation, leading to angiogenesis, metastasis, and tumor invasion¹⁸⁵. PMCA2 and FAK are therefore promising cancer drug targets. While we have identified these potential biomarkers in thyroid colloid, the true prevalence of this proteins can only be established in larger study sets.

Even though mean comparisons of protein signaling intensity values of epithelial cells resulted in no statistical differences between PTC, FTA and non-carcinoma samples, autophagy markers displayed increased protein expression in PTC samples. The process of autophagy occurs all the time at a basal level, whether a cell is starving or not^{86,186}. Under normal conditions autophagy removes damaged proteins and organelles to prevent cell damage. However, under stress (e.g., starvation, the absence of growth factors, or the lack of oxygen), the assembly of phagosomes increases. Under these conditions, intracellular molecules are digested to provide the nutrients the cell needs to survive¹⁹⁴. In this study, autophagy activation suggests that cellular proteins and organelles are being degraded/recycled for energy while depleting essential proteins from the colloid, thus creating constant cell stress contributing to tumor proliferation. Metabolic stress induces autophagy, which is sustained when apoptosis is blocked. It has been reported that autophagy is required for tumor cells with defects in apoptosis to survive metabolic stress.

DNA damage/repair signaling pathway activation was observed in PTC samples with a subgroup consistently showing higher protein expression of ATM S1981, ATR S428, ERCC1, and H2AX S139 but not DNA-PKcs T2609. Cells that accumulate damaged DNA may have reduced viability and loss of function, which could potentially lead to autophagy or tissue atrophy⁵⁹. The formation of DNA adducts in epithelial cells could also be a result of DNA damage or breakage and grants further investigation since H2AX was also found in our earlier MS analysis of the colloid.

Thyroid biomarker research has become an area of active interest over recent years not only for early detection, but also for identifying recurrent disease, and predicting the effectiveness of surgical tumor removal, radioiodine ablation, and chemotherapy^{6,71}. Biomarker discovery has now expanded to include the analysis of the proteome to investigate protein expression, along with changes in protein activity taking into account post-translational modifications that are not detected at the mRNA level. Identification of early molecular changing events is important in disease progression and mapping activated protein-signaling pathways representing each thyroid disease state will allow distinction between thyroid disorders and carcinomas preventing in many cases unnecessary surgery. Establishing signature post-translational modifications characteristic within the colloid and epithelial cells of follicular adenoma and papillary carcinoma could potentially be useful in effectively categorizing patients accordingly and it may aid in the early identification of those patients showing key modifications indicative of tumor progression.

Furthermore, there is now increased interest in metabolomics as a potential tool to support cancer research. The identification of differential metabolites in cancer cells undergoing metabolic transformations would be helpful in understanding thyroid cancer biology and ultimately in biomarker development. Recent innovations in these two areas have shown great potential in the search for specific markers to distinguish thyroid diseases and new potential targets for therapy and prevention. Thyroid proteomics and metabolomics together are seen as essential tools representing a new direction in thyroid

cancer research aiming to enhance the biochemical underpinnings of thyroid disease ^{196–198}.

Novel targeted therapies are still needed for those PTC patients who fail to respond to current approaches based on surgery plus radioiodine therapy. Efforts should be made to elucidate the molecular mechanisms underlying the aggressiveness of certain PTCs. The lack of responsiveness to radioiodine of recurrent/metastatic PTC lesions is largely the result of de-differentiation, in particular, the downregulated or abrogated expression of a functioning form of the sodium/iodide symporter^{15,22}. Loss of differentiation, which is usually accompanied by dysregulated cell proliferation, is the result of genetic and epigenetic alterations that are characteristic of more aggressive PTCs^{199,200}. Therefore, identifying biomarkers to reflect a molecular profile signature for each tumor type at any given stage would be ideal since thyroid cancer phenotypes vary in respect to morphology, molecular underpinnings, prognosis, and even therapy. With this concept in mind, a redefined goal of molecular profiling is to map the cellular circuitry so as to define the optimal set of interconnected drug targets for an individualized therapy to decrease unwanted toxic side-effects¹⁸⁴.

This study is the first to examine both thyroid colloid content and epithelial cell proteome utilizing laser capture microdissection, mass spectrometry, and reverse phase protein arrays for proteomic analysis. This is the first study to identify a myriad of cell signaling proteins and exosome proteins within the thyroid colloid. The proteomic information archive in thyroid colloid has the potential to provide diagnostic, prognostic, and therapeutic information.

Future Studies.

1) Explore methodology for identifying metabolites in thyroid tissue

Optimize protocols for isolating and identifying metabolites in normal and diseased thyroid tissue. Biologically active metabolites, including iodinated metabolites essential for developmental growth and metabolic processes ²⁰¹.

2) Discover the prevalence of hormone-linked nucleotides or chemical linked nucleotides in DNA from thyroid cancer and benign tissue specimens. DNA damage is linked with hormonal dysregulation. Electrophilic metabolites that enter the nucleus may covalently bond with the nucleobases, forming DNA-adducts. If not repaired, these adducts can create points of mutagenesis.

APPENDIX 1–

Validated antibodies used with Reverse Phase Microarrays

Antibody	Company	Species	Function
Acetyl-CoenzymeA Carboxylase (S79)	Cell Signaling	Rabbit	Hypoxia/Lipid Metabolism
Actin, Beta	Cell Signaling	Rabbit	Cytoskeletal
AMPK β 1 (S108)	Cell Signaling	Rabbit	Hypoxia/Stress
Annexin II	BD Biosciences	Mouse	Adhesion/Calcium binding
ATF-2 (T71)	Cell Signaling	Rabbit	Thyroid
ATG5	Cell Signaling	Rabbit	Autophagy
ATM (S1981) (D6H9)	Cell Signaling	RmAb	DNA Damage/repair
ATR (S428)	Cell Signaling	Rabbit	DNA Damage/repair
Beclin 1	Cell Signaling	Rabbit	Autophagy
Catenin, Beta (T41/S45)	Cell Signaling	Rabbit	Adhesion/Differentiation
CD63	Abcam	Rabbit	Exosome Marker
CD9	Stressgen Biotechnologies	Mouse	Exosome Marker
Cofilin (D59)	Cell Signaling	Rabbit	Motility/Adhesion/Phagocytosis
Cu/Zn Superoxide Dismutase (SOD)	Stressgen Biotechnologies	Rabbit	Hypoxia Response/ Oxidative Response
Cytokeratin 8	Santa Cruz Biotechnology	Mouse	Cytoskeletal
DNAPK T2609	Abcam	Mouse	DNA Damage/repair
ERCC1 (4F9)	OriGene	Mouse	DNA Damage/repair
ERK (T202/Y204)	Cell Signaling	Rabbit	Growth and Prosurvival
Estrogen Receptor α (S118) (16JR)	Cell Signaling	Mouse	Transcription Regulation
FAK (Y397) (18)	BD Biosciences	Mouse	Adhesion
Fibronectin (IST-9)	Abcam	Mouse	Adhesion
Galectin 3	Cell Signaling	Rabbit	Adhesion/Growth Regulation
GAPDH (D16H1)	Cell Signaling	RmAb	Apoptosis/Gene expression
GSK-3 α/β (S21/9)	Cell Signaling	Rabbit	Glucose Metabolism
H2AX S139	Cell Signaling	Rabbit	DNA Damage/Repair
HSP70 (C92F3A-5)	Stressgen Biotechnologies	Mouse	Chaperon Protein/Vesicle Formation

HSP90a (T5/7)	Cell Signaling	Rabbit	Chaperon Protein/Vesicle Formation
IGF-1R (Y1135/36)/IR (Y1150/51)	Cell Signaling	RmAb	Insulin Receptor/Glucose Metabolims
IL-6	BioVision	Rabbit	Cytokine/Inflammation
IRS-1 (S612)	Cell Signaling	Rabbit	Glucose/Metabolism
Jak1 (Y1022/1023)	Cell Signaling	Rabbit	Cytokine Signaling /Transcription
LC3B	Cell Signaling	Rabbit	Autophagy
MMP-9	Cell Signaling	Rabbit	Invasion
Na/I Symporter (NIS)	Abcam	Rabbit	Thyroid/Iodide Transport
MSH6 (L990)	Cell Signaling	Rabbit	DNA Damage Repair/
mTOR (S2448)	Cell Signaling	Rabbit	Growth/Prosurvival
NF-kappaB p65 (S536)	Cell Signaling	Rabbit	Proteosome Degradation/Inflammation
p90RSK (S380)	Cell Signaling	Rabbit	Growth/Differentiation
Paxillin (Y118)	Cell Signaling	Rabbit	Cytoskeletal
PD-L1 (28-8)	Abcam	Rabbit	Immune Response
PI3-Kinase	BD Biosciences	Mouse	Growth/Prosurvival
PMCA2	Thermo Fisher Scientific	Rabbit	Calcium Regulation/Transport
Prolactin	Epitomics	Rabbit	Hormone Regulation/Cell Proliferation
S100A7 calcium binding protein	Abnova	Mouse	Calcium Regulation/Transport
Stat3 (S727)	Cell Signaling	Rabbit	Stress/Inflammation
Sumo-2/3	Cell Signaling	Rabbit	Ubiquitination/Protein Folding
Thyroid Peroxidase	Thermo Fisher Scientific	Mouse	Chaperon Protein/Vesicle Formation
TR α 1/ β 1 Antibody (C4)	Santa Cruz Biotechnology	Mouse	Thyroid Hormone/Nuclear Receptor
TSH β Antibody (D-6)	Santa Cruz Biotechnology	Mouse	Thyroid
Type3 DIO3	Thermo Fisher Scientific	Rabbit	Thyroid
VEGF Receptor 2 (55B11)	Cell Signaling	Rabbit	Angiogenesis
Vimentin	Cell Signaling	Rabbit	Cytokine Signaling

REFERENCES

1. Siegel, R. L., Miller, K. D. & Jemal, A. Cancer statistics, 2017. *CA: A Cancer Journal for Clinicians* **67**, 7–30 (2017).
2. Kondo, T., Ezzat, S. & Asa, S. L. Pathogenetic mechanisms in thyroid follicular-cell neoplasia. *Nature Reviews Cancer* **6**, 292–306 (2006).
3. Rivera, M. *et al.* Histopathologic characterization of radioactive iodine-refractory fluorodeoxyglucose-positron emission tomography-positive thyroid carcinoma. *Cancer* **113**, 48–56 (2008).
4. *Diagnostic pathology and molecular genetics of the thyroid*. (Wolters Kluwer Health/Lippincott Williams & Wilkins, 2012).
5. Ravetto, C., Colombo, L. & Dottorini, M. E. Usefulness of fine-needle aspiration in the diagnosis of thyroid carcinoma: a retrospective study in 37,895 patients. *Cancer* **90**, 357–363 (2000).
6. Grogan, R. H., Mitmaker, E. J. & Clark, O. H. The evolution of biomarkers in thyroid cancer-from mass screening to a personalized biosignature. *Cancers (Basel)* **2**, 885–912 (2010).
7. Netea-Maier, R. T. *et al.* Discovery and validation of protein abundance differences between follicular thyroid neoplasms. *Cancer Res.* **68**, 1572–1580 (2008).
8. M. Gomez Saez, J. Diagnostic and Prognostic Markers in Differentiated Thyroid Cancer. *Current Genomics* **12**, 597–608 (2011).

9. Brown, R. A., Al-Moussa, M. & Beck, J. Histometry of normal thyroid in man. *J. Clin. Pathol.* **39**, 475–482 (1986).
10. Gerber, H. *et al.* Colloidal aggregates of insoluble inclusions in human goiters. *Biochimie* **81**, 441–445 (1999).
11. Garrett, J. E. *et al.* Calcitonin-secreting cells of the thyroid express an extracellular calcium receptor gene. *Endocrinology* **136**, 5202–5211 (1995).
12. Morillo-Bernal, J. *et al.* Functional expression of the thyrotropin receptor in C cells: new insights into their involvement in the hypothalamic-pituitary-thyroid axis. *Journal of Anatomy* **215**, 150–158 (2009).
13. Boron, W. F. & Boulpaep, E. L. *Medical physiology: a cellular and molecular approach*. (Elsevier Saunders, 2005).
14. Riedel, C., Levy, O. & Carrasco, N. Post-transcriptional Regulation of the Sodium/Iodide Symporter by Thyrotropin. *Journal of Biological Chemistry* **276**, 21458–21463 (2001).
15. Kogai, T. & Brent, G. A. The sodium iodide symporter (NIS): Regulation and approaches to targeting for cancer therapeutics. *Pharmacology & Therapeutics* **135**, 355–370 (2012).
16. Dohán, O. & Carrasco, N. Advances in Na⁺/I[−] symporter (NIS) research in the thyroid and beyond. *Molecular and Cellular Endocrinology* **213**, 59–70 (2003).
17. Bizhanova, A. & Kopp, P. The Sodium-Iodide Symporter NIS and Pendrin in Iodide Homeostasis of the Thyroid. *Endocrinology* **150**, 1084–1090 (2009).

18. Andrade, B. M. & de Carvalho, D. P. Perspectives of the AMP-activated kinase (AMPK) signalling pathway in thyroid cancer. *Bioscience Reports* **34**, 181–187 (2014).
19. Levy, O. *et al.* Characterization of the thyroid Na⁺/I⁻ symporter with an anti-COOH terminus antibody. *Proc. Natl. Acad. Sci. U.S.A.* **94**, 5568–5573 (1997).
20. Dohán, O., Baloch, Z., Bánrévi, Z., Livolsi, V. & Carrasco, N. RAPID COMMUNICATION: Predominant Intracellular Overexpression of the Na⁺/I⁻ Symporter (NIS) in a Large Sampling of Thyroid Cancer Cases. *The Journal of Clinical Endocrinology & Metabolism* **86**, 2697–2700 (2001).
21. Pesce, L. *et al.* TSH Regulates Pendrin Membrane Abundance and Enhances Iodide Efflux in Thyroid Cells. *Endocrinology* **153**, 512–521 (2012).
22. Chen, X. *et al.* The Effect on Sodium/Iodide Symporter and Pendrin in Thyroid Colloid Retention Developed by Excess Iodide Intake. *Biological Trace Element Research* **172**, 193–200 (2016).
23. *Werner & Ingbar's the thyroid: a fundamental and clinical text.* (Wolters Kluwer/Lippincott Williams & Wilkins Health, 2013).
24. Gérard, A.-C. *et al.* Correlation between the Loss of Thyroglobulin Iodination and the Expression of Thyroid-Specific Proteins Involved in Iodine Metabolism in Thyroid Carcinomas. *The Journal of Clinical Endocrinology & Metabolism* **88**, 4977–4983 (2003).

25. Targovnik, H. M., Citterio, C. E. & Rivolta, C. M. Iodide handling disorders (NIS, TPO, TG, IYD). *Best Practice & Research Clinical Endocrinology & Metabolism* **31**, 195–212 (2017).
26. Many, M. C., Mestdagh, C., van den Hove, M. F. & Denef, J. F. In vitro study of acute toxic effects of high iodide doses in human thyroid follicles. *Endocrinology* **131**, 621–630 (1992).
27. Poncin, S. *et al.* Oxidative Stress in the Thyroid Gland: From Harmlessness to Hazard Depending on the Iodine Content. *Endocrinology* **149**, 424–433 (2008).
28. Leoni, S. G., Kimura, E. T., Santisteban, P. & De la Vieja, A. Regulation of Thyroid Oxidative State by Thioredoxin Reductase Has a Crucial Role in Thyroid Responses to Iodide Excess. *Molecular Endocrinology* **25**, 1924–1935 (2011).
29. Ruf, J. & Carayon, P. Structural and functional aspects of thyroid peroxidase. *Archives of Biochemistry and Biophysics* **445**, 269–277 (2006).
30. Huang, S. A. & Bianco, A. C. Reawakened interest in type III iodothyronine deiodinase in critical illness and injury. *Nature Clinical Practice Endocrinology & Metabolism* **4**, 148–155 (2008).
31. Gereben, B. *et al.* Cellular and Molecular Basis of Deiodinase-Regulated Thyroid Hormone Signaling ¹. *Endocrine Reviews* **29**, 898–938 (2008).
32. Larsen, P. R. & Zavacki, A. M. Role of the Iodothyronine Deiodinases in the Physiology and Pathophysiology of Thyroid Hormone Action. *European Thyroid Journal* (2012). doi:10.1159/000343922

33. Laboratory Support for the Diagnosis and Monitoring of Thyroid Disease. *Thyroid* **13**, 3–3 (2003).
34. Rotteveel-de Groot, D. M. *et al.* Evaluation of the highly sensitive Roche thyroglobulin II assay and establishment of a reference limit for thyroglobulin-negative patient samples. *Practical Laboratory Medicine* **5**, 6–13 (2016).
35. Pascual, A. & Aranda, A. Thyroid hormone receptors, cell growth and differentiation. *Biochimica et Biophysica Acta (BBA) - General Subjects* **1830**, 3908–3916 (2013).
36. Köhrle, J. Thyroid Hormones and Derivatives: Endogenous Thyroid Hormones and Their Targets. in *Thyroid Hormone Nuclear Receptor* (eds. Plateroti, M. & Samarut, J.) **1801**, 85–104 (Springer New York, 2018).
37. Flamant, F. *et al.* International Union of Pharmacology. LIX. The Pharmacology and Classification of the Nuclear Receptor Superfamily: Thyroid Hormone Receptors. *Pharmacological Reviews* **58**, 705–711 (2006).
38. Lemansky, P., Popp, G. M., Tietz, J. & Herzog, V. Identification of iodinated proteins in cultured thyrocytes and their possible significance for thyroid hormone formation. *Endocrinology* **135**, 1566–1575 (1994).
39. Seljelid, R. Endocytosis in thyroid follicle cells. V. On the redistribution of cytosomes following stimulation with thyrotropic hormone. *J. Ultrastruct. Res.* **18**, 479–488 (1967).
40. Seljelid, R. Endocytosis in thyroid follicle cells. *Journal of Ultrastructure Research* **18**, 237–256 (1967).

41. Smeds, S. A Microgel Electrophoretic Analysis of the Colloid Proteins in Single Rat Thyroid Follicles. I. The Qualitative Protein Composition of the Colloid in Normal Thyroids. *Endocrinology* **91**, 1288–1299 (1972).
42. Smeds, S. A Microgel Electrophoretic Analysis of the Colloid Proteins in Single Rat Thyroid Follicles. II. The Protein Concentration of the Colloid in Single Rat Thyroid Follicles. *Endocrinology* **91**, 1300–1306 (1972).
43. Gerber, H. *et al.* Reaccumulation of thyroglobulin and colloid in rat and mouse thyroid follicles during intense thyrotropin stimulation. A clue to the pathogenesis of colloid goiters. *Journal of Clinical Investigation* **68**, 1338–1347 (1981).
44. Berry, J. P., Escaig, F., Lange, F. & Galle, P. Ion microscopy of the thyroid gland: a method for imaging stable and radioactive iodine. *Lab. Invest.* **55**, 109–119 (1986).
45. Fragu, P., Briançon, C., Halpern, S. & Larras-Regard, E. Changes in iodine mapping in rat thyroid during the course of iodine deficiency: imaging and relative quantitation by analytical ion microscope. *Biol. Cell* **62**, 145–155 (1988).
46. Herzog, V., Berndorfer, U. & Saber, Y. Isolation of insoluble secretory product from bovine thyroid: extracellular storage of thyroglobulin in covalently cross-linked form. *J. Cell Biol.* **118**, 1071–1083 (1992).
47. Schmutzler, C. *et al.* Selenoproteins of the thyroid gland: expression, localization and possible function of glutathione peroxidase 3. *Biological Chemistry* **388**, (2007).
48. Cazarin, J., Andrade, B. & Carvalho, D. AMP-Activated Protein Kinase Activation Leads to Lysome-Mediated Na^+/I^- -Symporter Protein Degradation in Rat Thyroid Cells. *Hormone and Metabolic Research* **46**, 313–317 (2014).

49. Nava-Villalba, M. & Aceves, C. 6-Iodolactone, key mediator of antitumoral properties of iodine. *Prostaglandins & Other Lipid Mediators* **112**, 27–33 (2014).
50. Gerber, H., Studer, H. & Grunigen, C. V. Paradoxical Effects of Thyrotropin on Diffusion of Thyroglobulin in the Colloid of Rat Thyroid Follicles after Long Term Thyroxine Treatment*. *Endocrinology* **116**, 303–310 (1985).
51. Smeds, S., Ekholm, R. & Ericson, L. E. Protein concentration of the rat thyroid colloid during thyroxine treatment. *Acta Endocrinol.* **84**, 768–773 (1977).
52. Hartoft-Nielsen, M. L., Rasmussen, A. K., Feldt-Rasmussen, U., Buschard, K. & Bock, T. Estimation of number of follicles, volume of colloid and inner follicular surface area in the thyroid gland of rats. *Journal of Anatomy* **207**, 117–124 (2005).
53. Stelow, E. B. *et al.* Interobserver Variability in Thyroid Fine-Needle Aspiration Interpretation of Lesions Showing Predominantly Colloid and Follicular Groups. *American Journal of Clinical Pathology* **124**, 239–244 (2005).
54. Bartalena, L., Chiovato, L. & Vitti, P. Management of hyperthyroidism due to Graves' disease: frequently asked questions and answers (if any). *Journal of Endocrinological Investigation* **39**, 1105–1114 (2016).
55. Kahaly, G. J. *et al.* 2018 European Thyroid Association Guideline for the Management of Graves' Hyperthyroidism. *European Thyroid Journal* **7**, 167–186 (2018).
56. Xu, C. *et al.* Excess iodine promotes apoptosis of thyroid follicular epithelial cells by inducing autophagy suppression and is associated with Hashimoto thyroiditis disease. *Journal of Autoimmunity* **75**, 50–57 (2016).

57. Rao-Rupanagudi, S., Heywood, R. & Gopinath, C. Age-related Changes in Thyroid Structure and Function in Sprague-Dawley Rats. *Veterinary Pathology* **29**, 278–287 (1992).
58. Faggiano, A. *et al.* Age-dependent variation of follicular size and expression of iodine transporters in human thyroid tissue. *J. Nucl. Med.* **45**, 232–237 (2004).
59. Lee, J. *et al.* Morphological and Functional Changes in the Thyroid Follicles of the Aged Murine and Humans. *Journal of Pathology and Translational Medicine* **50**, 426–435 (2016).
60. Brandler, T. C. *et al.* Can noninvasive follicular thyroid neoplasm with papillary-like nuclear features be distinguished from classic papillary thyroid carcinoma and follicular adenomas by fine-needle aspiration?: Distinguishing NIFTP, PTC, and FA on FNA. *Cancer Cytopathology* **125**, 378–388 (2017).
61. McHenry, C. R. & Phitayakorn, R. Follicular Adenoma and Carcinoma of the Thyroid Gland. *The Oncologist* **16**, 585–593 (2011).
62. Yoo, S.-K. *et al.* Comprehensive Analysis of the Transcriptional and Mutational Landscape of Follicular and Papillary Thyroid Cancers. *PLOS Genetics* **12**, e1006239 (2016).
63. Davies, H. *et al.* Mutations of the BRAF gene in human cancer. *Nature* **417**, 949–954 (2002).
64. Proietti, A. *et al.* Follicular-derived neoplasms: Morphometric and genetic differences. *Journal of Endocrinological Investigation* (2013). doi:10.3275/9063

65. Clark, D. P. & Faquin, W. C. Colloid-Predominant Lesions. in *Thyroid Cytopathology* **8**, 55–67 (Springer US, 2010).
66. de Matos, L. *et al.* Expression of ck-19, galectin-3 and hbme-1 in the differentiation of thyroid lesions: systematic review and diagnostic meta-analysis. *Diagnostic Pathology* **7**, 97 (2012).
67. Dunderović, D. *et al.* Defining the value of CD56, CK19, Galectin 3 and HBME-1 in diagnosis of follicular cell derived lesions of thyroid with systematic review of literature. *Diagnostic Pathology* **10**, (2015).
68. Kitahara, C. M. & Sosa, J. A. The changing incidence of thyroid cancer. *Nature Reviews Endocrinology* **12**, 646–653 (2016).
69. Enewold, L. *et al.* Rising Thyroid Cancer Incidence in the United States by Demographic and Tumor Characteristics, 1980-2005. *Cancer Epidemiology Biomarkers & Prevention* **18**, 784–791 (2009).
70. Kim, Y. J., Hong, H. S., Jeong, S. H., Lee, E. H. & Kwak, J. J. Papillary Thyroid Carcinoma Arising Within a Follicular Adenoma: A Case Report, Ultrasound Features, and Considerations. *Ultrasound Quarterly* **33**, 62–65 (2017).
71. Carpi, A., Mechanick, J. I., Saussez, S. & Nicolini, A. Thyroid tumor marker genomics and proteomics: Diagnostic and clinical implications. *Journal of Cellular Physiology* **224**, 612–619 (2010).
72. Sadow, P. M., Heinrich, M. C., Corless, C. L., Fletcher, J. A. & Nosé, V. Absence of BRAF, NRAS, KRAS, HRAS Mutations, and RET/PTC Gene Rearrangements

- Distinguishes Dominant Nodules in Hashimoto Thyroiditis from Papillary Thyroid Carcinomas. *Endocrine Pathology* **21**, 73–79 (2010).
73. Kim, S. *et al.* BRAFV600E Mutation is Associated with Tumor Aggressiveness in Papillary Thyroid Cancer. *World Journal of Surgery* **36**, 310–317 (2012).
 74. Mizushima, N., Levine, B., Cuervo, A. M. & Klionsky, D. J. Autophagy fights disease through cellular self-digestion. *Nature* **451**, 1069–1075 (2008).
 75. Morselli, E. *et al.* Anti- and pro-tumor functions of autophagy. *Biochimica et Biophysica Acta (BBA) - Molecular Cell Research* **1793**, 1524–1532 (2009).
 76. Yang, M. *et al.* Expression of autophagy-associated proteins in papillary thyroid carcinoma. *Oncology Letters* **14**, 411–415 (2017).
 77. Mizushima, N. The exponential growth of autophagy-related research: from the humble yeast to the Nobel Prize. *FEBS Letters* **591**, 681–689 (2017).
 78. Mathew, R., Karantza-Wadsworth, V. & White, E. Role of autophagy in cancer. *Nature Reviews Cancer* **7**, 961–967 (2007).
 79. Apel, A., Zentgraf, H., Büchler, M. W. & Herr, I. Autophagy-A double-edged sword in oncology. *International Journal of Cancer* **125**, 991–995 (2009).
 80. Levine, B. & Klionsky, D. J. Development by self-digestion: molecular mechanisms and biological functions of autophagy. *Dev. Cell* **6**, 463–477 (2004).
 81. Shintani, T. Autophagy in Health and Disease: A Double-Edged Sword. *Science* **306**, 990–995 (2004).
 82. Qu, X. *et al.* Promotion of tumorigenesis by heterozygous disruption of the beclin 1 autophagy gene. *Journal of Clinical Investigation* **112**, 1809–1820 (2003).

83. Klionsky, D. J. *et al.* Guidelines for the use and interpretation of assays for monitoring autophagy. *Autophagy* **8**, 445–544 (2012).
84. Degenhardt, K. *et al.* Autophagy promotes tumor cell survival and restricts necrosis, inflammation, and tumorigenesis. *Cancer Cell* **10**, 51–64 (2006).
85. Kim, H., Kim, E.-S. & Koo, J. Expression of Autophagy-Related Proteins in Different Types of Thyroid Cancer. *International Journal of Molecular Sciences* **18**, 540 (2017).
86. Swart, C., Du Toit, A. & Loos, B. Autophagy and the invisible line between life and death. *European Journal of Cell Biology* **95**, 598–610 (2016).
87. Janku, F., McConkey, D. J., Hong, D. S. & Kurzrock, R. Autophagy as a target for anticancer therapy. *Nature Reviews Clinical Oncology* **8**, 528–539 (2011).
88. Vidal, A. P. *et al.* AMP-activated protein kinase signaling is upregulated in papillary thyroid cancer. *European Journal of Endocrinology* **169**, 521–528 (2013).
89. Luo, Z., Zang, M. & Guo, W. AMPK as a metabolic tumor suppressor: control of metabolism and cell growth. *Future Oncology* **6**, 457–470 (2010).
90. Knauf, J. A. & Fagin, J. A. Role of MAPK pathway oncoproteins in thyroid cancer pathogenesis and as drug targets. *Current Opinion in Cell Biology* **21**, 296–303 (2009).
91. Rivas, M. & Santisteban, P. TSH-activated signaling pathways in thyroid tumorigenesis. *Molecular and Cellular Endocrinology* **213**, 31–45 (2003).
92. Souza, E. C. L. de *et al.* MTOR downregulates iodide uptake in thyrocytes. *Journal of Endocrinology* **206**, 113–120 (2010).

93. Choi, H.-J. *et al.* The influence of the BRAF V600E mutation in thyroid cancer cell lines on the anticancer effects of 5-aminoimidazole-4-carboxamide-ribonucleoside. *Journal of Endocrinology* **211**, 79–85 (2011).
94. Jung, C. H. *et al.* ULK-Atg13-FIP200 Complexes Mediate mTOR Signaling to the Autophagy Machinery. *Molecular Biology of the Cell* **20**, 1992–2003 (2009).
95. Li, X., Li, Z., Song, Y., Liu, W. & Liu, Z. The mTOR Kinase Inhibitor CZ415 Inhibits Human Papillary Thyroid Carcinoma Cell Growth. *Cellular Physiology and Biochemistry* **46**, 579–590 (2018).
96. Xing, M. Oxidative stress: a new risk factor for thyroid cancer. *Endocrine-Related Cancer* **19**, C7–C11 (2012).
97. Liu, Z. *et al.* Highly Prevalent Genetic Alterations in Receptor Tyrosine Kinases and Phosphatidylinositol 3-Kinase/Akt and Mitogen-Activated Protein Kinase Pathways in Anaplastic and Follicular Thyroid Cancers. *The Journal of Clinical Endocrinology & Metabolism* **93**, 3106–3116 (2008).
98. Davuluri, G. *et al.* Activated VEGF receptor shed into the vitreous in eyes with wet AMD: a new class of biomarkers in the vitreous with potential for predicting the treatment timing and monitoring response. *Arch. Ophthalmol.* **127**, 613–621 (2009).
99. Li, L., Liu, G., Zhang, X. & Li, Y. Autophagy, a novel target for chemotherapeutic intervention of thyroid cancer. *Cancer Chemotherapy and Pharmacology* **73**, 439–449 (2014).
100. Espina, V. *et al.* Malignant precursor cells pre-exist in human breast DCIS and require autophagy for survival. *PLoS ONE* **5**, e10240 (2010).

101. Cazarin, J., Andrade, B. & Carvalho, D. AMP-Activated Protein Kinase Activation Leads to Lysome-Mediated Na^+/I^- -Symporter Protein Degradation in Rat Thyroid Cells. *Hormone and Metabolic Research* **46**, 313–317 (2014).
102. Carvalho, D. P. & Ferreira, A. C. F. The importance of sodium/iodide symporter (NIS) for thyroid cancer management. *Arq Bras Endocrinol Metabol* **51**, 672–682 (2007).
103. Li, L., Liu, G., Zhang, X. & Li, Y. Autophagy, a novel target for chemotherapeutic intervention of thyroid cancer. *Cancer Chemotherapy and Pharmacology* **73**, 439–449 (2014).
104. Matuszczyk, A. *et al.* Chemotherapy with Doxorubicin in Progressive Medullary and Thyroid Carcinoma of the Follicular Epithelium. *Hormone and Metabolic Research* **40**, 210–213 (2008).
105. Paglin, S. *et al.* A novel response of cancer cells to radiation involves autophagy and formation of acidic vesicles. *Cancer Res.* **61**, 439–444 (2001).
106. Muñoz-Gámez, J. A. *et al.* PARP-1 is involved in autophagy induced by DNA damage. *Autophagy* **5**, 61–74 (2009).
107. Paweletz, C. P. *et al.* Reverse phase protein microarrays which capture disease progression show activation of pro-survival pathways at the cancer invasion front. *Oncogene* **20**, 1981–1989 (2001).
108. Espina, V. *et al.* Protein microarrays: Molecular profiling technologies for clinical specimens. *PROTEOMICS* **3**, 2091–2100 (2003).

109. Petricoin, E. F. *et al.* Phosphoprotein Pathway Mapping: Akt/Mammalian Target of Rapamycin Activation Is Negatively Associated with Childhood Rhabdomyosarcoma Survival. *Cancer Research* **67**, 3431–3440 (2007).
110. Espina, V. *et al.* Laser-capture microdissection. *Nat Protoc* **1**, 586–603 (2006).
111. Tamburro, D. *et al.* Multifunctional Core–Shell Nanoparticles: Discovery of Previously Invisible Biomarkers. *Journal of the American Chemical Society* **133**, 19178–19188 (2011).
112. Gallagher, R. I., Silvestri, A., Petricoin, E. F., Liotta, L. A. & Espina, V. Reverse Phase Protein Microarrays: Fluorometric and Colorimetric Detection. in *Protein Microarray for Disease Analysis* (ed. Wu, C. J.) **723**, 275–301 (Humana Press, 2011).
113. Zhou, W. *et al.* Proteomic analysis of pancreatic ductal adenocarcinoma cells reveals metabolic alterations. *J. Proteome Res.* **10**, 1944–1952 (2011).
114. Zhou, W., Liotta, L. A. & Petricoin, E. F. Cancer metabolism: what we can learn from proteomic analysis by mass spectrometry. *Cancer Genomics Proteomics* **9**, 373–381 (2012).
115. Cochand-Priollet, B. *et al.* Immunocytochemistry with cytokeratin 19 and anti-human mesothelial cell antibody (HBME1) increases the diagnostic accuracy of thyroid fine-needle aspirations: preliminary report of 150 liquid-based fine-needle aspirations with histological control. *Thyroid* **21**, 1067–1073 (2011).

116. Navas-Carrillo, D., Rodriguez, J. M., Montoro-García, S. & Orenes-Piñero, E. High-resolution proteomics and metabolomics in thyroid cancer: Deciphering novel biomarkers. *Critical Reviews in Clinical Laboratory Sciences* **54**, 446–457 (2017).
117. Paris, L. *et al.* Urine lipoarabinomannan glycan in HIV-negative patients with pulmonary tuberculosis correlates with disease severity. *Sci Transl Med* **9**, (2017).
118. Raiszadeh, M. M. *et al.* Proteomic Analysis of Eccrine Sweat: Implications for the Discovery of Schizophrenia Biomarker Proteins. *Journal of Proteome Research* **11**, 2127–2139 (2012).
119. Guo, D. *et al.* Cytokeratin-8 in Anaplastic Thyroid Carcinoma: More Than a Simple Structural Cytoskeletal Protein. *Int J Mol Sci* **19**, (2018).
120. Takano, T., Miyauchi, A., Yoshida, H., Kuma, K. & Amino, N. High-throughput differential screening of mRNAs by serial analysis of gene expression: decreased expression of trefoil factor 3 mRNA in thyroid follicular carcinomas. *Br. J. Cancer* **90**, 1600–1605 (2004).
121. Wojtas, B. *et al.* Gene Expression (mRNA) Markers for Differentiating between Malignant and Benign Follicular Thyroid Tumours. *Int J Mol Sci* **18**, (2017).
122. Eun, Y. G. *et al.* Associations between promoter polymorphism -106A/G of interleukin-11 receptor alpha and papillary thyroid cancer in Korean population. *Surgery* **151**, 323–329 (2012).
123. Chu, P. G. & Weiss, L. M. Keratin expression in human tissues and neoplasms. *Histopathology* **40**, 403–439 (2002).

124. Domanski, D. *et al.* A Multiplexed Cytokeratin Analysis Using Targeted Mass Spectrometry Reveals Specific Profiles in Cancer-Related Pleural Effusions. *Neoplasia* **18**, 399–412 (2016).
125. Sakamoto, K. *et al.* Down-regulation of keratin 4 and keratin 13 expression in oral squamous cell carcinoma and epithelial dysplasia: a clue for histopathogenesis. *Histopathology* **58**, 531–542 (2011).
126. Ghavami, S. *et al.* S100A8/A9 induces autophagy and apoptosis via ROS-mediated cross-talk between mitochondria and lysosomes that involves BNIP3. *Cell Res.* **20**, 314–331 (2010).
127. Patel, S. R. *et al.* Differential roles of microtubule assembly and sliding in proplatelet formation by megakaryocytes. *Blood* **106**, 4076–4085 (2005).
128. Stoupa, A. *et al.* TUBB1 mutations cause thyroid dysgenesis associated with abnormal platelet physiology. *EMBO Molecular Medicine* **10**, e9569 (2018).
129. Karantza, V. Keratins in health and cancer: more than mere epithelial cell markers. *Oncogene* **30**, 127–138 (2011).
130. Ku, N.-O., Toivola, D. M., Strnad, P. & Omary, M. B. Cytoskeletal keratin glycosylation protects epithelial tissue from injury. *Nat. Cell Biol.* **12**, 876–885 (2010).
131. Toivola, D. M., Tao, G.-Z., Habtezion, A., Liao, J. & Omary, M. B. Cellular integrity plus: organelle-related and protein-targeting functions of intermediate filaments. *Trends Cell Biol.* **15**, 608–617 (2005).

132. Kang, Y. *et al.* A multigenic program mediating breast cancer metastasis to bone. *Cancer Cell* **3**, 537–549 (2003).
133. Bresnick, A. R. S100 proteins as therapeutic targets. *Biophys Rev* **10**, 1617–1629 (2018).
134. Ahmed, K. A. & Xiang, J. Mechanisms of cellular communication through intercellular protein transfer. *J. Cell. Mol. Med.* **15**, 1458–1473 (2011).
135. Ogawa, Y. *et al.* Proteomic analysis of two types of exosomes in human whole saliva. *Biol. Pharm. Bull.* **34**, 13–23 (2011).
136. György, B. *et al.* Membrane vesicles, current state-of-the-art: emerging role of extracellular vesicles. *Cell. Mol. Life Sci.* **68**, 2667–2688 (2011).
137. Li, P., Kaslan, M., Lee, S. H., Yao, J. & Gao, Z. Progress in Exosome Isolation Techniques. *Theranostics* **7**, 789–804 (2017).
138. Bard, M. P. *et al.* Proteomic analysis of exosomes isolated from human malignant pleural effusions. *Am. J. Respir. Cell Mol. Biol.* **31**, 114–121 (2004).
139. Kowal, J., Tkach, M. & Théry, C. Biogenesis and secretion of exosomes. *Curr. Opin. Cell Biol.* **29**, 116–125 (2014).
140. Hoshino, A. *et al.* Tumour exosome integrins determine organotropic metastasis. *Nature* **527**, 329–335 (2015).
141. Laurenzana, I. *et al.* Extracellular Vesicles: A New Prospective in Crosstalk between Microenvironment and Stem Cells in Hematological Malignancies. *Stem Cells Int* **2018**, 9863194 (2018).

142. Narayanan, A. *et al.* Exosomes derived from HIV-1-infected cells contain trans-activation response element RNA. *J. Biol. Chem.* **288**, 20014–20033 (2013).
143. Zhou, M. *et al.* Effects of RSC96 Schwann Cell-Derived Exosomes on Proliferation, Senescence, and Apoptosis of Dorsal Root Ganglion Cells In Vitro. *Med. Sci. Monit.* **24**, 7841–7849 (2018).
144. Matsuura, Y. *et al.* Exosomal miR-155 Derived from Hepatocellular Carcinoma Cells Under Hypoxia Promotes Angiogenesis in Endothelial Cells. *Dig. Dis. Sci.* **64**, 792–802 (2019).
145. Kahlert, C. & Kalluri, R. Exosomes in tumor microenvironment influence cancer progression and metastasis. *J. Mol. Med.* **91**, 431–437 (2013).
146. Fujita, Y., Yoshioka, Y. & Ochiya, T. Extracellular vesicle transfer of cancer pathogenic components. *Cancer Sci.* **107**, 385–390 (2016).
147. Colao, I. L., Corteling, R., Bracewell, D. & Wall, I. Manufacturing Exosomes: A Promising Therapeutic Platform. *Trends in Molecular Medicine* **24**, 242–256 (2018).
148. Kim, S. J. *et al.* Increased serum 90K and Galectin-3 expression are associated with advanced stage and a worse prognosis in diffuse large B-cell lymphomas. *Acta Haematol.* **120**, 211–216 (2008).
149. Sciacchitano, S. *et al.* Galectin-3: One Molecule for an Alphabet of Diseases, from A to Z. *Int J Mol Sci* **19**, (2018).
150. Pan, S. *et al.* Quantitative glycoproteomics analysis reveals changes in N-glycosylation level associated with pancreatic ductal adenocarcinoma. *J. Proteome Res.* **13**, 1293–1306 (2014).

151. Sikorska, J., Gawel, D., Domek, H., Rudzińska, M. & Czarnocka, B. Podoplanin (PDPN) affects the invasiveness of thyroid carcinoma cells by inducing ezrin, radixin and moesin (E/R/M) phosphorylation in association with matrix metalloproteinases. *BMC Cancer* **19**, 85 (2019).
152. Ghoneim, C., Soula-Rothhut, M. & Rothhut, B. Thrombospondin-1 in differentiated thyroid cancer: Dr. Jekyll and Mr. Hyde. *Connect. Tissue Res.* **49**, 257–260 (2008).
153. Maji, S. *et al.* Exosomal Annexin II Promotes Angiogenesis and Breast Cancer Metastasis. *Mol. Cancer Res.* **15**, 93–105 (2017).
154. Lam, K. Y., Lui, M. C. & Lo, C. Y. Cytokeratin expression profiles in thyroid carcinomas. *European Journal of Surgical Oncology (EJSO)* **27**, 631–635 (2001).
155. Lucas, S. D. *et al.* Tumor-specific deposition of immunoglobulin G and complement in papillary thyroid carcinoma. *Hum. Pathol.* **27**, 1329–1335 (1996).
156. Pio, R., Corrales, L. & Lambris, J. D. The role of complement in tumor growth. *Adv. Exp. Med. Biol.* **772**, 229–262 (2014).
157. Xia, S. *et al.* Fibronectin 1 promotes migration and invasion of papillary thyroid cancer and predicts papillary thyroid cancer lymph node metastasis. *Onco Targets Ther* **10**, 1743–1755 (2017).
158. Fryknäs, M. *et al.* Molecular markers for discrimination of benign and malignant follicular thyroid tumors. *Tumour Biol.* **27**, 211–220 (2006).

159. Rodrigues, R. *et al.* Comparative genomic hybridization, BRAF, RAS, RET, and oligo-array analysis in aneuploid papillary thyroid carcinomas. *Oncol. Rep.* **18**, 917–926 (2007).
160. Vasko, V. *et al.* Gene expression and functional evidence of epithelial-to-mesenchymal transition in papillary thyroid carcinoma invasion. *Proc. Natl. Acad. Sci. U.S.A.* **104**, 2803–2808 (2007).
161. da Silveira Mitteldorf, C. A. T., de Sousa-Canavez, J. M., Leite, K. R. M., Massumoto, C. & Camara-Lopes, L. H. FN1, GALE, MET, and QPCT overexpression in papillary thyroid carcinoma: molecular analysis using frozen tissue and routine fine-needle aspiration biopsy samples. *Diagn. Cytopathol.* **39**, 556–561 (2011).
162. Sponziello, M. *et al.* Fibronectin-1 expression is increased in aggressive thyroid cancer and favors the migration and invasion of cancer cells. *Mol. Cell. Endocrinol.* **431**, 123–132 (2016).
163. Baietti, M. F. *et al.* Syndecan-syntenin-ALIX regulates the biogenesis of exosomes. *Nat. Cell Biol.* **14**, 677–685 (2012).
164. Kulkarni, R. & Prasad, A. Exosomes Derived from HIV-1 Infected DCs Mediate Viral trans-Infection via Fibronectin and Galectin-3. *Sci Rep* **7**, 14787 (2017).
165. Roucourt, B., Meeussen, S., Bao, J., Zimmermann, P. & David, G. Heparanase activates the syndecan-syntenin-ALIX exosome pathway. *Cell Res.* **25**, 412–428 (2015).

166. Ilan, N., Elkin, M. & Vlodavsky, I. Regulation, function and clinical significance of heparanase in cancer metastasis and angiogenesis. *Int. J. Biochem. Cell Biol.* **38**, 2018–2039 (2006).
167. Thompson, C. A., Purushothaman, A., Ramani, V. C., Vlodavsky, I. & Sanderson, R. D. Heparanase regulates secretion, composition, and function of tumor cell-derived exosomes. *J. Biol. Chem.* **288**, 10093–10099 (2013).
168. Monteith, G. R., Prevarskaya, N. & Roberts-Thomson, S. J. The calcium-cancer signalling nexus. *Nat. Rev. Cancer* **17**, 367–380 (2017).
169. Stewart, T. A., Yapa, K. T. D. S. & Monteith, G. R. Altered calcium signaling in cancer cells. *Biochim. Biophys. Acta* **1848**, 2502–2511 (2015).
170. Cheng, N., Chytil, A., Shyr, Y., Joly, A. & Moses, H. L. Transforming growth factor-beta signaling-deficient fibroblasts enhance hepatocyte growth factor signaling in mammary carcinoma cells to promote scattering and invasion. *Mol. Cancer Res.* **6**, 1521–1533 (2008).
171. Lee, Y., El Andaloussi, S. & Wood, M. J. A. Exosomes and microvesicles: extracellular vesicles for genetic information transfer and gene therapy. *Hum. Mol. Genet.* **21**, R125-134 (2012).
172. Li, W. *et al.* Role of exosomal proteins in cancer diagnosis. *Mol. Cancer* **16**, 145 (2017).
173. Abd Elmageed, Z. Y. *et al.* Neoplastic reprogramming of patient-derived adipose stem cells by prostate cancer cell-associated exosomes. *Stem Cells* **32**, 983–997 (2014).

174. Melo, S. A. *et al.* Cancer exosomes perform cell-independent microRNA biogenesis and promote tumorigenesis. *Cancer Cell* **26**, 707–721 (2014).
175. Henderson, M. C. & Azorsa, D. O. The Genomic and Proteomic Content of Cancer Cell-Derived Exosomes. *Frontiers in Oncology* **2**, (2012).
176. Zhang, X. *et al.* Exosomes in cancer: small particle, big player. *J Hematol Oncol* **8**, 83 (2015).
177. Lokman, N. A., Ween, M. P., Oehler, M. K. & Ricciardelli, C. The role of annexin A2 in tumorigenesis and cancer progression. *Cancer Microenviron* **4**, 199–208 (2011).
178. Wang, C.-Y. & Lin, C.-F. Annexin A2: its molecular regulation and cellular expression in cancer development. *Dis. Markers* **2014**, 308976 (2014).
179. Yang, C. & Robbins, P. D. The roles of tumor-derived exosomes in cancer pathogenesis. *Clin. Dev. Immunol.* **2011**, 842849 (2011).
180. Kholia, S. *et al.* Extracellular vesicles as new players in angiogenesis. *Vascul. Pharmacol.* **86**, 64–70 (2016).
181. Solier, S. *et al.* Heat shock protein 90 α (HSP90 α), a substrate and chaperone of DNA-PK necessary for the apoptotic response. *Proc. Natl. Acad. Sci. U.S.A.* **109**, 12866–12872 (2012).
182. Liotta, L. A., Kohn, E. C. & Petricoin, E. F. Clinical proteomics: personalized molecular medicine. *JAMA* **286**, 2211–2214 (2001).

183. Petricoin, E. F., Zoon, K. C., Kohn, E. C., Barrett, J. C. & Liotta, L. A. Clinical proteomics: translating benchside promise into bedside reality. *Nat Rev Drug Discov* **1**, 683–695 (2002).
184. Wulfkuhle, J., Espina, V., Liotta, L. & Petricoin, E. Genomic and proteomic technologies for individualisation and improvement of cancer treatment. *Eur. J. Cancer* **40**, 2623–2632 (2004).
185. O'Brien, S. *et al.* FAK inhibition with small molecule inhibitor Y15 decreases viability, clonogenicity, and cell attachment in thyroid cancer cell lines and synergizes with targeted therapeutics. *Oncotarget* **5**, 7945–7959 (2014).
186. Kenific, C. M., Thorburn, A. & Debnath, J. Autophagy and metastasis: another double-edged sword. *Current Opinion in Cell Biology* **22**, 241–245 (2010).
187. Ha, J., Guan, K.-L. & Kim, J. AMPK and autophagy in glucose/glycogen metabolism. *Mol. Aspects Med.* **46**, 46–62 (2015).
188. So, A., Le Guen, T., Lopez, B. S. & Guirouilh-Barbat, J. Genomic rearrangements induced by unscheduled DNA double strand breaks in somatic mammalian cells. *The FEBS Journal* **284**, 2324–2344 (2017).
189. Krohn, K. *et al.* Molecular pathogenesis of euthyroid and toxic multinodular goiter. *Endocr. Rev.* **26**, 504–524 (2005).
190. Song, Y. *et al.* Roles of Hydrogen Peroxide in Thyroid Physiology and Disease. *The Journal of Clinical Endocrinology & Metabolism* **92**, 3764–3773 (2007).
191. Zambrano, A. *et al.* The thyroid hormone receptor β induces DNA damage and premature senescence. *J. Cell Biol.* **204**, 129–146 (2014).

192. Zhang, N. *et al.* Metallothionein-I/II Knockout Mice Aggravate Mitochondrial Superoxide Production and Peroxiredoxin 3 Expression in Thyroid after Excessive Iodide Exposure. *Oxidative Medicine and Cellular Longevity* **2015**, 1–11 (2015).
193. Kalifa, L. *et al.* DNA double-strand breaks activate ATM independent of mitochondrial dysfunction in A549 cells. *Free Radic. Biol. Med.* **75**, 30–39 (2014).
194. Sinha, R. A. *et al.* Thyroid hormone stimulates hepatic lipid catabolism via activation of autophagy. *Journal of Clinical Investigation* **122**, 2428–2438 (2012).
195. Wulfkühle, J. D. *et al.* Molecular analysis of HER2 signaling in human breast cancer by functional protein pathway activation mapping. *Clin. Cancer Res.* **18**, 6426–6435 (2012).
196. Sofiadis, A. *et al.* Proteomic profiling of follicular and papillary thyroid tumors. *Eur. J. Endocrinol.* **166**, 657–667 (2012).
197. Zhou, W., Liotta, L. A. & Petricoin, E. F. Cancer metabolism: what we can learn from proteomic analysis by mass spectrometry. *Cancer Genomics Proteomics* **9**, 373–381 (2012).
198. Torregrossa, L. *et al.* Toward the reliable diagnosis of indeterminate thyroid lesions: a HRMAS NMR-based metabolomics case of study. *J. Proteome Res.* **11**, 3317–3325 (2012).
199. Carneiro, R. M., Carneiro, B. A., Agulnik, M., Kopp, P. A. & Giles, F. J. Targeted therapies in advanced differentiated thyroid cancer. *Cancer Treat. Rev.* **41**, 690–698 (2015).

200. Spitzweg, C., Bible, K. C., Hofbauer, L. C. & Morris, J. C. Advanced radioiodine-refractory differentiated thyroid cancer: the sodium iodide symporter and other emerging therapeutic targets. *Lancet Diabetes Endocrinol* **2**, 830–842 (2014).
201. Rathmann, D., Rijntjes, E., Lietzow, J. & Köhrle, J. Quantitative Analysis of Thyroid Hormone Metabolites in Cell Culture Samples Using LC-MS/MS. *European Thyroid Journal* **4**, 51–58 (2015).

BIOGRAPHY

Rosa Isela Gallagher received her Bachelor of Science from the University of Texas-Pan American in 2000 and her Master of Science from the University of Texas-Pan American in 2006. She was employed as a Biochemistry Technician at USDA-Agriculture Research Service in Weslaco, TX for 4 years. She later moved to Virginia and was hired by George Mason University at the Center for Applied Proteomics and Molecular Medicine in 2006 as a Research and Laboratory Specialist.